



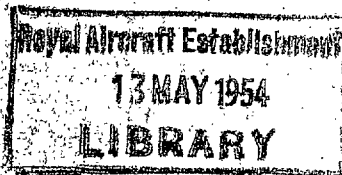
MINISTRY OF SUPPLY

AERONAUTICAL RESEARCH COUNCIL
REPORTS AND MEMORANDA

**Heat Transference and Pressure Loss
for Air Flowing in
Passages of Small Dimensions**

BY

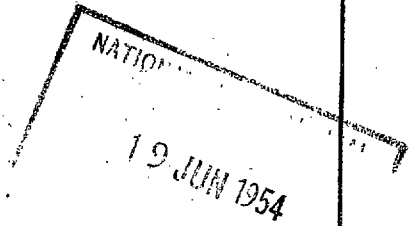
J. REMFRY, Ph.D., A.C.G.I., D.I.C., Wh. Sch.



LONDON: HER MAJESTY'S STATIONERY OFFICE

1954

PRICE 18s 6d NET



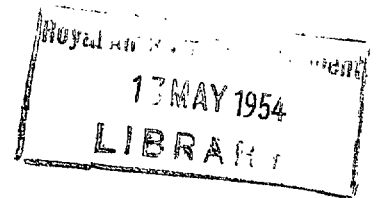
MINISTRY OF SUPPLY

AERONAUTICAL RESEARCH COUNCIL
REPORTS AND MEMORANDA

Heat Transference and Pressure Loss
for Air Flowing in
Passages of Small Dimensions

BY

J. REMFRY, Ph.D., A.C.G.I., D.I.C., Wh. Sch.



LONDON: HER MAJESTY'S STATIONERY OFFICE

1954

Work proposed for the Ph.D. degree, University of London, and approved by the University for the award of this degree. The date of presentation to the University was June 1947. The original thesis as presented to the University of London has been reduced for the purpose of publication in the Aeronautical Research Council Reports and Memoranda. The original thesis is deposited in the library of the University of London.

PRINTED AND PUBLISHED BY HER MAJESTY'S STATIONERY OFFICE

To be purchased from

York House, Kingsway, LONDON, W.C.2 423 Oxford Street, LONDON, W.1

P.O. Box 569, LONDON, S.E.1

13a Castle Street, EDINBURGH, 2 1 St. Andrew's Crescent, CARDIFF

39 King Street, MANCHESTER, 2 Tower Lane, BRISTOL, 1

2 Edmund Street, BIRMINGHAM, 3 80 Chichester Street, BELFAST

or from any Bookseller

1954

Price 18s 6d net

S.O. Code No. 23-2638

Heat Transference and Pressure Loss for Air Flowing in Passages of Small Dimensions

CONTENTS

		PAGE			PAGE
SUMMARY					iv
		PAGE			PAGE
Section I			Section IV		
1.0	INTRODUCTION	1	4.0	ANALYSIS OF RESULTS	10
1.1	Usual Methods of Estimation	1	4.1	Determination of Heat-Transfer Coefficients	10
1.2	Turbulence and Roughness	1	4.2	Determination of Coefficients of Pressure Drop	10
1.3	Turbulence and Heat Transfer	2	4.3	Determination of Friction Coefficients	10
1.4	The Relation Between Friction and Heat Transfer	2	4.4	Determination of End Losses	11
1.5	Practical Applications	2	4.5	Determination of Losses Due to Waving or Bulging	11
1.6	Objects of Investigation	2			
Section II			Section V		
2.0	THEORETICAL ANALYSIS	2	5.0	DISCUSSION OF RESULTS	11
2.1	Velocity and Temperature Distributions	3	5.1	Heat Transfer	12
2.2	Heat Transfer and Friction in a Passage	3	5.2	End-Loss Coefficients	12
2.3	The Relation Between the Friction and Heat-Transfer Coefficients	4	5.3	Losses Due to Waving and Bulging	13
2.4	Effect of Contraction at Entry	5	5.4	Limitations Due to Approximate Method of Analysis	13
2.5	Effect of Expansion at Exit	5	5.5	Range of Investigation	14
2.6	The Net End Effect	5			
2.7	Pressure Loss Due to Apparent Roughness	5	Section VI		
2.8	Pressure Loss in the Passages	6	6.0	METHOD OF USING EXPERIMENTAL RESULTS	14
2.9	Coefficients of Pressure Drop	7	6.1	Heat Interchange	14
Section III			6.2	Friction	14
3.0	EXPERIMENTAL WORK	7	6.3	Pressure Losses	14
3.1	Types of Passage	8	6.4	Typical Values of Coefficients	15
3.2	Range of Investigation	8	References		15
3.3	Experimental Plant	9			
3.4	Experimental Method	9			

APPENDICES

APPENDIX I	General Data and Collected Results.
SYMBOLS.	
TABLE 1	General Particulars of Experimental Units.
FIGURE 1	Effective Temperature Difference in Cross Flow.
FIGURE 2	Relation Between Friction and Heat-Transfer Coefficients.
FIGURE 3	Heat-Transfer Coefficients.
FIGURE 4	End-Loss Coefficients.
FIGURE 5	Coefficients of Pressure Loss Due to Waves and Bulges.
APPENDIX II	Descriptions of Test Units.
APPENDIX III	Curves of End-Loss Coefficients.
APPENDIX IV	Curve of Coefficients of Pressure Loss Due to Waves and Bulges.
APPENDIX V	Curves of Pressure-Drop Coefficients for Cold Units.

SUMMARY

This investigation had as its primary object the experimental determination of the heat-transfer and pressure-loss characteristics for air flowing in small triangular, square, hexagonal and round passages. The heat interchanger models, with a frontage six inches square, each comprised from just under 150 to over 2,250 passages, according to their size and spacing. The hydraulic diameter of the smallest tubes was about 0.08 inch. Previously, little information of this kind had been available for any except round tubes of more than 0.5 inch diameter.

The heat transfer in small smooth passages was found to be less than that usually measured for turbulent flow in tubes of larger size, and there was a tendency for a prolonged transition.

The investigation was extended to determine the greater heat flow obtained in bulged or waved passages and outside a nest of hexagonal tubes. The influence of

variation of passage length, pitch and end shape was also examined.

A simplified theoretical analysis furnished a basis for separation of the components of pressure loss due to friction, increase of momentum, turbulence and end losses. Because of the uncertainty regarding conditions in transitional flow, a more precise theoretical treatment was considered to be unjustified. The interdependence of friction and heat transfer was emphasised by estimating the useful friction from the measured heat transfer coefficient, using the relationship deduced by von Kármán on the hypothesis of the existence of a buffer layer between the laminar boundary flow and the turbulent core.

The pressure losses measured in the experiments were found to be represented with good accuracy by coefficients, which may confidently be used to predict the air pressure drop in similar types of passage when the rate of heat transference is known.

Heat Transference and Pressure Loss for Air Flowing in Passages of Small Dimensions

REPORTS AND MEMORANDA No. 2638*

JUNE, 1947

SECTION I

1.0. INTRODUCTION

In assessing the suitability of heat interchangers for specified duties it is necessary to be able to estimate both their performance as a means of transferring heat and the characteristics of their passages as channels for fluid flow. It is sometimes overlooked that these two essential qualities of a heat interchanger are not unrelated. Their mutual affinity is apparent in their common dependence on the nature of the fluid flow in the passages and, in particular, on the degree of turbulence that is maintained in this flow. In the following pages it is the object, in the first place, to provide fundamental information, derived from experimental work, on the heat-transfer and pressure-drop characteristics of certain types of passage for which previously such information has been lacking and, secondly, to present this data in a way that will emphasise the interdependence of these characteristics and will, at the same time, furnish a comparatively simple and practical method of using the data for reasonably accurate performance estimates.

1.1. Usual Methods of Estimation

Heat transference from one fluid to another is effected in heat interchangers of the types common in engineering practice by causing the fluids to pass on opposite sides of a metal surface which serves primarily to prevent mixing of the fluids. This metal surface is frequently in the form of a tube or tubes within which one fluid flows, surrounded by a jacket or container for the other fluid, which flows in the passage or passages between the tubes. The motion of each fluid along its system of passages is resisted by fluid friction, and a difference of pressure is therefore needed between the ends of the system to maintain the flow. For the purpose of estimating the heat transferred from the surface of the passages to the fluid and the pressure required to maintain the flow, it is the usual practice to obtain factors or coefficients of heat transfer and friction from published data. It is sometimes possible to obtain from such sources, coefficients applicable to the precise dimensions and shape of the passages and to the flow conditions expected in them; in such cases the friction coefficient and the heat-transfer coefficient are obtainable uniquely for each condition of flow and the relation between the coefficients

is established. More frequently some difference of passage dimension or shape makes published data not directly applicable, and recourse is then had to information of a more general nature, giving average values of the coefficients over a range of Reynolds numbers for passages of certain standard types. In these cases the heat-transfer and friction factors are chosen separately. This method usually yields results of sufficient accuracy for practical engineering purposes, where an error of, say, 10 per cent or more in the estimation of performance is frequently tolerable.

There are cases, however, where greater accuracy is necessary as, for example, when a comparison of the performance of rather similar types of heat interchanger is required and the difference between them is small. In certain fields, too, there is a lack of accurate information. One such field is that of flow in small passages, particularly in the range of Reynolds numbers corresponding to flow of the transitional kind between fully turbulent and fully laminar, where the nature of the flow in a passage is dependent on the degree of turbulence, vorticity or other disturbance introduced at entry to the passage, and maintained within the passage on account of its shape, or because of surface roughness possibly introduced intentionally for this purpose.

1.2. Turbulence and Roughness

The initial turbulence engendered in a smooth passage by the entry conditions may increase or decrease as flow proceeds along the passage, according as the flow is greater or less than that corresponding to the critical range of Reynolds number. The degree and scale of turbulence that is maintained depends also on the physical roughness of the surface, such as is usually represented by a friction factor and measured by the rate of pressure drop along the passage; in general, the greater the roughness, the more readily is turbulence maintained. The apparent roughness, as distinct from the physical roughness, of a surface may be increased by various means, which result in the introduction of additional turbulence into the fluid flow. This turbulence is usually the result of the interaction of vortices arising from the configuration of the passage (*e.g.*, because of its shape or curvature) or from partial obstruction to the flow, and

* A condensed version of a thesis for a London University Ph.D. degree.

is invariably accompanied by an increased rate of pressure drop. So, pressure drop, which is a measure of the roughness, may also be interpreted as a measure of the turbulence.

1.3. Turbulence and Heat Transfer

When a difference of temperature exists between the walls of a passage and the fluid flowing in it, the degree of turbulence maintained in the fluid is also associated with the rate of interchange of heat between the fluid and the walls, which is usually expressed by the coefficient of heat transfer. Any increase of turbulence enforced by the configuration of the passage or otherwise, therefore may result, not only in a greater pressure drop along its length, but also in a greater rate of convection of heat between the walls and the fluid. Since, in those parts of the transitional range approaching the laminar flow region, considerable control of the degree of turbulence and of heat transfer may be exerted by increasing the apparent roughness, it is essential, when estimating the performance of a heat interchanger operating with fluid flows in this range, that the appropriate rate of heat transfer and the friction factor to be associated with it are determined for identical conditions, if any reasonable degree of accuracy is to be achieved.

1.4. The Relation between Friction and Heat Transfer

For conditions of fully turbulent or laminar flow, the pioneer work of Reynolds, Taylor and Prandtl has shown that, because of its identical mechanism, the transference of friction effects and of temperature effects from a passage wall into the fluid stream are related quantitatively. Von Kármán's extension of this theorem for the case of turbulent flow, introducing a 'buffer layer' of intermediate characteristics between the laminar boundary and main fluid flows, has resulted in a refinement of the theoretical relation between friction and heat transfer which gives good correlation with experimentally determined values when the physical properties of the fluid are taken into account. It may be assumed in the absence of definite information about flow in the transition range, that until a state of laminar flow is approached the relation between friction and heat transfer in this range is similar to that in the turbulent region. This means that for a given rate of heat transfer, a corresponding and limited resistance to flow may be considered as 'useful' friction: any pressure drop in excess of this may be considered as 'parasitic'. The losses that occur at entrance and exit and in the wake of obstructions in a passage, in so far at least as they do not increase the

rate of heat transfer, must be placed in the latter category. Paradoxically, however, some loss of this kind may be unavoidable if a high rate of heat transfer and the flow of heated fluid are to be maintained. The problem of economical heat transfer then becomes one of maintaining a high degree of useful friction with a minimum of unessential excess pressure loss.

1.5. Practical Applications

In certain heat interchangers, such as, for example, radiators and charge coolers for reciprocating engines in aircraft, and in other applications where weight or bulk is a disadvantage, the size of passages for fluid flow is reduced as much as is possible consistent with economical production of the metallic parts and satisfactory performance of the units. At the fluid velocities that are practicable, the flows are frequently in the transition range of Reynolds number, and because of the need in such cases to produce heat interchangers with the best possible performance for a given bulk and weight, the passages must be designed so that as much turbulence as possible is enforced with the minimum of cost in pressure losses. Reliable information of the heat transfer and friction to be expected in these cases for passages of the relevant size and shape is not available in published data and in order to assess the relative merit of various methods of enforcing turbulence it is necessary to augment existing knowledge of the friction and heat-transfer characteristics of these small passages, and to determine the increase of pressure drop that must be associated with the increase of heat transference brought about by artificially induced turbulence.

1.6. Objects of Investigation

This investigation supplies this extension of existing knowledge for the case of air flow in certain small passages of round, hexagonal, rectangular and triangular cross-section and, in particular, relates the improvement of heat transfer to the associated loss of pressure when, in the transitional flow range, turbulent flow is induced in an otherwise smooth passage by means of waves or bulges along its length.

It is also established that, provided the entry conditions are not materially changed, the flow conditions in the passages in the transition range are repeatable and not unpredictable nor unstable.

It is suggested that the influence of entry conditions and the distance between bulges on the heat-transfer and pressure-drop characteristics might be the subject of a further investigation.

SECTION II

2.0. THEORETICAL ANALYSIS

As a preliminary to attempting to analyse into its components the pressure difference existing between the ends of a heated passage through which a fluid is flowing, it is essential to consider the possible changes or losses of

energy that may occur in the stream. In general, except in special cases as, for example, in fully established isothermal laminar flow, the fluid motion is so complex that several simplifying assumptions must be made before the problem of analysis becomes at all tractable. In

order to limit the variables, the case of air will be considered, and the assumption will first be made that it follows the usual 'laws' of a perfect gas.

With the further assumption of certain idealised conditions of flow, the equations of motion for compressible flow may be solved, but the solutions are not convenient for general use. Because of the relatively low velocities to be considered in the present application and the assumptions that must be made on account of the unknown conditions of flow, little accuracy is lost by ignoring the compressibility of the air and thus further assuming that its density and temperature are unaltered by the small adiabatic changes of pressure and velocity that occur at the entrance and exit of a passage. For simplicity, too, the increase of velocity of the air in passing through the passage is assumed to be proportional to the increase in temperature caused by the heat transfer. The impact of these approximations upon the accuracy of the pressure coefficients is discussed later. Their justification lies in the consistency with which the experimental results are represented, and the facility with which the derived coefficients may be used to estimate, with reasonable accuracy, the performance of heat interchangers of similar form to those used in the experiments.

2.1. Velocity and Temperature Distributions

For the fluids in a heat interchanger, the majority of the quantities and physical properties that are of importance in its performance are variable over any cross-section of a passage, and also along the passage length; there may also be variation between one passage and another. It is, in general, necessary to express all quantities in terms of average values for the cross-section or field under consideration. This usually entails an arbitrary selection of a factor to represent the degree of variation, since the manner of the variation is seldom known precisely. This is especially true of the flow in the transition zone where the indeterminate thickness of the boundary and buffer layers, and the fluctuations of velocity in the latter and in the turbulent parts of the stream with time, all add to the uncertainty of the velocity and temperature distributions across any section.

The average temperature at any cross-section of a passage depends upon the variation of viscosity and turbulence over the section, neither of which are usually known functions. The average temperature over any field will be defined as :

$$T = \frac{\int T' dM}{M} \quad \dots \quad (1)$$

where T' is the local temperature and M is the mass flowing in unit time. The average density ρ over the same field will be derived from the gas law, using this average temperature and the static pressure assumed in the passage. If A_t is the throughway area of the passage, the average velocity is then given by

$$V = \frac{M}{\rho A_t} \quad \dots \quad (2)$$

In a passage of constant area, the product ρV is conveniently constant throughout. Variation of momentum and kinetic energy across a section, which reflect the velocity distribution, may be expressed by stating average values in terms of the average velocity. Thus the average momentum and kinetic energy per unit mass may be written as

$$e'V$$

and

$$e \frac{V^2}{2}$$

respectively. These definitions enable the flow conditions over the whole system of passages in a unit to be dealt with on a statistical basis, the only practicable approach since, with cross flow of the two fluids, the conditions are not the same for all passages of the system. The values of the coefficients e' and e may vary, from unity for a flat velocity profile (as at entry to a passage) to two or more for viscous fluid flow with a steep velocity gradient over a considerable part of the section.

2.2. Heat Transfer and Friction in a Passage

When heat is transferred between an element of passage wall and the fluid flowing in it, the energy balance gives, since the heat is added at substantially constant pressure,

$$\frac{dH}{M} = S dT + eV dV, \quad \dots \quad (3)$$

where H is the heat transferred in unit time and S is the average specific heat (at constant pressure).

When H and the kinetic energy term are expressed in consistent units, the latter is relatively small and can be ignored where only differences of energy are required. Thus for the heat balance it can be assumed that, for the whole unit,

$$H = MS \Delta T, \quad \dots \quad (4)$$

where ΔT is the total temperature rise.

If a difference of temperature δT exists between the element of passage wall and the fluid at an average temperature T , the local rate of heat transference may be expressed by the non-dimensional heat-transfer coefficient k_H , defined in any consistent system of units, by the relation :

$$H = \rho V S k_H A_a \delta T \quad \dots \quad (5)$$

where A_a is the effective surface area.

The average value of k_H for a passage or system of passages is similarly defined by replacing the local temperature difference δT by the mean effective difference for the passage or system.

If A_t is the throughway area, and k_F the average non-dimensional coefficient of friction for a passage, the pressure drop F in the passage due to friction may be expressed in any consistent system of units as :

$$F = \rho V^2 k_F \frac{A_a}{A_t} \quad \dots \quad (6)$$

or, if L is the passage length and D the hydraulic diameter,

$$F = \rho V^2 k_F \frac{4L}{D} \quad \dots \quad (7)$$

In what follows, k_F will be taken to represent the useful friction, that is, the skin friction that corresponds to the transfer of heat from the passage walls.

2.3. The Relation between the Friction and Heat-Transfer Coefficients

In a laminar flow heat and friction are transmitted between the fluid adjacent to the boundary wall and the main body of the fluid by the same molecular motion, and the coefficients k_H and k_F are quantitatively related. By making some simplifying assumptions, the relation between them can be determined approximately.

Thus, the heat H transferred in unit time to an element of fluid of thickness dy is given by

$$\frac{H}{A_a} = -k \frac{dT}{dy}, \quad \dots \quad (8)$$

where k is the coefficient of conductivity of the fluid, and the conduction in the direction of flow is neglected. Similarly, the shearing stress τ is expressed by

$$\tau = \mu \frac{dV}{dy}, \quad \dots \quad (9)$$

where μ is the coefficient of viscosity.

If these expressions are integrated to give the change of velocity and temperature between the wall and some arbitrary point, then

$$T - T_w = - \int_0^y \frac{H}{A_a k} dy \quad \dots \quad (10)$$

and

$$V - V_w = \int_0^y \frac{\tau}{\mu} dy \quad \dots \quad (11)$$

For air, the Prandtl number $\sigma = S\mu/k$ is practically independent of temperature, and it is also known that the velocity and temperature fields in a laminar flow are very similar, so that representative mean values of T and V (defined in any similar way) may be related to the values of H_w and τ_w at the walls by the expression

$$\frac{T - T_w}{V - V_w} = - \frac{H_w \sigma}{A_a S \tau_w} \quad \dots \quad (12)$$

The velocity at the wall is zero, and if δT is written for $(T_w - T)$

$$\frac{\delta T}{V} = \frac{H_w \sigma}{A_a S \tau_w} \quad \dots \quad (13)$$

From equations (5) and (6), by definition,

$$\frac{H_w}{A_a \rho V S \delta T} = k_H, \quad \dots \quad (14)$$

and

$$\frac{\tau_w}{\rho V^2} = k_F, \quad \dots \quad (15)$$

since

$$FA_t = \tau_w A_a; \quad \dots \quad (16)$$

hence,

$$\frac{k_F}{k_H} = \sigma \quad \dots \quad (17)$$

The ratio between these coefficients for laminar flow may thus be expected to be of the same order as the Prandtl number, *i.e.*, 0.72 for air.

In a turbulent stream, on the other hand, the laminar boundary layer has little effect on the velocity field, but nevertheless has a controlling influence on the heat transfer. The interposition of a buffer layer between the turbulent flow and the laminar layer as postulated by von Kármán leads, with suitable simplifying assumptions, to the following relation between the friction and heat-transfer coefficients for any fluid ;

$$\frac{k_F}{k_H} = 1 + 5 (k_F)^{1/2} [(\sigma - 1) + \log_e \{1 + \frac{5}{6} (\sigma - 1)\}] \quad \dots \quad (18)$$

This relationship, which is based on Nikuradse's measurements of velocity distribution of fluid in pipes, appears to be well substantiated by experimental results.

It may be noted in passing that the ratio between the coefficients is unity, according to the equations (17) and (18), for both types of flow, if the Prandtl number σ itself is unity.

It may be demonstrated experimentally that flow in the transitional range is composed of a system of eddies or vortices superimposed on a laminar regime. The amount and extent of the vorticity is dependent on the entry conditions, the velocity of flow and the roughness, in its broadest sense, of the walls of the passage. The vorticity may persist along the length of the passage or may increase or decrease according to the relative importance of these factors. Since a considerable length of passage (some sixty to a hundred diameters for the velocities and passages here considered) is necessary for the full establishment of a laminar regime, in any system in which a degree of turbulence exists it is reasonably certain that the establishment of a velocity or temperature distribution corresponding to that in laminar flow will be effectively prevented. Consequently, in transitional flow, the friction and heat-transfer characteristics are likely to resemble those of turbulent flow rather than those of laminar flow. Hence, in what follows, the assumption has been made that the relation between the friction and heat-transfer coefficients in the transitional region is similar to that in turbulent flow. The quantitative error introduced by this assumption for air, even in a case of pure laminar flow is unlikely to exceed about 10 per cent, and because no laminar regime can be established while any turbulence exists the error will be appreciably less than this for the cases under consideration.

Therefore, the expression for the ratio k_F/k_H deduced by von Kármán for turbulent flow, viz., the above equation (18),

$$\frac{k_F}{k_H} = 1 + 5 (k_F)^{1/2} [(\sigma - 1) + \log_e \{1 + \frac{5}{8} (\sigma - 1)\}]$$

will be taken to apply over the whole range of flows covered by the following work.

In addition to the pressure required to overcome the friction of the flow, there are a number of energy changes that occur in the stream which result in pressure losses. Losses occur at entrance and exit and wherever turbulence and vortices are produced by discontinuities of surface or by other forms of apparent roughness. Pressure is also needed to cause any acceleration of flow.

2.4. Effect of Contraction at Entry

The reduction of pressure of a fluid entering a passage is due in part to the increase of velocity at the sudden contraction, and in part also to the loss caused by any breakaway of the flow at the edges of the entry. This loss is small for smooth, rounded or tapered, converging entries, where the favourable pressure gradient assists in maintaining laminar conditions near the surface. Any breakaway tends to initiate turbulence, which in addition to causing a reduction of pressure, increases both the friction and the rate of heat transfer. Entry shape may thus exert an appreciable influence on the flow conditions in a passage near the entry.

The pressure loss due to the turbulence at a contraction may be expressed as $K_c \frac{1}{2} \rho V^2$ where K_c is a non-dimensional coefficient depending on the contraction ratio and the Reynolds number of the flow. The quantities ρ and V are here local mean values.

Suppose fluid to be flowing from a duct of area A_d into a system of tubular passages of total area A_t . If the static pressure is denoted by p , average velocity by V , and suffixes d and t refer to conditions in the duct and tubes respectively, then with the assumption of incompressible flow, the application of Bernoulli's equation to the flow at the entrance gives :

$$p_d - p_t = \frac{1}{2} \rho e_t V_t^2 - \frac{1}{2} \rho e_d V_d^2 + K_c \frac{1}{2} \rho V_t^2, \quad \dots \quad (19)$$

where e_t and e_d are factors to take account of the variation of velocity across the sections, and K_c also is an average value for the system of passages.

Since for continuity, $\rho V_t A_t = \rho V_d A_d$, this becomes

$$p_d - p_t = \frac{1}{2} \rho V_t^2 \left\{ e_t - e_d \left(\frac{A_t}{A_d} \right)^2 + K_c \right\}, \quad \dots \quad (20)$$

giving the change of static pressure occurring at the entrance face.

2.5. Effect of Expansion at Exit

Similarly, a fluid experiences a pressure loss in turbulence produced in the expansion at exit from a passage. Except in so far as it may affect the velocity distribution

upstream, the turbulence increases neither the friction nor the heat transfer, as it occurs outside the passage and is completely lost to the system. The loss is minimised when the expansion is gradual and breakaway does not occur. For a sudden expansion the loss is usually taken as

$$\frac{1}{2} \rho (\text{relative velocity})^2.$$

For a more gradual expansion, the more convenient form $K_e \frac{1}{2} \rho V^2$ may be taken, where ρ and V are again local mean values and where K_e is a factor depending on the exit shape and Reynolds number.

By the application of Bernoulli's equation to the flow, and if the suffix h is used to denote conditions in the fluid at exit, the pressure difference between the duct of area A_d and the passages of area A_t becomes :

$$p_{dh} - p_{th} = \frac{1}{2} \rho e_{th} V_{th}^2 - \frac{1}{2} \rho e_{dh} V_{dh}^2 - K_e \frac{1}{2} \rho V_{th}^2, \quad (21)$$

or by the use of the continuity relation

$$\rho_h V_{th} A_t = \rho_h V_{dh} A_d, \quad \dots \quad (22)$$

$$p_{dh} - p_{th} = \frac{1}{2} \rho_h V_{th}^2 \left\{ e_{th} - e_{dh} \left(\frac{A_t}{A_d} \right)^2 - K_e \right\}, \quad (23)$$

where all the quantities again denote average values for the system of passages.

2.6. The Net End Effect

By subtracting equations (20) and (23), and using the condition for continuity of flow and constant cross-section,

$$\rho_h V_{th} = \rho V_t, \quad \dots \quad (24)$$

the net difference between the pressure drop in the duct and that which exists between the ends of the passages is found to be :

$$(p_d - p_{dh}) - (p_t - p_{th}) = \frac{1}{2} \rho V_t^2 \left[\left\{ K_c - e_d \left(\frac{A_t}{A_d} \right)^2 + e_t \right\} + \frac{V_{th}}{V_t} \left\{ K_e + e_{dh} \left(\frac{A_t}{A_d} \right)^2 - e_{th} \right\} \right]. \quad \dots \quad (25)$$

This expression, in addition to its obvious dependence upon velocity and throughway/frontal-area ratio, may also vary to some extent with degree of heat transfer and length of passage, since these may influence the velocity distribution and thus the values of the various coefficients. Neither of these effects is likely to be very great, however, in the case of air.

2.7. Pressure Loss due to Apparent Roughness

When flow in a passage is disturbed by changes of section, by projections into the passage, by changes of direction or other causes, the resulting turbulence, which may increase both the apparent friction and the heat transfer, is accompanied by a reduction of pressure along the passage. This is in part the result of an increase in local velocities and therefore of the shearing forces, but is a measure also of the energy dissipated in the vortices

arising from the disturbances. Any increase in heat transfer is related to the increase in local velocities and to the rearrangement of the temperature field. The ideal to be achieved in introducing such forced turbulence is to attain as nearly as possible, throughout the length of the passage, and without causing excessive losses, the kind of uniform velocity and temperature fields that are favourable to high rates of heat transfer, such as those existing near the entry. This may be attempted, for example, by introducing into the passage a series of bulges, that is, sudden expansions followed by sudden contractions. The energy losses accompanying such changes of section may, however, in extreme cases be disproportionate to the improvement in heat transfer. In cases where such enforced turbulence is introduced, the coefficient of heat transfer may be regarded as a measure of the useful turbulence; pressure losses in excess of the corresponding skin friction may be expressed for each disturbance as $C \frac{1}{2} \rho V^2$, where ρ and V are local mean values. The coefficient C depends upon the Reynolds number of the flow and upon the form of artificial roughness. For N such disturbances in a passage of uniform cross-section—for which ρV is a constant—the total loss may be written as

$$\frac{1}{2} \rho V_t^2 N C \frac{V_m}{V_t}, \quad \dots \quad (26)$$

where V_m is the average velocity for the N disturbances.

2.8. Pressure Loss in the Passages

With the symbols previously used, the momentum equation for the flow in a system of passages of uniform section is :

$$p_t - p_{th} = e_{th}' \rho_n V_{th}^2 - e_t' \rho V_t^2 + F + \frac{1}{2} \rho V_t^2 N C \frac{V_m}{V_t}, \quad (27)$$

where e_{th}' and e_t' are factors taking account of the variations in momentum across the sections, and F is the pressure required to overcome the skin friction. As in equation (7)

$$F = \frac{1}{2} \rho V_t^2 \frac{8L}{D} k_F \frac{V_m}{V_t}, \quad \dots \quad (28)$$

where V_m is again the relevant average velocity for the passages. The expression $\frac{8L}{D} k_F$ will be replaced by C_{pf} , the coefficient of pressure drop due to friction in the passages.

With the condition of continuity in the passages,

$$\rho_n V_{th} = \rho V_t, \quad \dots \quad (29)$$

equation (27) becomes :

$$p_t - p_{th} = \frac{1}{2} \rho V_t^2 \left\{ C_{pf} \frac{V_m}{V_t} + N C \frac{V_m}{V_t} - 2e_t' + 2e_{th}' \frac{V_{th}}{V_t} \right\}, \quad (30)$$

and, by addition, equation (25),

$$(p_a - p_{ah}) - (p_t - p_{th}) = \frac{1}{2} \rho V_t^2 \left[\left\{ K_c - e_a \left(\frac{A_t}{A_d} \right)^2 + e_t \right\} + \frac{V_{th}}{V_t} \left\{ K_e + e_{ah} \left(\frac{A_t}{A_d} \right)^2 - e_{th} \right\} \right],$$

then gives for the pressure drop measured in the duct :

$$p_a - p_{ah} = \frac{1}{2} \rho V_t^2 \left[\left(\frac{V_{th}}{V_t} - 1 \right) \left\{ 1 + \left(\frac{A_t}{A_d} \right)^2 \right\} + \left\{ C_{pf} \frac{V_m}{V_t} + N C \frac{V_m}{V_t} \right\} + \left\{ K_c - (e_a - 1) \left(\frac{A_t}{A_d} \right)^2 - (2e_t' - e_t - 1) \right\} + \frac{V_{th}}{V_t} \left\{ K_e + (e_{ah} - 1) \left(\frac{A_t}{A_d} \right)^2 + (2e_{th}' - e_{th} - 1) \right\} \right]. \quad \dots \quad (31)$$

The last two terms in the square brackets are seen to contain, for the two end sections, all the arbitrary coefficients of energy loss.

It is reasonable to suppose that the velocity distribution in the passages at the entrance, represented by the coefficients e_t' and e_t , is a flat one and that these coefficients differ very little from unity, so that the expression $(2e_t' - e_t - 1)$ is negligible. The contraction coefficient K_c itself is probably small; with the subtraction of the second expression $(e_a - 1) \left(\frac{A_t}{A_d} \right)^2$, the whole term is considered to be negligible in relation to the other terms and has therefore been omitted.

The term containing K_e includes other small expressions depending on the throughway/frontal-area ratio and the velocity distributions in the passages and duct at the exit end. These may be considered to be included in an 'end-loss' coefficient λ , such that

$$\lambda = K_e + (e_{ah} - 1) \left(\frac{A_t}{A_d} \right)^2 + (2e_{th}' - e_{th} - 1). \quad (32)$$

It should be noted that this term will attract to itself any small remainder in the preceding term that has been ignored.

When this coefficient is included, the expression

$$p_a - p_{ah} = \frac{1}{2} \rho V_t^2 \left[\left(\frac{V_{th}}{V_t} - 1 \right) \left\{ 1 + \left(\frac{A_t}{A_d} \right)^2 \right\} + \left(C_{pf} \frac{V_m}{V_t} + N C \frac{V_m}{V_t} \right) + \lambda \frac{V_{th}}{V_t} \right] \quad \dots \quad (33)$$

represents a rational form of the pressure difference measured in the duct.

It remains to assess the values of the velocity ratios V_{th}/V_t and V_m/V_t which depend on the change of temperature and pressure in the passages. It will be convenient and sufficiently accurate (assuming that the interruptions are symmetrically disposed with respect to

the ends) to take the same effective average velocity V_m for the skin friction and turbulence loss terms. If this is assumed to be equal to the arithmetic mean of the velocities at the ends (which involves very little error) then, approximately,

$$\frac{V_{ih}}{V_t} = 1 + \frac{\Delta T}{T} + \frac{\Delta p}{p_{ah}} \dots \dots \dots (34)$$

and

$$\frac{V_m}{V_t} = 1 + \frac{1}{2} \frac{\Delta T}{T} + \frac{1}{2} \frac{\Delta p}{p_{ah}}, \dots \dots (35)$$

where T is the absolute temperature of the fluid at entry, and ΔT and Δp are the temperature and pressure changes, respectively, in the passages. If Δp is written for $(p_a - p_{ah})$, equation (33) takes the form :

$$\begin{aligned} \frac{\Delta p}{\frac{1}{2}\rho V_t^2} = & \left[\left\{ \frac{\Delta T}{T} + \frac{\Delta p}{p_{ah}} \right\} \left\{ 1 + \left(\frac{A_t}{A_d} \right)^2 \right\} \right. \\ & + (C_{pf} + NC) \left(1 + \frac{1}{2} \frac{\Delta T}{T} + \frac{1}{2} \frac{\Delta p}{p_{ah}} \right) \\ & \left. + \lambda \left(1 + \frac{\Delta T}{T} + \frac{\Delta p}{p_{ah}} \right) \right] \dots \dots \dots (36) \end{aligned}$$

or the expression for the pressure drop is :

$$\begin{aligned} \frac{\Delta p}{\frac{1}{2}\rho V_t^2} = & \frac{\left[\frac{\Delta T}{T} \left\{ 1 + \left(\frac{A_t}{A_d} \right)^2 \right\} + (C_{pf} + NC) \left(1 + \frac{1}{2} \frac{\Delta T}{T} \right) + \lambda \left(1 + \frac{\Delta T}{T} \right) \right]}{1 - \frac{\frac{1}{2}\rho V_t^2}{p_{ah}} \left[\left\{ 1 + \left(\frac{A_t}{A_d} \right)^2 \right\} + \frac{1}{2} C_{pf} + \frac{1}{2} NC + \lambda \right]} \dots \dots \dots (37) \end{aligned}$$

This expression can be used where the pressure drop is an appreciable part of the static pressure. If, however, the final assumption can be made that the velocity in the passages is proportional to the temperature (thus ignoring the relatively small changes of pressure) the convenient approximate value :

$$\begin{aligned} \Delta p = \frac{1}{2}\rho V_t^2 & \left[\frac{\Delta T}{T} \left\{ 1 + \left(\frac{A_t}{A_d} \right)^2 \right\} + C_{pf} \left(1 + \frac{1}{2} \frac{\Delta T}{T} \right) \right. \\ & \left. + NC \left(1 + \frac{1}{2} \frac{\Delta T}{T} \right) + \lambda \left(1 + \frac{\Delta T}{T} \right) \right] \dots (38) \end{aligned}$$

is obtained for the rational form of the pressure drop.

3.0. EXPERIMENTAL WORK

The experimental work for the simultaneous measurement of the heat transfer and air pressure loss in small passages was carried out at the Royal Aircraft Establishment, Farnborough, during the years 1937-44 on a number of assemblies of tubes that were typical of or feasible for aero-engine heat interchangers, in which cooling air flows in one group of passages. The airflow and the air pressure drop in these passages together

This is the form that has been used in the analysis and presentation of the following experimental results. Because of the uncertainty about the conditions of flow, and the many assumptions that must be made, it is considered that a more precise analysis is not justified. It was in fact found possible to represent the experimental results with satisfactory accuracy by means of the simplified equation (38), and although rather better correlation was obtained by more complex methods, the accuracy gained did not merit the additional complication involved in using them.

2.9. Coefficients of Pressure Drop

The coefficient λ contains small components that may vary with the degree of heat transfer that takes place ; similarly C the coefficient for the turbulence losses may vary with local temperature conditions. It is, therefore, necessary to distinguish between the values of these coefficients for cold conditions and for conditions of heat transfer. Suffixes x and o will be used for the hot and cold conditions respectively.

The pressure difference $p_a - p_{ah}$ may also conveniently be expressed as a coefficient of the dynamic pressure $\frac{1}{2}\rho V_t^2$ at the tube entrance. Thus if

$$\frac{p_a - p_{ah}}{\frac{1}{2}\rho V_t^2} = C_{px} \text{ or } C_{po} \dots \dots (39)$$

for the hot or cold conditions respectively then the coefficients of pressure loss are :

$$\begin{aligned} C_{px} = & \frac{\Delta T}{T} \left\{ 1 + \left(\frac{A_t}{A_d} \right)^2 \right\} + C_{pf} \left(1 + \frac{1}{2} \frac{\Delta T}{T} \right) \\ & + NC_x \left(1 + \frac{1}{2} \frac{\Delta T}{T} \right) + \lambda_x \left(1 + \frac{\Delta T}{T} \right) \dots (40) \end{aligned}$$

and

$$C_{po} = C_{pf} + NC_o + \lambda_o \dots \dots (41)$$

The validity of the assumptions made can be checked by a comparison of the values of λ_o and C_o with the values of λ_x and C_x obtained experimentally with different rates of heat transfer. Coincidence of the respective values would indicate an approach to that Utopia of the theorist where the relevant natural conditions are all satisfactorily represented.

SECTION III

determine, for the heat dissipation duty, the price to be paid in cooling drag of the aircraft installation. Since this is of primary importance it was natural that the investigation was directed towards obtaining information for the cooling air passages of these units, and that the passages chosen for the investigation were those considered suitable in size and form for this airflow.

The tubes were assembled into units suitable either for radiators or charge coolers ; in the experiments, air was

DETAILS OF PASSAGES

Unit No.	Nominal passage shape			Pitch	Throughway Area Ratio	End Shape	Bulges or Waves
	Section	Height or Diameter	Length				
1	Triangular	0.1 in.	3.6 in.	Wide	0.464	Rounded	Straight
2	Triangular	0.1 in.	6 in.	Wide	0.440	Rounded	Straight
3	Triangular	0.1 in.	6 in.	Wide	0.454	Sharp	Straight
4	Triangular	0.1 in.	6 in.	Wide	0.467	Rounded	22 Waves
5	Triangular	0.1 in.	6 in.	Wide	0.474	Sharp	22 Waves
6	Triangular	0.1 in.	6 in.	Close	0.650	Sharp	22 Waves
7	Triangular	0.1 in.	6 in.	Close	0.698	Sharp	Straight
8	Round	5 mm	140 mm	Close	0.570	Sharp	Straight
9	Round	5 mm	140 mm	Close	0.562	Sharp	8 Waves
10	Hexagonal	5 mm	140 mm	Close	0.655	Sharp	Straight
11	Hexagonal	5 mm	240 mm	Close	0.638	Sharp	3 Bulges
12	Hexagonal	5 mm	320 mm	Close	0.627	Sharp	3 Bulges
13	Hexagonal	5 mm	360 mm	Close	0.621	Sharp	3 Bulges
14	Hexagonal	7 mm	320 mm	Close	0.700	Sharp	2 Bulges
15	Hexagonal	7 mm	320 mm	Close	0.681	Sharp	2 Bulges
16	Hexagonal	7 mm	320 mm	Very Close	0.714	Sharp	2 Bulges
17	Hexagonal	5 mm	300 mm	Close	0.705	Sharp	37 Bulges
18	Hexagonal	5 mm	300 mm	Wide	0.381	Sharp	Straight
19	Rectangular	2.6 mm	Outside 5 mm	Hexagonal	0.481	—	22 Rows
20	Square	5 mm	300 mm	Close	0.667	Sharp	24 Bulges
21	Square	10 mm	316 mm	Close	0.757	Sharp	24 Bulges

used as the cooling medium in one set of passages and heat was supplied to these by hot water flowing in the alternative passages.

3.1. Types of Passage

Of the twenty-one sets of passages examined, and for which details are shown above, twenty were of tubular form of triangular, square, hexagonal or round cross-sections. The other set consisted of the passages outside a block of hexagonal tubes; in these passages the air repeatedly divided and rejoined the neighbouring stream as it flowed around each tube.

Seven of the tubular types of passage were of triangular cross-section; of these, four were smooth and straight except for the end expansions, and three were waved in the direction of airflow. Two types of passage were round in section, one smooth and straight, the other waved. Of the nine types of passage of hexagonal cross-section, two were smooth and straight; six others (three of each of two sizes) were smooth except for two or three small bulges, and one was bulged alternately on two opposite flats to an approximate wave form. The two types of square passage, which were of different size, both had numerous bulges. The tubes were of various lengths and hydraulic diameters and differed also in the amount of their end expansions.

The units, although carefully assembled and as far as possible free from major imperfections, were nevertheless intended to be representative of good production workmanship. For this reason a few tubes near the outside

of some of the assemblies, which had inadvertently become blocked with solder during construction of the units, were allowed to remain in this condition. The thickness of the soldered edges of the tubes was not controlled, although one unit was rejected on account of excessive thickening of the entry edges with solder. A number of 'half-tubes' were used to complete some of the assemblies. These have been assumed to be fully effective, as this assumption was estimated to lead to a very close approximation to their influence on the performance of the complete unit.

The precise form and dimensions of each of the types of passage and the experimental units are described in Appendix II and shown in the Tables and Figures there enumerated. A list of the units is also given in Appendix I.

3.2. Range of Investigation

The characteristics of each unit were obtained experimentally for a number of air flows up to the maximum capacity of the equipment. In most cases this allowed an air velocity of 200 ft/sec in the passages and a maximum Reynolds number of more than 20,000, except in the case of the smaller passages and those of high resistance, where the highest velocity and Reynolds number obtainable were about 150 ft/sec and 6,000 respectively. For the smaller passages Reynolds numbers down to 2,000 were used.

The size of the passages varied from a nominal height of 0.1 inch and an hydraulic diameter of rather under 0.007 ft for the triangular passages, to a nominal height

of 10 mm and an hydraulic diameter of about 0.03 ft for the larger square passages. The hexagonal and round passages were of intermediate size ; nominally 5 mm and 7 mm tubes, their cross-sections had hydraulic diameters of about 0.015 and 0.022 ft respectively. These tubes are smaller than those for which heat-transfer and pressure-loss information is usually quoted in published data. The form of some of them is also unusual.

The length/diameter ratios of the tubes ranged from about 30 to about 65 including the entrance lengths, and the throughway/frontal-area ratio or 'transparency' from about 0.76 for the larger square tubes and 0.7 for the close spaced hexagonal tubes to about 0.38 for the wide spaced hexagonal tubes.

Two methods of inducing turbulence in tubes were investigated. The one consisted of bulging the tube at intervals, giving a sudden local area increase of from 30 to 50 per cent : the other of waving the passage with a wavelength of about 3 tube diameters and a semi-amplitude of about 10 per cent of the passage diameter. Some effects of passage entrance shape were also noted. Full particulars of the passage shapes are given in Appendix II.

The average temperature of the tube walls in the experiments was about 95 deg C, and the average air temperature about 20 deg C.

3.3. Experimental Plant

Each experimental unit, which had a frontal area of approximately 6 inches square, was inserted in a horizontal air duct of the same size, having a flared entry. The unit was attached to flanges on the duct by means of a pair of wooden frames carefully trimmed internally to the shape of unit and duct, so that there was no abrupt step at the face of the unit.

Air from the laboratory was drawn through the duct and unit by a fan, belt driven from a variable speed motor. The air was discharged outside the building, giving steady temperature conditions in the laboratory and at the duct entry. A variable orifice on the fan discharge, together with the speed control enabled any desired airflow to be obtained.

Heat was supplied to the unit by hot water passed in an upwards direction through it. The water was circulated from a sump by a centrifugal pump through a number of electrical heaters, and thence to a gravity tank where any entrained air was released. The water supply to the units was from this tank under approximately 15 ft head, the flow being controlled by a valve on the outlet side. An overflow pipe from the gravity tank returned the surplus water direct to the sump and control of the overflow gave a fine regulation of water flow through the unit. By this system the unit was supplied with a full flow of hot water under only a small pressure and free from entrained air. Water discharged from the top of the unit was led to a weighing tank and

thence returned to the sump. In the weighing tank 150 lb were collected in a time registered by stopwatch.

Static pressure at the walls of the air duct was measured by a pressure ring around the duct at a distance of 18 inches behind the flared entry and 18 inches in front of the face of the unit. Together with a second pressure ring 18 inches behind the unit, this ring enabled the static pressure drop through the unit to be measured. Pressure measurements from the first ring, after calibration by a pitot traverse, also served as a means of measuring airflow. For the later experiments a number of calibrated orifices in a box fitted over the duct entry was used for the measurement of airflow, as this arrangement permitted small airflows to be measured with greater accuracy.

Air temperatures were measured by mercury-in-glass thermometers inserted into the duct 9 inches downstream from each pressure ring. Mercury-in-glass thermometers in pockets were used to measure the temperature of the water entering and leaving the unit. The pockets were designed to give average water temperatures.

3.4. Experimental Method

For each test unit the heat dissipation and air pressure drop were measured at each of a number of air and water flow rates, after temperatures had become stable. Several readings of each instrument were taken during the time occupied by three weighings and average values of these readings were adopted for the analysis. The air pressure drop for the cold unit was also measured for the experimental range of air flow before and after the heat dissipation experiments.

All the instruments were calibrated, and it was the aim to obtain all measured quantities with an error not exceeding ± 1 per cent. Corrections were applied to the readings of the spirit manometers for variation of atmospheric temperature ; and in measuring the air pressure drop through the units, allowance was made for the resistance offered by the thermometer in the entry duct and for the friction of the duct between measuring points. It was found that atmospheric dust tended to collect at the entrances to the passages and increase the resistance to flow. Throughout the tests precautions were taken therefore to ensure that the edges of the passages facing upstream were kept clean and free from dust.

Because of the difference of temperature field in the air duct behind the unit for the various conditions of heat flow, the measurements of air temperature at this position did not give dependable average values. The heat quantity was therefore obtained from the more reliable water measurements. The air temperature measurements were used only as an approximate check on the heat balance. The air temperature rise used in the analysis was computed from the heat transfer and the known airflow. Corrections were made for radiation losses.

SECTION IV

4.0. ANALYSIS OF RESULTS

In analysing the results the assumption has been made that the heat transference occurs in cross flow without mixing of either fluid. This is very nearly true for the flow (usually air) inside the tubes of the units, and probably nearly true also for the flow (usually water) outside the tubes. Because of their construction, in the case of the units with triangular passages it is very nearly true for both fluids. The effective temperature difference for this kind of flow can—as shown by Nusselt—be expressed as a function of the temperature changes in the two fluids and of the extreme temperature difference between them at entry.

Thus, if E is the extreme temperature difference and if $\Delta T_a = \eta_a E$ and $\Delta T_b = \eta_b E$ are the temperature changes of the two fluids, and ζE is the effective temperature difference, then ζ is a function of η_a and η_b only. A chart showing the values of ζ for given values of η_a and η_b is appended as Fig. 1. This relation has been used to determine from the experimental results the average effective overall heat-transfer coefficient.

4.1. Determination of Heat-Transfer Coefficients

The heat quantity per degree of extreme temperature difference, H/E , determined from the experiments, was first faired to eliminate small variations from the intended values of air flow. The quantity $\zeta E/H$ —the resistance to heat transfer—was then plotted against a power function of the reciprocal of the water flow and extrapolated to conditions of infinite waterflow, for which it was assumed the resistance to heat transfer on the water side was negligible, as was also the temperature drop through the thin metal walls. The remaining resistance $\zeta' E'/H'$ is that of the air side and from it the average heat-transfer coefficient k_H has been calculated from the relationship of equation (5) in the form

$$\frac{H'}{\zeta' E'} = \frac{M}{A_t} S k_H A_a, \quad \dots \quad (42)$$

where W is the airflow and A_t the throughway area for air. The accented symbols here refer to conditions of infinite waterflow.

The curves of heat-transfer coefficient, plotted against the Reynolds number for the air at the temperature of entrance to the passages are given in Fig. 3.

In computing the values of k_H for the triangular passages the efficiency of the secondary surface formed by the corrugated sheets has been treated as unity. The actual value in the cases of greatest heat flow is seldom less than 99 per cent, and the analysis is not appreciably affected by treating the fin surfaces as fully effective. There are no secondary surfaces in any of the other passages.

4.2. Determination of Coefficients of Pressure Drop

The difference of static pressure between the two measuring points in the experimental duct has been expressed, for the conditions both with and without heat transfer, as a coefficient of $\frac{1}{2} \rho V_t^2$ the dynamic head of the cold air at entrance to the passages. The coefficients have been analysed into their components by deducting from them those parts representing the increase of momentum and the skin friction, and from the remainder deducing, in the case of the straight smooth passages, the 'end-loss' coefficient. For the waved and bulged passages values for the 'end loss' have been assumed and after deduction of the corresponding quantity from the pressure-drop coefficient, the remaining pressure has been attributed to the ineffectual turbulence caused by the waves and bulges.

The values of C_{p0} , the coefficient of pressure drop for the cold units, have been plotted in Appendix V. They are given merely for comparison with other results. They cannot be used directly in deducing the pressure drop when heat transfer is taking place.

4.3. Determination of Friction Coefficients

If the relation between the friction and heat-transfer coefficients is assumed to be as deduced by von Kármán, viz., as in equation (18)

$$\frac{k_F}{k_H} = 1 + 5 (k_F)^{1/2} [(\sigma - 1) + \log_e \{1 + \frac{5}{6} (\sigma - 1)\}],$$

and if σ for air is taken as 0.72, a figure based on physical constants given by Gröber, then k_F can readily be found from

$$\frac{k_F}{k_H} = 1 - 2.729 (k_F)^{1/2}. \quad \dots \quad (43)$$

A curve showing this ratio for a range of values of k_H is given as Fig. 2.

The symbol C_{pf} has been used to denote that part of the coefficient of pressure drop due to skin friction in the cold passages. Then, as in equation (7)

$$C_{pf} = \frac{8L}{D} k_F, \quad \dots \quad (44)$$

where L and D are respectively the length and hydraulic diameter of the passages. For a heated passage with an average velocity greater in the ratio $\left(1 + \frac{1}{2} \frac{\Delta T}{T}\right)$ the corresponding quantity is

$$C_{pf} \left(1 + \frac{1}{2} \frac{\Delta T}{T}\right) \quad \dots \quad (45)$$

where T is the temperature of the air at entrance and ΔT the air temperature rise.

4.4. Determination of End Losses

The small loss due to the contraction at entry has been neglected, and the coefficient λ representing the loss due to expansion at the passage outlet has been found for the straight smooth passages by deducting from the total pressure loss expressed in equation (40) those components due to skin friction, determined as above, and to the increase of momentum for the hot passages.

Thus, the values of λ_o for the cold passages were found from the expression :

$$\lambda_o = C_{po} - C_{pf}, \quad \dots \quad (46)$$

and those of λ_x from

$$\lambda_x = \frac{C_{px} - \frac{\Delta T}{T} \left\{ 1 + \left(\frac{A_t}{A_d} \right)^2 \right\} - C_{pf} \left\{ 1 + \frac{1}{2} \frac{\Delta T}{T} \right\}}{\left(1 + \frac{\Delta T}{T} \right)}. \quad (47)$$

The values of λ_x and λ_o for each of the units with straight passages are shown in Appendix III, plotted on a base of Reynolds number for the air at the temperature of entry of the passages. The values of λ_x are compared in Fig. 4.

4.5. Determination of Losses due to Waving or Bulging

For those passages in which the turbulence was increased by waving or bulging, that part of the pressure loss required to produce the turbulence not usefully employed in increasing the heat transfer can be estimated only when the other losses, including those due to the end expansion, have been evaluated. It was therefore necessary, in analysing the losses in these passages to assume that the values of λ obtained from the analyses of the losses in the straight passages were applicable to the more turbulent flow in the artificially roughened passages.

5.0. DISCUSSION OF RESULTS

In order to fulfil the primary intention of providing fundamental information on the characteristics of certain forms of passages that might be used for heat interchangers, the experimental units chosen for this investigation included a number of variations from which it was hoped to discover the more important facts concerning the influence of such details as passage shape and size, entry shape, tube length and tube spacing as well as the relative merit of bulges and waves in creating useful turbulence, and the desirable or economical limit to such enforced turbulence at low Reynolds numbers.

With the variations included in the group of Units Nos. 1 to 7, for example, it was the intention to learn for triangular passages, the effect of passage spacing and entrance shape. This objective enquiry was limited to

By deducting these losses and the pressure drops due to skin friction and increase of momentum as before, the coefficients C_o and C_x for the ineffectual turbulence or shock losses were obtained from the expressions

$$C_o = \frac{C_{po} - C_{pf} - \lambda_o}{N} \quad \dots \quad (48)$$

for the cold passages, and from

$$C_x = \frac{C_{px} - \frac{\Delta T}{T} \left\{ 1 + \left(\frac{A_t}{A_d} \right)^2 \right\} - C_{pf} \left\{ 1 + \frac{1}{2} \frac{\Delta T}{T} \right\} - \lambda_x \left\{ 1 + \frac{\Delta T}{T} \right\}}{N \left(1 + \frac{1}{2} \frac{\Delta T}{T} \right)} \quad \dots \quad (49)$$

for the heated passages, where N is the number of sources of loss in each passage.

It was considered reasonable that a loss would occur at each abrupt change of section or of direction of flow. Thus there was assumed to be one source of loss at each small bulge or change of direction and one at each reversal of curvature in a waved passage. The mechanism of turbulence in each of these cases is the same, viz., the interaction of the vortices formed at the change of direction of flow and the interference of the intermingling streams. In some instances, for example for flow outside the hexagonal tubes, the losses are much greater than the losses for the waved tubes, and are doubtless not comparable, but the magnitude of this loss can be regarded as a measure of the shock loss, which it is desirable to avoid in order to obtain heat transfer most economically.

The values of C_x and C_o are plotted against Reynolds number in the curves of Appendix IV. In Fig. 5 the values of C_x obtained for all the cases are shown for comparative purposes.

SECTION V

some extent by the subjective need for information on current designs of aircraft heat interchangers. As a result of this limitation, the range of variation of any of these details was small. The general effect of each of the variations can, however, be observed and quantitative values of the various coefficients can be quoted.

The majority of published data on heat transfer in tubes have been obtained from experiments with tubes larger than those used in this work. Few results are available for tubes smaller than 0.5 inch diameter, and very little information has been published on other than straight tubes of round section, even in the larger sizes.

The results of this experimental work, therefore, extend the available knowledge to include heat-transfer and pressure-drop characteristics of tubes of various forms and of hydraulic diameters down to about 0.08 inch.

5.1. Heat Transfer

The small deviation of the experimental points from the mean lines of resistance to heat flow showed the very consistent instrument indication, even if the absolute accuracy of the readings was not necessarily shown in this way. The scattering of the points was seldom more than ± 2 per cent and on the average was considerably less than this.

For the purpose of comparison, all the curves of heat-transfer coefficient k_H have been reproduced in Fig. 3. These coefficients are representative of the values that can be obtained with passages of the kinds shown in Appendix II, when the 'end effect' with its favourable conditions for heat transfer is included. There is very good agreement between the values of heat-transfer coefficient obtained for all the hexagonal tubes. The progressive deterioration with tube length, and also the effect of the few intermediate bulges in raising the value, is well shown for the 5 mm tubes in Fig. 3.

The average value of the heat-transfer coefficient for the turbulent flow of fluids in round tubes, based on a review* of the large number of published results, is represented very closely by the empirical equation :

$$k_H (\sigma_w)^{2/3} = 0.023 \left(\frac{\rho V D}{\mu_w} \right)^{-0.2}, \quad \dots \quad (50)$$

where the suffix w represents the condition at a film temperature, assumed to be the arithmetic mean between that of the wall and the bulk of the fluid. With the value of $\sigma = 0.733$ for air (as used in this Reference) and μ_w greater by 17.5 per cent than the value at the inlet temperature (an average value estimated for these experiments) the expression for k_H for comparison with the measured values becomes

$$k_H = 0.0292 R^{-0.2} \quad \dots \quad (51)$$

The curve represented by this equation is shown in Fig. 3. It agrees well with other published empirical curves. The values of the friction coefficient derived from it by the use of equation (43) also agree closely with published values for smooth tubes.

For streamline flow, an average* value is approximately

$$k_H (\sigma_w)^{2/3} = 1.5 \left(\frac{D}{L} \right)^{1/3} \left(\frac{\rho V D}{\mu_w} \right)^{-2/3}, \quad (52)$$

or, with the same values as above for σ and μ_w ,

$$k_H = 0.523 R^{2/3} \quad \dots \quad (53)$$

for a length/diameter ratio of 60, a typical value for the experiments. This curve is also shown for comparison in Fig. 3.

It would be reasonable to suppose that the effect of surface roughness would be more pronounced with smaller tubes and consequently that these experiments would show relatively high values of heat-transfer coefficient. It is a little surprising, therefore, to find that,

* *The Principles of Chemical Engineering*, by W. H. Walker, W. K. Lewis, W. H. McAdams and E. R. Gilliland. (McGraw Hill, 1937.)

in general the experimental values are lower for the small tubes, despite the inclusion of the entrance length. The use of the effective temperature chart for cross flow, Fig. 1, gives an effective temperature difference slightly less than the arithmetic mean upon which the majority of published data are based. This fails, therefore, to account for the difference in values. Although it might be expected that the more angular tube sections used in this work would encourage the growth of thicker boundary layers than in round tubes, it is notable that the only unit with straight round tubes should itself show a low value of heat-transfer coefficient and an early deterioration in passing from the turbulent to the transition region.

It can only be concluded that these smaller passages show a marked tendency towards a prolonged transition range, in which the heat dissipation is well below the value for turbulent flow at the same Reynolds number in passages of greater diameter. Certainly for Reynolds numbers less than 10,000, a value below the average is shown for all passages in which turbulence is not artificially induced.

It is also seen by reference to Fig. 3 that the heat-transfer coefficients for the various tube shapes are well correlated in the turbulent region by taking the hydraulic diameter as the representative length for the Reynolds number. In the transition range the value of the coefficient depends to a small extent on the entry conditions, being less for those passages with the smaller throughway/frontal-area ratio, and the rounded entry edges.

With enforced turbulence, values considerably greater than those obtained in smooth tubes may be reached for all Reynolds numbers, but particularly in the transition range. The more severely bulged tubes and the waved round tubes all show values above the average for smooth tubes, and there is no obvious advantage as regards heat transfer, to be claimed for either. For the smaller, triangular passages the waving, although approximately proportionate in respect of wavelength and amplitude to the hydraulic diameter, appears to have relatively less effect in raising the heat-transfer coefficient than in the case of the larger round tubes. The effect of entry conditions can be only transitory in the passages with enforced turbulence, but the same tendencies are apparent as in the case of the smooth tubes. The indications are that the smooth tube length between interruptions or changes of direction is probably the feature that exerts the greatest control over the rate of heat transfer.

The heat-transfer coefficient for the outside surface of the hexagonal tubes is about five times as great as for the other passages, but there is a much greater increase of resistance to flow.

5.2. End-Loss Coefficients

The values of the end-loss coefficients for the straight tubes are plotted together in Fig. 4. It is seen that the values are of the same order for the tubes of all sections, but, in general, larger values are obtained for the greater

end expansions. This variation is not, however, more than a general one. Nor is any consistent variation with tube length apparent. The loss is shown to be at least 0.4 for the majority of the tubes, *i.e.*, nearly one half of the dynamic head is lost due to the sudden enlargement at exit; this is rather more than might have been expected from theoretical considerations, but, as stated previously, the value obtained from the analysis, as it is derived by difference, includes all losses not specifically accounted for and also the effect of all the approximations in the theory. Another rather unexpected result is the tendency for very high values to be deduced for low Reynolds numbers.

The end losses fall very roughly into two groups according to the values of throughway/frontal-area ratio, but end shape appears to influence the loss to a considerable extent. It is perhaps not without significance that the low value obtained with Unit No. 15, in comparison with the 5 mm and the other 7 mm hexagonal tubes, is associated with a small metal thickness at the ends of the tubes where they are attached to one another. The same feature appears to be relevant in the case of the other hexagonal tubes. The same effect is also noticeable in the case of the triangular passages, where the sharp edged ends of the 'b' passages in Unit No. 3 are associated with smaller end losses than the rounded edges of No. 2. The sharp ends of No. 7 are also associated with small losses, although in this case the throughway/frontal-area ratio is greater, and these passages on this account are perhaps more comparable with the 7 mm hexagonal tubes, for which the end losses are, however, still smaller. The contrary effect may be observed, too, in Unit No. 1, for which the well rounded edges have a low loss. It should be noted that, in comparison with No. 1, the edges of units Nos. 2 and 4 were not so well rounded, being rather flattened during manufacture. It can be concluded that either well rounded or tapered exits with thin metal edges offer the least resistance in the form of end loss.

The comparisons between the values of λ_o and λ_w , some of which are given in the diagrams of Appendix III showed, for the most part, good agreement, and this indicates that no major losses influenced by the heating of the air have been neglected. In the majority of cases the curve for the cold condition lay below the curve for λ_w , but as there was no systematic variation of the values of λ_w with air temperature rise, and in some cases, too, the positions of the curves were reversed, this discrepancy would appear to be primarily something more than an effect of temperature. The scatter of the experimental points represented in the worst cases a total variation of less than 5 per cent in the pressure drop. This was greater than the scatter shown in the measurement of pressure in the cold condition, and is therefore probably greater than the experimental error.

These discrepancies are no doubt due to the approximations made in the analysis, and in particular to the assumption of negligible pressure drop in the passages made when estimating the air velocity at exit.

5.3. Losses due to Waving and Bulging

Figure 5 shows all the values of the coefficients of pressure loss due to the bulges and waves plotted on one diagram. It can be seen that the value of the loss for each change of direction is of the same order whether the passages were bulged or waved. This consistency is rather remarkable in view of the great difference in shape of the waves and bulges. The value for the 'wake' losses outside the hexagonal tubes is, however, unexpectedly much higher. This may be accounted for in part by the bad aerodynamic shape of the tubes and the resulting form drag, and in part also by the interference of the intermingling air streams. These losses, about twenty times those for the bulges or waved passages, appear to be out of proportion to the improvement in heat dissipation, but careful design, by taking advantage of the high rate of heat transfer, may nevertheless enable efficient heat interchangers to be made in this form for particular applications.

Leaving these high losses for Unit No. 19 out of consideration, the remaining shock or turbulence losses of Fig. 5 appear to divide into two main groups. This may in fact be largely an effect of Reynolds number, since it would be expected that the large values shown for Units Nos. 9, 17, 20 and 21 would be reduced as the air flow approached nearer the laminar condition. For the more nearly laminar flow in the small triangular passages the loss appears to approach zero for small values of Reynolds number.

In comparing the losses for the larger passages, there is seen to be a slight advantage of the waved form over the more severe bulge, a result which, though not unexpected, is of some importance since the rate of heat transference is very similar.

The scatter of the experimental points represented only about $\pm 2\frac{1}{2}$ per cent of the pressure drop for the whole passage. This scatter and the discrepancies between the values obtained for the coefficients for the hot and the cold conditions, no doubt again reflect the approximations made in the analysis. In this case they would appear to be almost within the limits of experimental error.

5.4. Limitations due to Approximate Method of Analysis

The accuracy of the heat-transfer and pressure measurements in these experiments is believed to be of a high order and, for units of similar construction intended to be used for similar conditions, the coefficients given can be used with confidence to predict performance. In the estimation of the coefficients for the pressure loss due to waving and bulging in those passages for which no comparable straight tube existed it was necessary to assume values for the pressure loss at the ends of the passages. For example, for Units Nos. 4, 5 and 6 where the results of Nos. 2, 3 and 7 were available these were used, and for Unit No. 17, the end losses for No. 10 were available. For No. 20, however, as no comparable straight tube had been examined, the results of No. 10 were again used. Similarly, for No. 21, end losses

deduced from No. 14 were used. Also in deducing end losses for the 5 mm and 7 mm hexagonal tubes a small allowance had to be made for the pressure loss at the two or three bulges. For this purpose the coefficients deduced for No. 20 were employed. If values from other units had been chosen for these purposes, slightly different numerical results would have been obtained: but the order of value of the coefficients would have been unchanged.

Because, however, of the simplifying assumptions made in the analysis some caution must be exercised if it is intended to use the derived quantities in estimating the pressure drop for units of very different length/diameter ratio, or for units operating with considerably greater velocities or temperature difference. For fluids other than air, too, in addition to the adjustment to k_H to take account of the difference of Prandtl number, the

coefficients should be used with caution in the absence of experimental verification that the same values can be assumed.

5.5. Range of Investigation

This investigation could usefully be extended to cover a wider range of Reynolds number for some of the passages. In particular, the experiments for some of the larger and more severely bulged passages were limited by the insensitivity of the earlier measuring equipment at low air speeds and further measurements at low velocities are required to give information about the characteristics of these passages nearer the laminar flow region. Other useful extensions to this work would be an investigation of the influence of entry conditions, and a determination of the effect of varying length of straight tube between bulges.

SECTION VI

6.0. METHOD OF USING EXPERIMENTAL RESULTS

The curves and tables in the Appendices, besides giving information about the characteristics of certain small passages when used as elements in a heat interchanger, present this data in a way that enables the evaluation of the heat transfer and pressure drop for such a heat interchanger to be accomplished in a convenient manner and with good accuracy. With the aid of this data, the estimation of the pressure drop through the passages is simplified in that once the coefficient of heat transfer has been determined no separate assessment of the skin friction coefficient is necessary. A value of the latter, compatible with the rate of heat transfer, is automatically fixed. For end-loss coefficients and other losses due to turbulence, values can be chosen which are representative of the shape of the passages, and the coefficient of pressure drop for any rate of heat interchange is then rapidly calculated as described below.

6.1. Heat Interchange

Suppose that H is the rate of heat interchange between two fluids when the effective temperature difference between them is ζE , where ζ represents the fractional part of the extreme temperature difference, E , between the fluids at entry that is effective in the heat interchange. The value of ζ may be found, for example, from the curves of Fig. 1.

If the thermal resistance of the metal is neglected, then the overall resistance of the interchanger to heat transfer (represented by $\zeta E/H$) may be expressed as the sum of the component resistance of each of the fluids. Thus,

$$\frac{\zeta E}{H} = \frac{1}{A_a \alpha_a} + \frac{1}{B_b \alpha_b}, \quad \dots \quad (54)$$

where A_a and B_b are the effective areas of the fluid swept surfaces, and α_a and α_b are their heat-transfer coefficients.

The values of these coefficients may be found from the relation:

$$\alpha = \rho V S k_H, \quad \dots \quad (55)$$

where the symbols have the meanings previously defined. The value of k_H for air can be obtained from the data of Fig. 3 (or from other published data) for the shape of passage most nearly resembling the shape chosen, and for the appropriate value of the Reynolds number $\rho V D / \mu$. For fluids other than air the value of k_H must, of course, be adjusted for differences in physical characteristics as expressed in the Prandtl number.

6.2. Friction

From the value of k_H determined in this manner the coefficient of friction k_F can be found for any fluid from the relation of equation (18), or in the case of air, from the curve of Fig. 2. The coefficient of pressure drop due to friction is then

$$C_{pf} = \frac{8L}{D} k_F \quad \dots \quad (56)$$

for a passage of length L and hydraulic diameter D .

6.3. Pressure Losses

For the specified Reynolds number and the appropriate passage shape, the values of the end-loss coefficient λ_n and the coefficient C_x for turbulence losses can be taken from Figs. 4 and 5 or the relevant curves of Appendices III and IV. For an initial absolute temperature T and a temperature rise ΔT of the fluid stream, determined from the known heat flow H , the equation

$$\Delta p = \frac{1}{2} \rho V_i^2 \left[\frac{\Delta T}{T} \left\{ 1 + \left(\frac{A_i}{A_d} \right)^2 \right\} + C_{pf} \left(1 + \frac{1}{2} \frac{\Delta T}{T} \right) + N C_x \left(1 + \frac{1}{2} \frac{\Delta T}{T} \right) + \lambda_n \left(1 + \frac{\Delta T}{T} \right) \right] \quad (57)$$

can then be used to give the pressure drop for the unit.

6.4. Typical Values of Coefficients

Although for accurate estimation of performance, precise values of the various coefficients must be chosen, applicable to the passage shape and to the conditions of flow, it may be useful to examine the range of values obtained in the experiments and to obtain some average values that may be used in cases where more exact evaluation is either not justifiable, or impracticable because of lack of detailed information about passage dimensions.

The heat-transfer coefficient for the smooth passages is seen to range from about 0.0025 to 0.0035, with the minimum increased to about 0.003 for those passages of small total length or with a small number of bulges. For the waved and bulged passages the values range from about 0.0035 to 0.005 or more at the low Reynolds numbers. For the outside of the hexagonal tubes the coefficients are about four times the latter values. For

all cases of flow inside the tubes the average value of the ratio k_F/k_H is about 0.85.

The end-loss coefficients range from about 0.3 to 0.5 for the more closely spaced passages, and 0.9 to 2.0 or more for the smaller passages and for those where the throughway/frontal-area ratio is less than 0.5. High values are appropriate to the lower Reynolds numbers.

The losses due to waving and bulging are represented by coefficients varying between 0.004 to 0.02 for the small waved passages, from 0.02 to 0.035 for the larger waved passages and from 0.025 to 0.04 for the severe and closely spaced bulges. For the sinuous path outside the hexagonal tubes the values are about twenty times those for the waved passages for each change of direction.

Thus the range of values of all these coefficients is not large for any one type of passage, and average values should give reasonable results for approximate calculations.

REFERENCES

No.	Author	Title, etc.
1	J. Remfry	Charge cooling with no intermediate fluid ; influence of airflow and pressure drop on passage size and shape, examined in conjunction with results of experiments on corrugated foil matrices. A.R.C. 5717. 1942. (Unpublished.)
2	J. Remfry	Ducted radiators ; performance characteristics of corrugated foil matrices with straight and waved air passages. A.R.C. 6119 1942. (Unpublished.)
3	C. Anderton Brown	Note on ducted radiators ; comparative performance of 'Sinuflo' and straight round tubes. A.R.C. 4157. 1939. (Unpublished.)
4	J. Remfry	Ducted radiators : performance characteristics of 5 mm hexagonal tubes, 140 mm long. R.A.E. Report No. Eng.4118. 1944. (Unpublished.)
5	C. Anderton Brown and J. Remfry ..	Ducted radiators : performance characteristics of 5 mm and 7 mm hexagonal tubes. R.A.E. Report No. E.3679. 1939. (Unpublished.)
6	J. Remfry	Ducted radiators : performance characteristics of wave-bulged 5 mm x 300 mm hexagonal tubes. A.R.C. 5948. 1942.
7	J. Remfry	Charge cooling : heat transfer and pressure drop characteristics of a honeycomb matrix with 5 mm x 300 mm hexagonal tubes at 7.6 mm pitch. R.A.E. Report No. E.4101. 1944. (Unpublished.)
8	J. Remfry	Ducted radiators : performance characteristics of radiator model with 'Gallay' matrix (System E) with airways 5 mm square x 300 mm long. A.R.C. 6118. 1942. (Unpublished.)
9	C. Anderton Brown	Ducted radiators : performance characteristics of radiator model with 'Gallay' matrix (System E). A.R.C. 4632. 1940. (Unpublished.)
10	J. Remfry	Thesis submitted for the Degree of Ph.D. University of London, which can be consulted at the Library, University of London. This Monograph bears the same title as the Thesis but some Appendices have been omitted.

TABLE 1
GENERAL PARTICULARS OF UNITS

Unit No.	Description	Passage Shape	Pitch	End Shape	Bulges or Waves
1	Corrugated-Foil Block 'A' ('a' passages)	Triangular	Wide	Rounded	Straight
2	Corrugated-Foil Block 'D' ('a' passages)	Triangular	Wide	Rounded	Straight
3	Corrugated-Foil Block 'D' ('b' passages)	Triangular	Wide	Sharp	Straight
4	Corrugated-Foil Block 'E' ('a' passages)	Triangular	Wide	Rounded	22 Waves
5	Corrugated-Foil Block 'E' ('b' passages)	Triangular	Wide	Sharp	22 Waves
6	Corrugated-Foil Block 'B' ('b' passages)	Triangular	Close	Sharp	22 Waves
7	Corrugated-Foil Block 'C' ('b' passages)	Triangular	Close	Sharp	Straight
8	5 mm × 140 mm Round Tube Radiator	Round	Close	Sharp	Straight
9	5 mm × 140 mm 'Sinuflo' Tube Radiator	Round	Close	Sharp	8 Waves
10	5 mm × 140 mm R.T.7. Radiator	Hexagonal	Close	Sharp	Straight
11	5 mm × 240 mm R.T.7. Radiator	Hexagonal	Close	Sharp	3 Bulges
12	5 mm × 320 mm R.T.7. Radiator	Hexagonal	Close	Sharp	3 Bulges
13	5 mm × 360 mm R.T.7. Radiator	Hexagonal	Close	Sharp	3 Bulges
14	7 mm × 320 mm R.T.5. Radiator	Hexagonal	Close	Sharp	2 Bulges
15	7 mm × 320 mm R.T.5. Radiator	Hexagonal	Close	Sharp	2 Bulges
16	7 mm × 320 mm R.T.6. Radiator	Hexagonal	Very Close	Sharp	2 Bulges
17	5 mm × 300 mm Wave-bulged Radiator	Hexagonal	Close	Sharp	37 Bulges
18	5 mm × 300 mm Charge Cooler	Hexagonal	Wide	Sharp	Straight
19	Outside 5 mm × 300 mm Tubes	Rectangular	—	—	22 Rows
20	5 mm × 300 mm 'Gallay' System E5	Square	Close	Sharp	24 Bulges
21	10 mm × 316 mm 'Gallay' System E	Square	Close	Sharp	24 Bulges

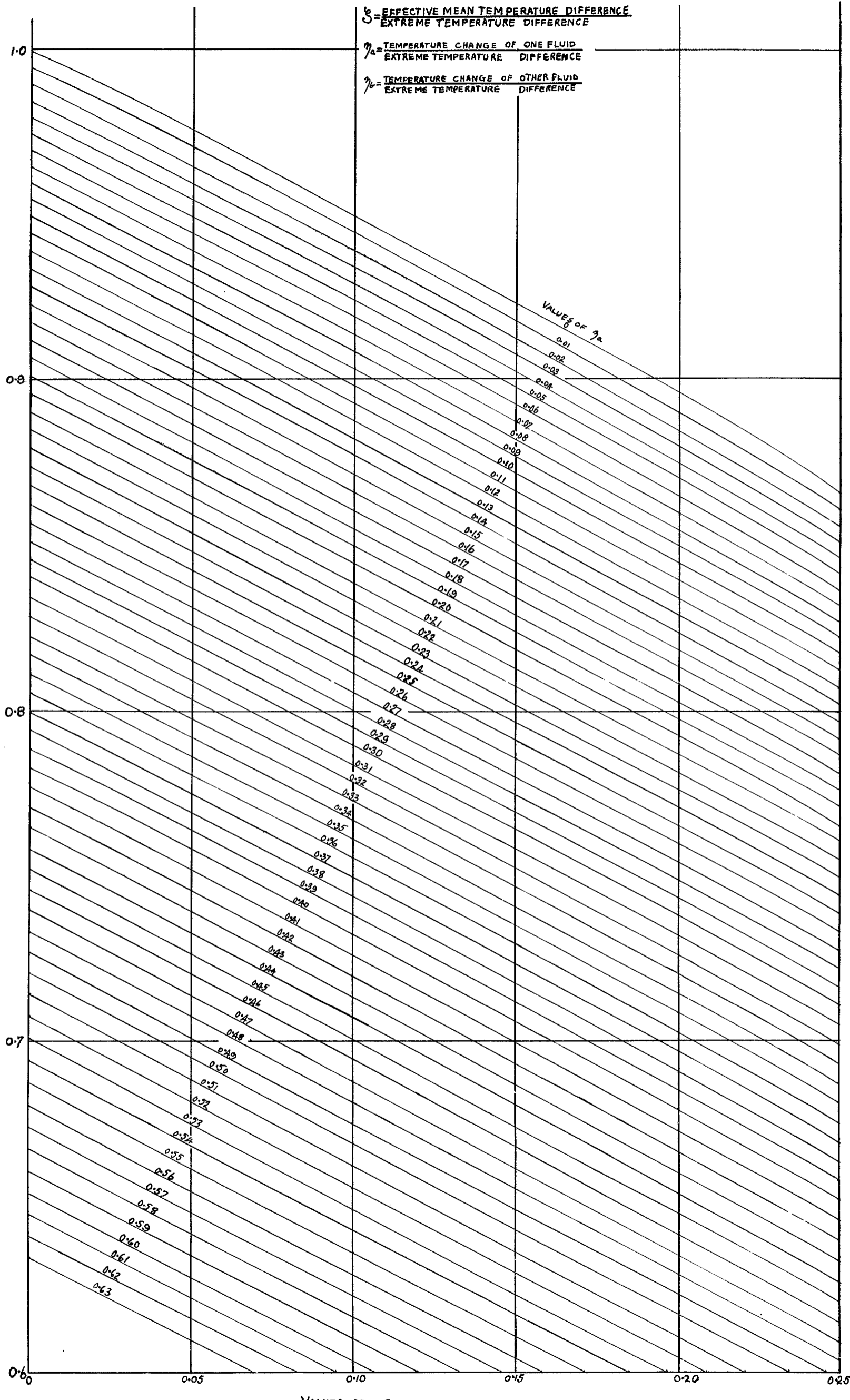


Fig. 1 Effective mean temperature difference for cross-flow cooler.

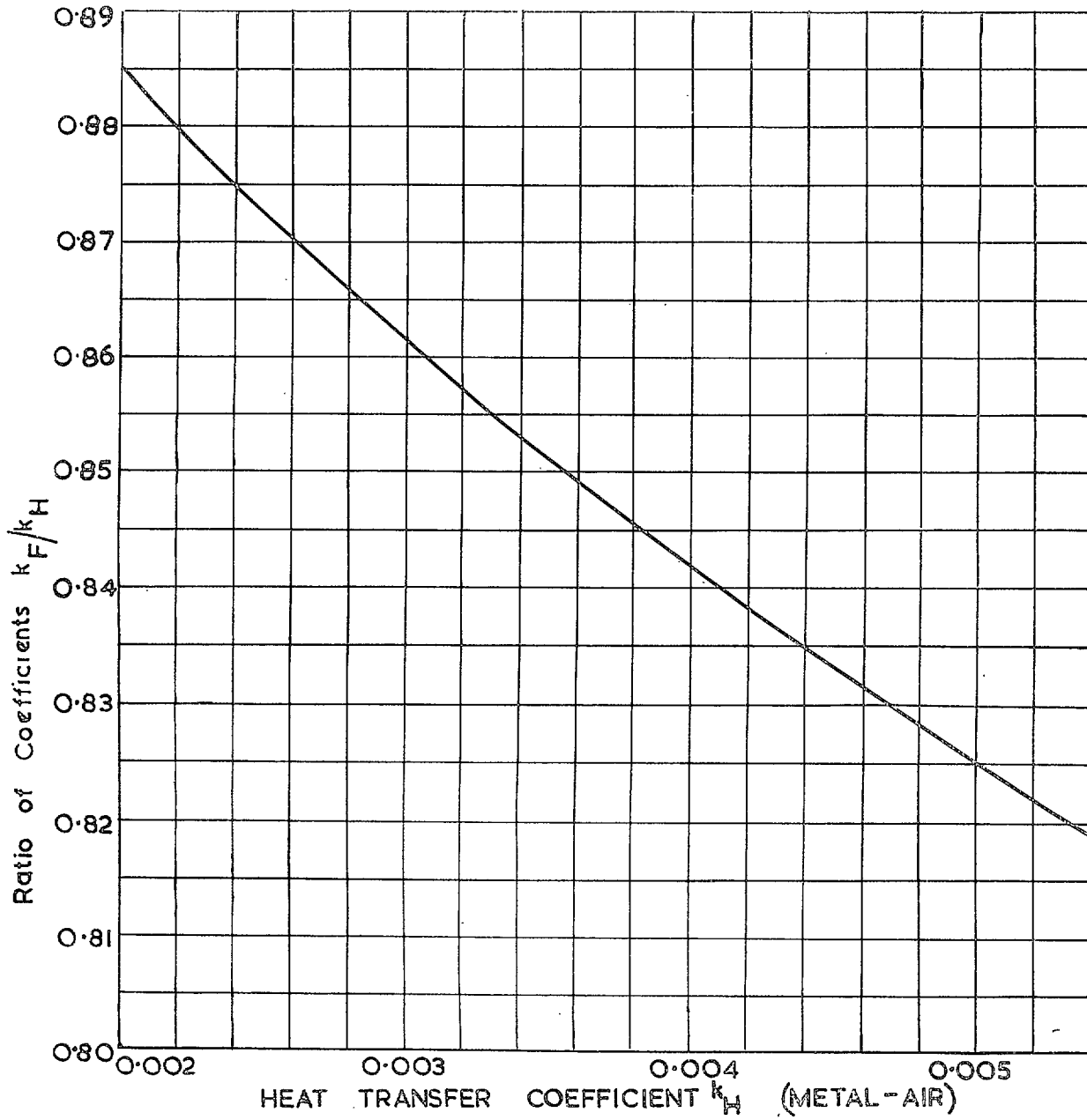


FIG. 2. Ratio of coefficients of friction and heat transfer for turbulent flow of air in tubes.
(From von Kármán's extension of the Reynolds' analogy.)

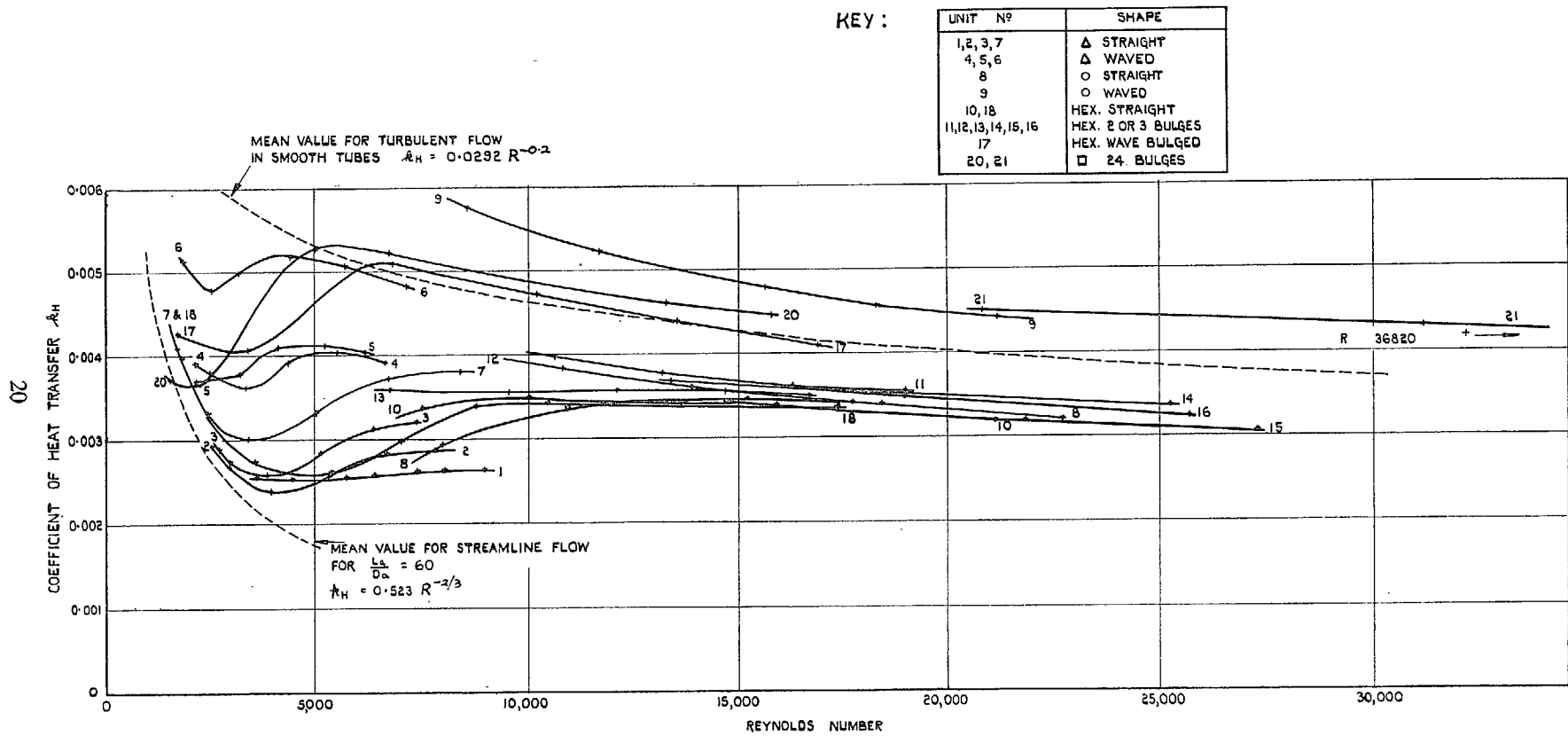


FIG. 3. Coefficient of heat transfer k_H .

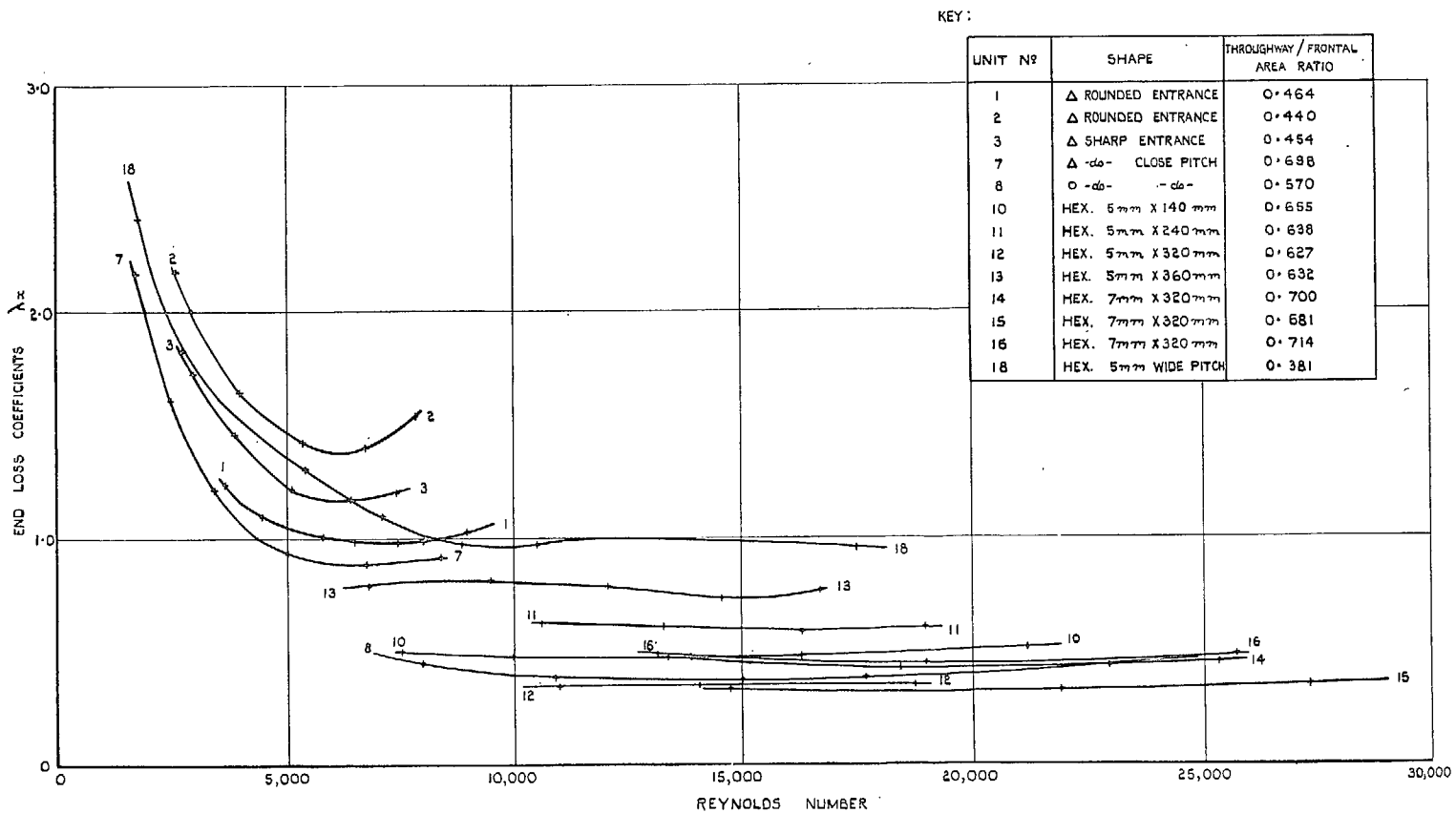


FIG. 4. Coefficient of pressure drop due to end losses for hot matrices.

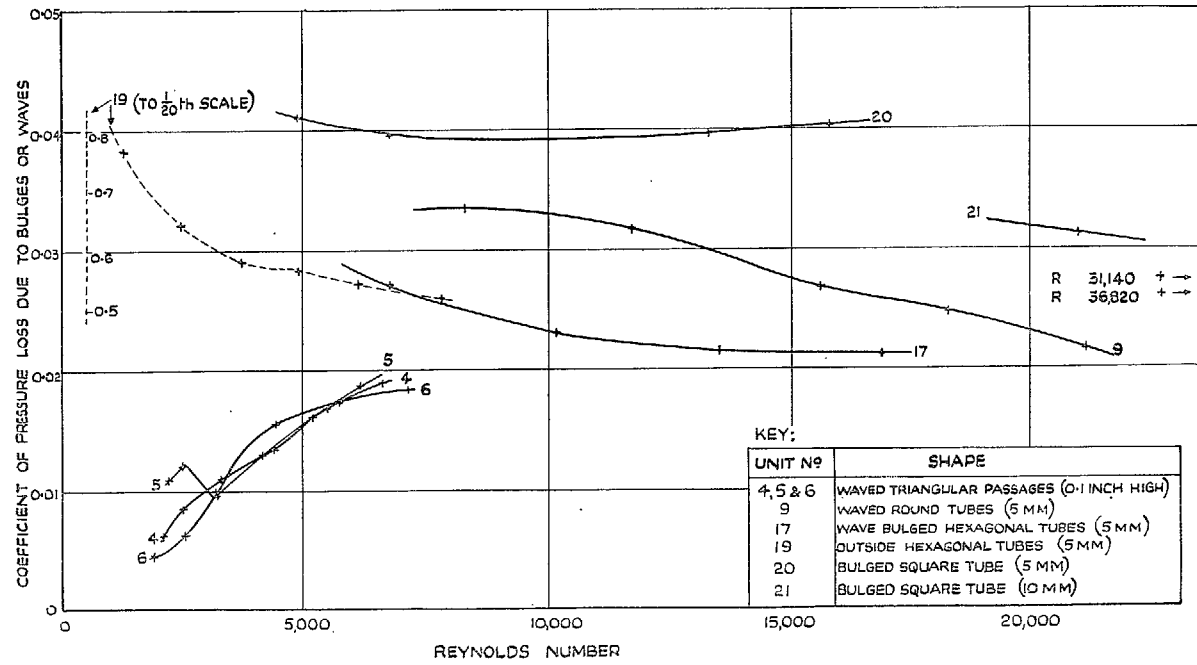


FIG. 5. Coefficients of pressure loss due to bulges or waves for hot matrices.

APPENDIX II

Description of Test Units, Tables of Dimensions and Diagrams of Passage Shape

1. Description of Test Units

A full description of each unit is given below, with an indication of the reason for its inclusion in the series examined. In this Appendix also is included a table of dimensions for each unit and photographs or drawings of the more important features.

2. Units Nos. 1, 2, 3, 4 and 5 (Ref. 1)

These units were generally of similar construction and made from copper foil 0.003 inch thick, plated electrically with a thickness of between 0.00025 and 0.0005 inch of tin on each side. All had a frontage approximately 6 by 6 inches, and were intended to be representative of a construction suitable for engine charge coolers. All these Units were designed and constructed at the Royal Aircraft Establishment.

No. 1 was formed by assembling, alternately, flat and corrugated strips with the direction of the corrugations in any corrugated strip arranged at right angles to the direction of the corrugations in the strips on each side. By placing the assembly under a small load in a furnace and raising the temperature to the melting point of the tin, subsequently allowing the unit to cool under the load, adherence of all the tinned parts in contact was effected and two sets of triangular passages mutually at right angles was obtained. The side seams were made by hand soldering. A photograph of the unit and details of this construction are shown in Plate 1 and Fig. 7. The entrances to the passages were all rounded in this construction. The air passages of Unit No. 1 were straight and approximately 3.6 inches long. In the 28 rows of passages in the Unit there were 1,727 whole tubes and 21 half-tubes effective, with 10 whole passages and 8 half passages in addition that were blocked with solder.

Units Nos. 2 and 4 were made in a similar manner but with a somewhat different method of assembly. A photograph of one of the units and details of the construction are shown in Plate 2, Figs. 8 and 9. The entrances and exits of one group of passages (marked 'a' passages or 'airways' in the diagrams) were rounded, while the other group (the 'b' or 'charge' passages) had seams made on flat extensions of the dividing plates, forming sharp or 'pointed' entrance and exit edges. Each unit was substantially cubical with passages 6 inches long and thus provided two groups of passages similar except for these end shapes. The units arranged for airflow in the passages with rounded entrances were designated Nos. 2 and 4. With the airflow in the alternative passages with sharp edged entries, the same units were called Nos. 3 and 5, respectively.

The difference between Nos. 2 and 4 (and therefore between Nos. 3 and 5 also) was in the form of the corrugations. Those in No. 2 assembly were straight in

the direction of flow for both groups of passages, while the corrugations in Unit No. 4, were waved as shown in Fig. 10, giving a slightly sinuous path for both groups of passages. There were 22 waves in each passage, with a length of 0.25 inch and an amplitude (half-range) of 0.01 inch. For the purpose of estimating the pressure losses due to these waves, there were considered to be 45 changes of direction of flow in each passage.

The passage shapes are shown in Fig. 6 and Table 2 gives further dimensions.

Unit No. 2 had 30 rows of passages with 1,500 whole passages and 35 halves.

No. 3 with 31 rows, had 1,581 whole passages and 58 halves.

No. 4 had 30 rows containing 1,500 whole passages and 59 halves.

No. 5 with 31 rows, had 1,581 passages and 62 halves.

3. Units Nos. 6 and 7 (Ref. 2)

The construction of Units Nos. 6 and 7 was similar to that of Nos. 3 and 5 except that the throughway/frontal-area ratio or 'transparency' was greater than in the case of Nos. 3 and 5. Both Units were approximately 6 inch cubes, constructed by assembling, alternately, flat tubes enclosing a corrugated strip (forming the airways), and finely corrugated sheets (forming the waterways). A photograph of one of the units and details of the construction are shown in Plate 3, Figs. 12 and 13. Both Units were made at the Royal Aircraft Establishment. The passages were substantially triangular with the dimensions shown in Fig. 11, while the entrances and exits were sharp edged and similar to those of Units Nos. 3 and 5.

The air passages of Unit No. 7 were straight while those of No. 6 were sinuous and similar to those of Units Nos. 4 and 5. There were 22 waves in each passage with a length of 0.25 inch and an amplitude (half-range) of 0.01 inch. The wave form is shown in Fig. 14.

Table 2 gives the dimensions of these units. Unit No. 6 had 2,240 passages in 43 rows: No. 7 also had 43 rows with a total of 2,268 passages.

4. Units Nos. 8 and 9 (Ref. 3)

These units were built up from round cupro-nickel tubes of 5 mm external diameter and 140 mm length, nominally 0.0045 inch thick. The hexagonal end expansions gave a nominal horizontal pitch of the tube centres of 6.4 mm and a diagonal pitch of 5.8 mm, but due to manufacturing tolerance the actual pitch distances for Unit No. 8 were 6.53 mm and 5.75 mm respectively; for Unit No. 9, they were 6.4 mm and 5.85 mm.

Unit No. 8 consisted of 736 straight round tubes. To complete the unit 32 half-tubes of elliptical cross-section were added, four of which were blocked with solder during assembly. The tubes were arranged in 32 rows, with 23 tubes and one half-tube in each row.

Unit No. 9 comprised 705 round tubes similar to those of No. 8 but waved in the direction of air flow, having eight waves of 0.53 mm amplitude (half-range) and 14.5 mm length. The waves were in the form of circular arcs of 12.7 mm mean radius and 33 deg subtended angle. To complete the unit 30 straight half-tubes of elliptical section were used; 4 of these became blocked with solder during assembly.

Plate 4 shows the tubes, and Plate 5 the Unit No. 9 after assembly of the tubes but before the addition of the water casing. The units were assembled at the Royal Aircraft Establishment. The dimensions are shown in Table 3.

5. Units Nos. 10, 11, 12 and 13

These units contained drawn copper tubes, hexagonal in section, measuring 5 mm externally across the flats. The nominal thickness of the metal was 0.1 mm. All tubes were of a type R.T.7, defined by the shape of the hexagonal end expansion, which gave the following dimensions for the widths of the waterways, measured outside the tubes, between adjacent flats.

Type No.	Vertical Waterways	Inclined Waterways
5 mm R.T.7.	1.4 mm	0.8 mm

The tubes were straight but with the exception of those in Unit No. 10, all had three bulges (in addition to the end expansions) equally spaced along the length.

The cross-section at the bulges was circular with a diameter of 5.64 mm externally. The centre bulge was 10 mm long, the intermediate ones 6 mm in length. A conical transition 1.5 mm long was made to the hexagon at each end of the bulge. The end expansions also had similar transitions 1.5 mm long. The tubes of Unit No. 10 had no bulges.

Unit No. 10 had 736 hexagonal tubes (Ref. 4) and was completed with 32 half-tubes of D section of which 4 were blocked with solder. The tubes were 140 mm long, including the end expansions, and were arranged in 32 rows. The unit was assembled at the Royal Aircraft Establishment. The other units were made by radiator manufacturers.

Unit No. 11 had 729 hexagonal tubes and 30 half-tubes, arranged in 31 rows. One whole tube and 8 half-tubes were blocked. This unit was 240 mm long (Ref. 5).

Unit No. 12, with 705 hexagonal tubes and 30 half-tubes had 8 half-tubes blocked. The tubes were arranged in 30 rows. The Unit was 320 mm long (Ref. 5).

Unit No. 13 had 729 tubes, arranged in 31 rows. All 30 half-tubes were blocked. It was 360 mm long (Ref. 5).

Other dimensions of the units are shown in Table 3 of this Appendix.

6. Units Nos. 14, 15 and 16 (Ref. 5)

The tubes of Units Nos. 14 to 16 were 7 mm hexagonal drawn copper tubes of nominal thickness 0.125 mm. Those of Nos. 14 and 15 were of type R.T.5: No. 16 had more closely spaced tubes of R.T.6 type. The details of these types of tube are:

Type No.	Vertical Waterways	Inclined Waterways
7 mm R.T.5.	1.5 mm	0.875 mm
7 mm R.T.6.	1.3 mm	0.70 mm

All tubes had two intermediate bulges (in addition to the end expansions). They were spaced 110 mm from the ends. The cross-section of the bulges was circular and of 7.89 mm diameter externally and 5.5 mm long with a conical transition to the hexagonal shape of the tube at each end, extending for 2 mm. The end expansions had a similar transition, 2 mm long. These units were made by radiator manufacturers.

Unit No. 14 had 403 hexagonal tubes and 22 half-tubes of D cross-section, arranged in 23 rows. All tubes were clear.

Unit No. 15 had 385 hexagonal tubes and 22 half-tubes with one half-tube blocked. The tubes were in 22 rows.

Unit No. 16 had 403 hexagonal tubes and 22 half-tubes; none was blocked. There were 23 rows of tubes.

All units had approximately a 6 inches square frontage. Full particulars are given in Tables 3 and 4.

7. Unit No. 17 (Ref. 6)

Unit No. 17 was made from 5 mm × 300 mm R.T.7, copper tubes, bulged alternately on two opposite flats of the cross-section to form a 'wave-bulged' passage as shown in the photographs of Plate 6. The dimensions of the dies used for bulging are shown in Fig. 15. The bulges in each flat were at 14 mm pitch and they were 0.7 mm deep, the contours being circular arcs of 12.7 mm radius. There were a total of 37 bulges in each tube, and for the purpose of estimating the pressure losses there were considered to be 39 changes of direction in a tube.

The unit, which had a frontal area approximately 5 inches square, contained 527 whole tubes and 26 half-tubes arranged in 27 rows. Of these 6 whole tubes and 10 half-tubes were blocked. The tubes were bulged and assembled at the Royal Aircraft Establishment. Table 4 contains particulars of the dimensions.

8. Units Nos. 18 and 19 (Ref. 7)

These units consisted of one block of frontal area approximately 6 by 6 inches containing 5 mm × 300 mm straight hexagonal, drawn copper tubes with regular hexagonal end expansions measuring 7.6 mm across the flats; there were 429 tubes in 22 rows. Eight of these were blocked. There were also 22 half-tubes of which three were effective. Details of the assembly are given in Fig. 16, and further dimensions in Table 4.

Unit No. 18 was arranged with airflow through the tubes. The same block, arranged for airflow outside the tubes, was designated Unit No. 19. There were 22 rows of tubes and for the purpose of estimating the pressure losses outside the tubes there were considered to be 44 changes of direction. The units were constructed at the Royal Aircraft Establishment.

9. Units Nos. 20 and 21 (Refs. 8 and 9)

The air passages of Units Nos. 20 and 21 were square in cross-section and had 24 bulges uniformly spaced along

the length. The units consisted of thin sheets of cupronickel, corrugated and folded to form tubular elements with a number of square airways. The method of assembling these elements is illustrated in Fig. 17. The units were constructed by radiator manufacturers.

Unit No. 20 was 300 mm long with airways approximately 5.76 mm square in cross-section. The bulges increased this dimension to 6.43 mm for a length of 3.25 mm at intervals of about 11.85 mm with a transitional length at each end inclined at 60 deg to the axis of the tube. There were 24 bulges along the length, each about 3.85 mm long. Table 4 gives full particulars of the dimensions of the unit, which contained 435 tubes.

Unit No. 21 was 316 mm long with airways approximately 10 mm square. The 24 bulges in this unit were arranged at intervals of about 12.6 mm, and were 11.3 mm square by 5 mm long approximately. There were 152 square tubes in 16 rows, with 36 half-tubes of triangular section to complete the assembly. Dimensions of this unit are given in Table 4.

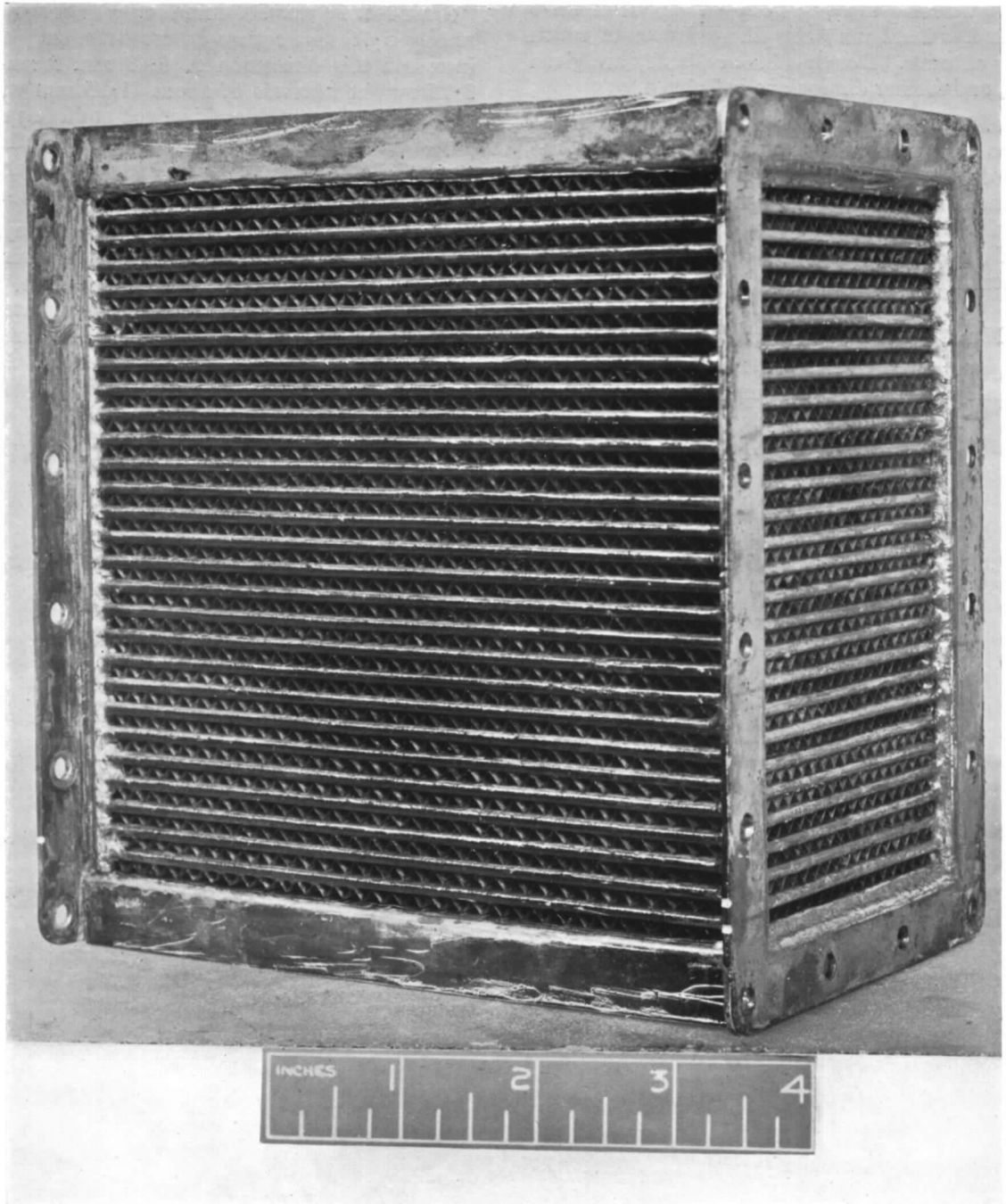


PLATE 1. Unit No. 1

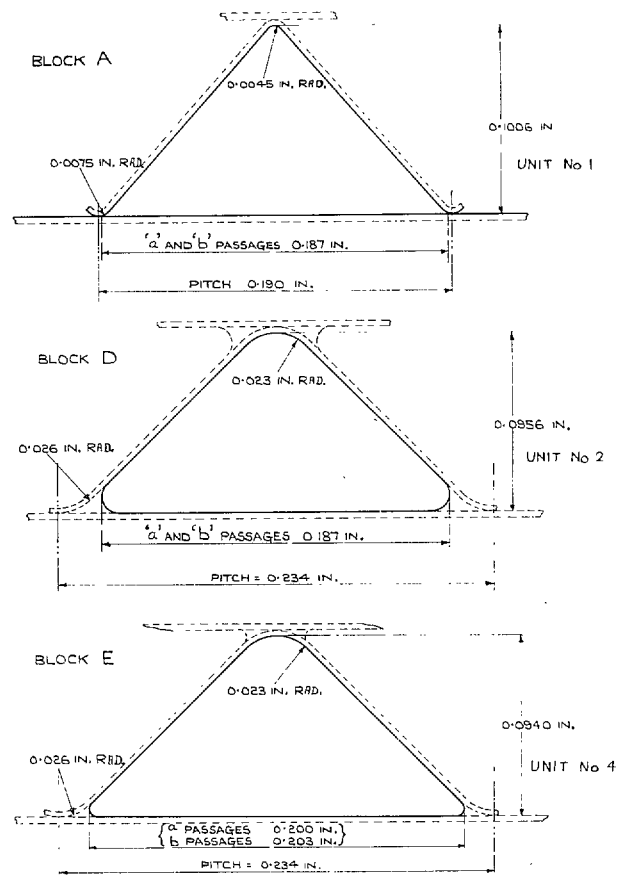


FIG. 6. Experimental charge coolers.
Average shape of passages.

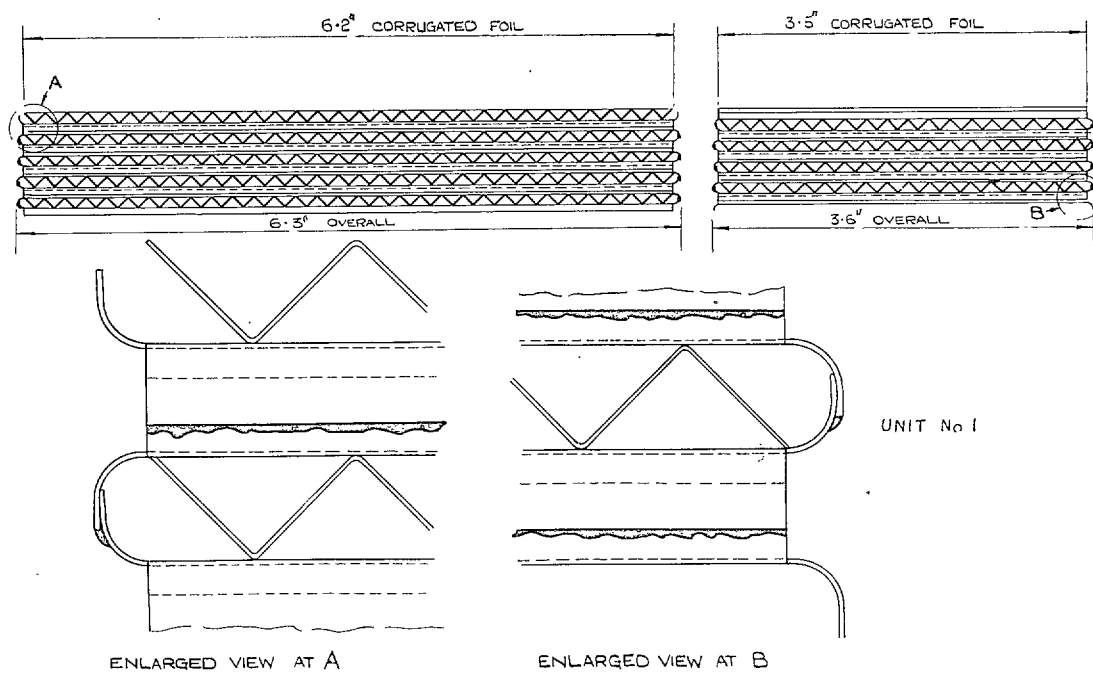


FIG. 7. Corrugated-foil charge cooler—constructional details.

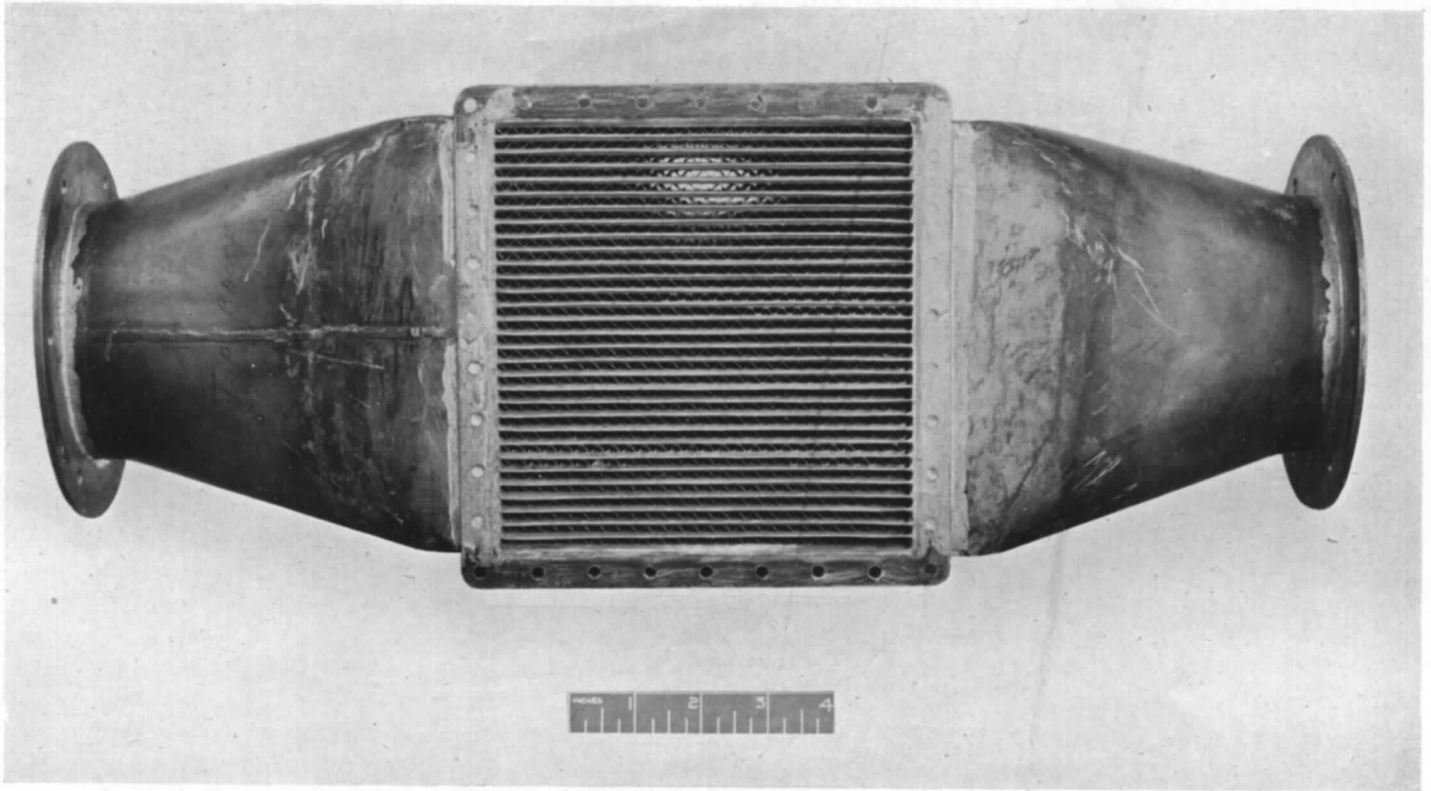


PLATE 2. Unit No. 2.

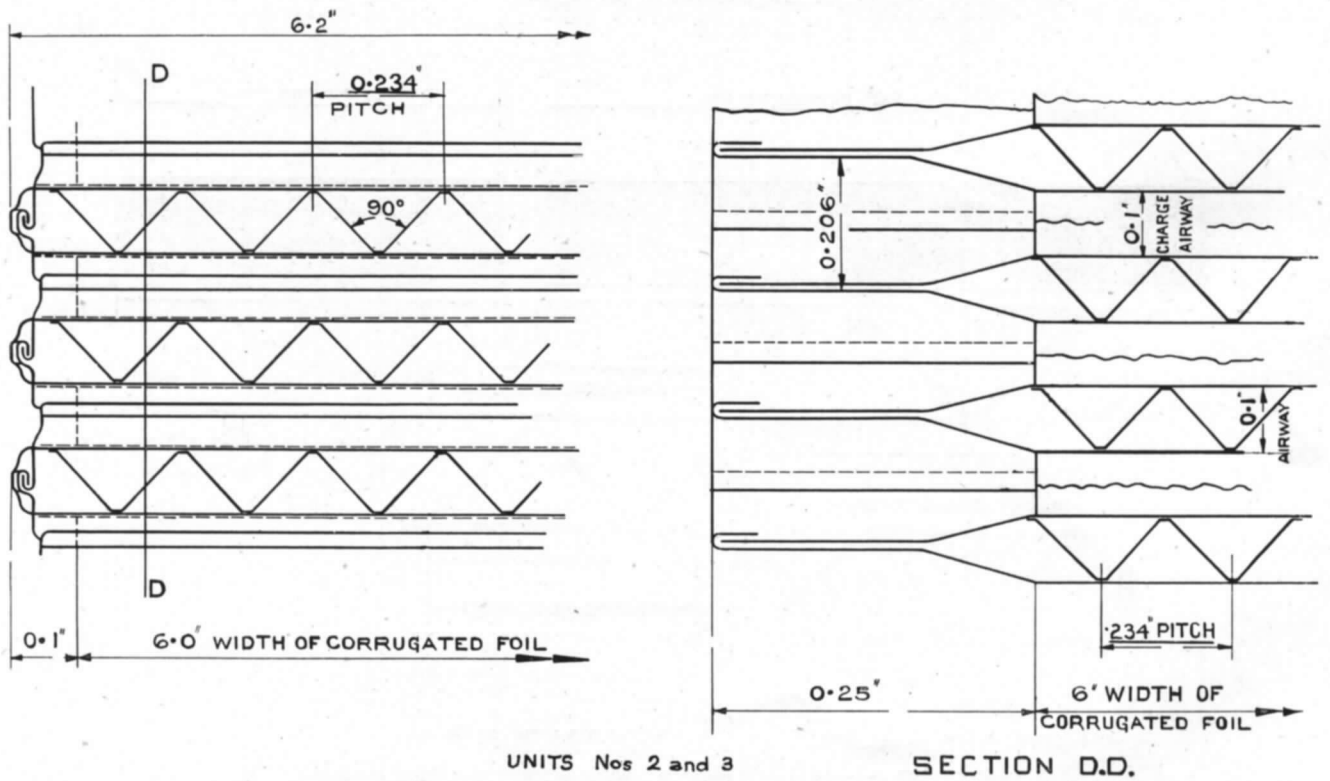
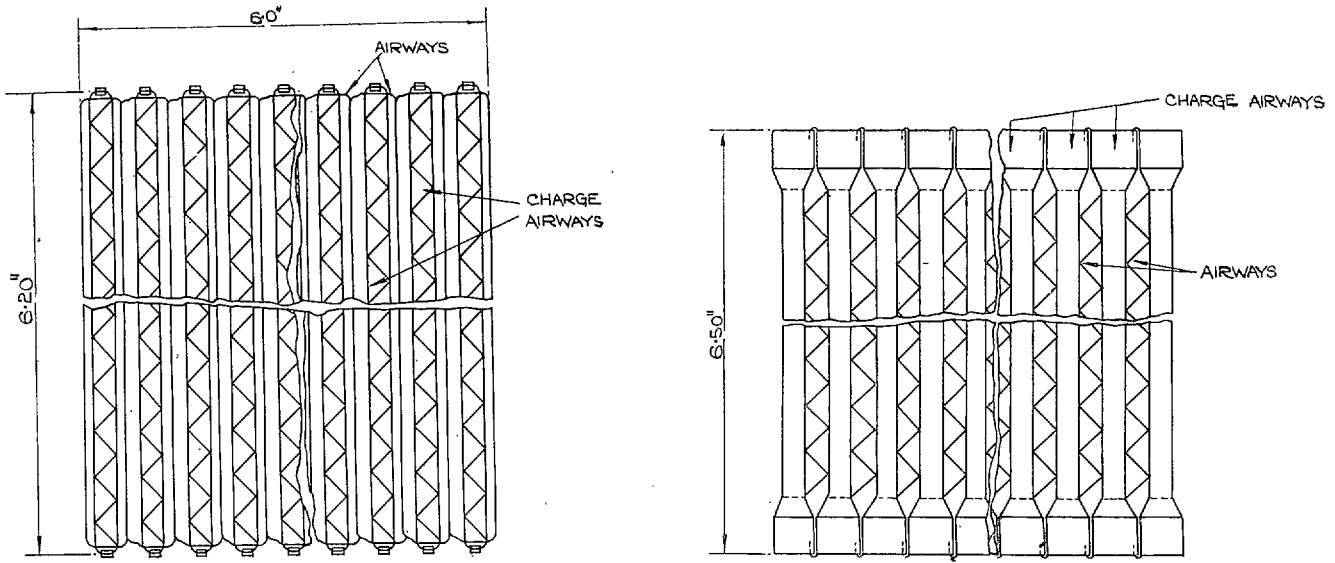
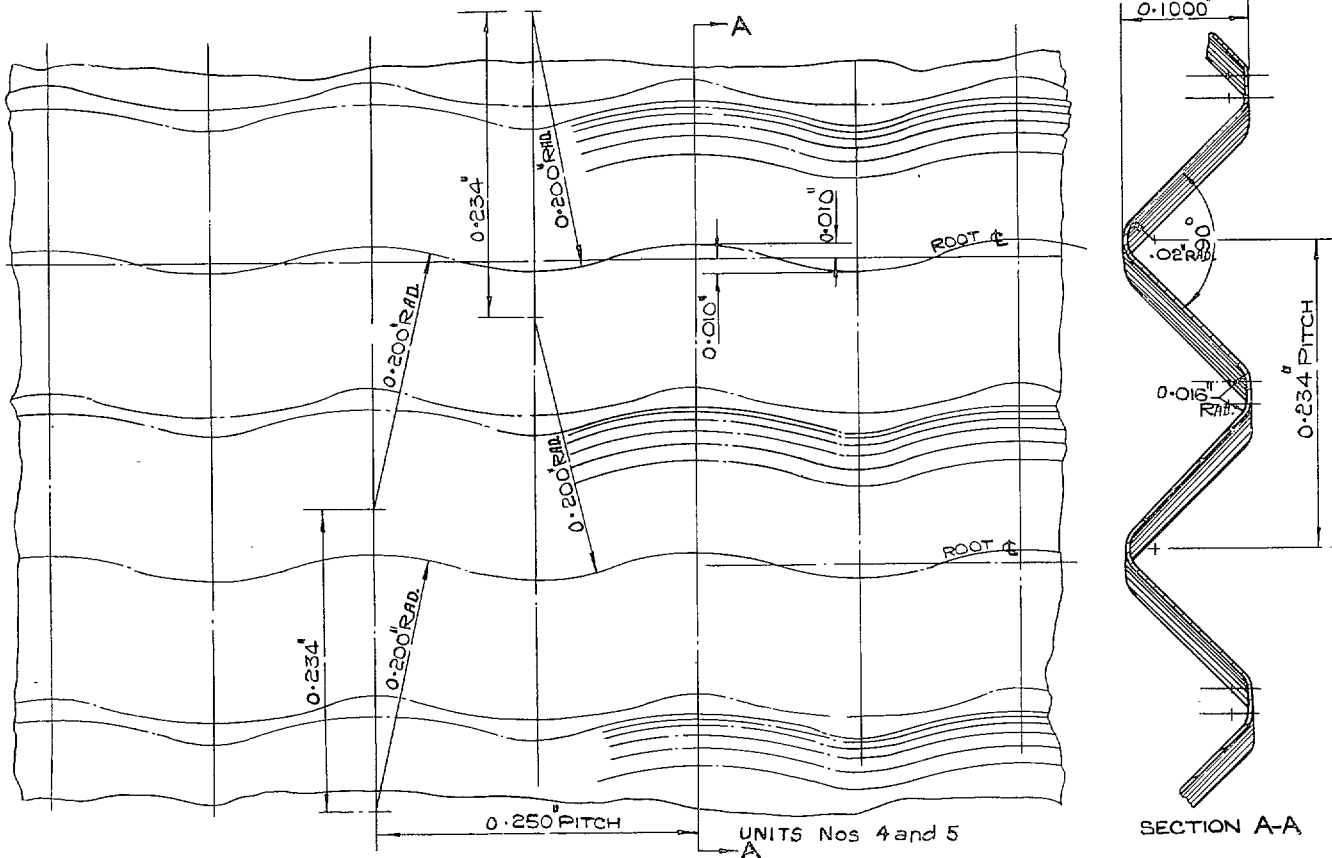


FIG. 8. Corrugated-foil charge cooler—constructional details.



UNITS Nos. 2 and 3

FIG. 9. Corrugated-foil charge cooler.



UNITS Nos 4 and 5

FIG. 10. Corrugated-foil for charge cooler.

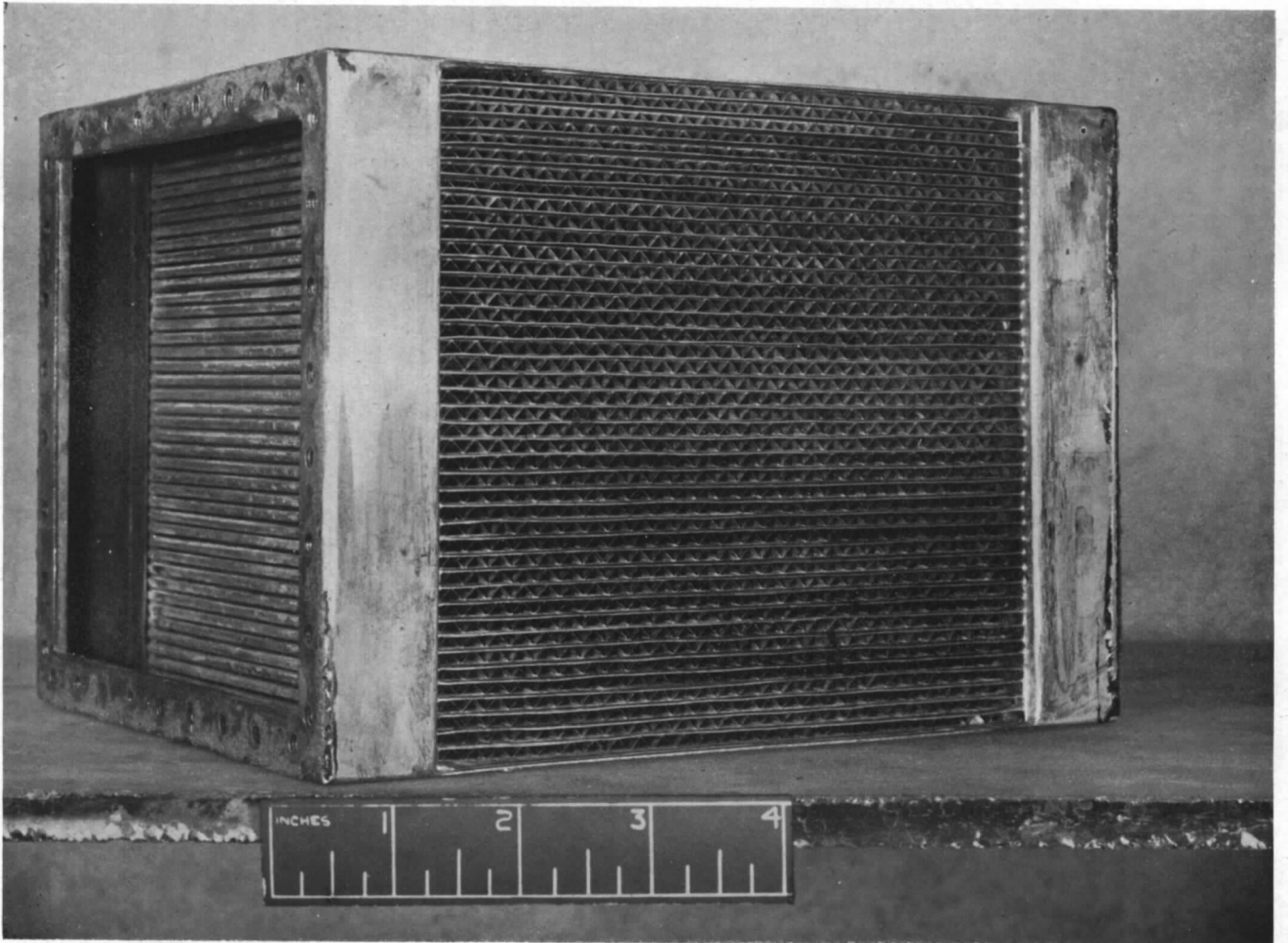


PLATE 3. Unit No. 6.

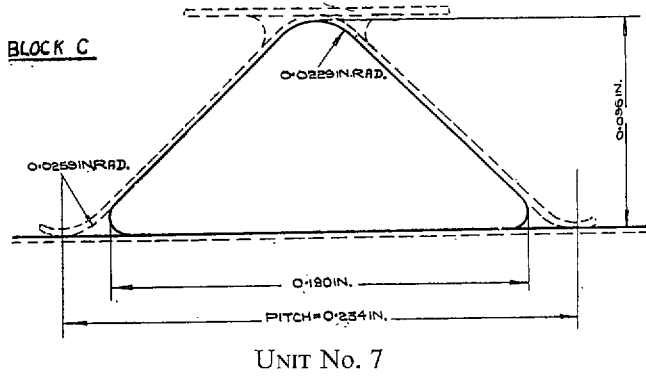
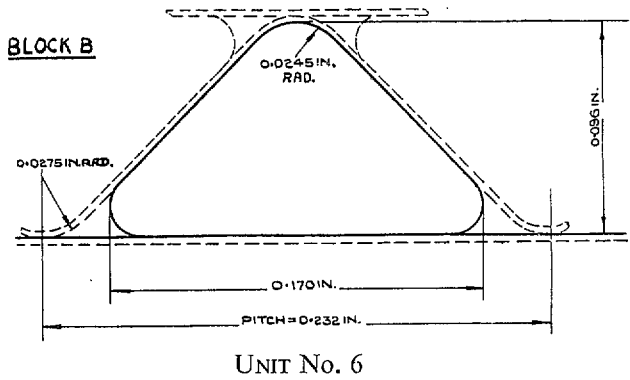


FIG. 11. Experimental radiators. Average shape of passages.

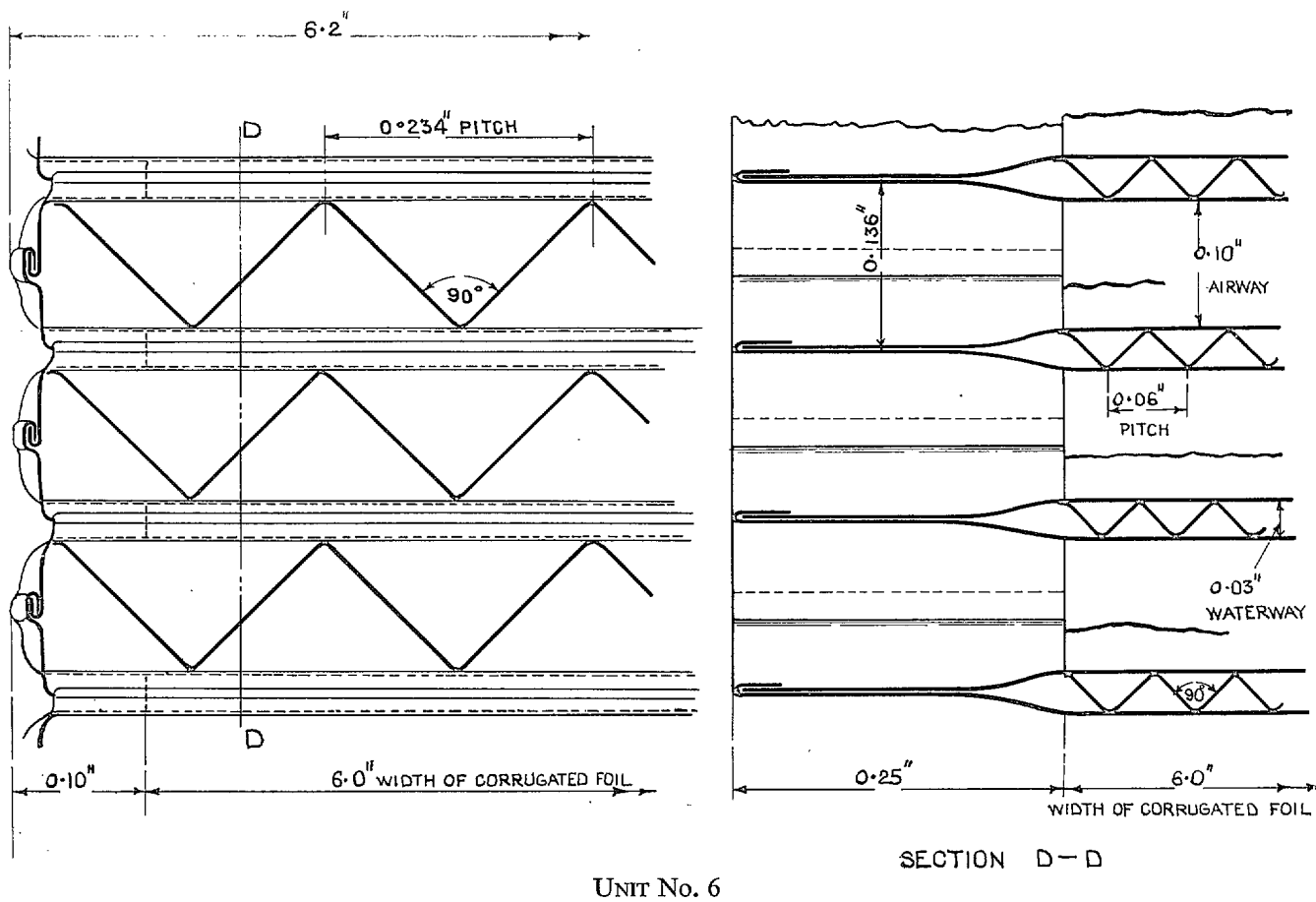


FIG. 12. Constructional details of corrugated-foil radiator.

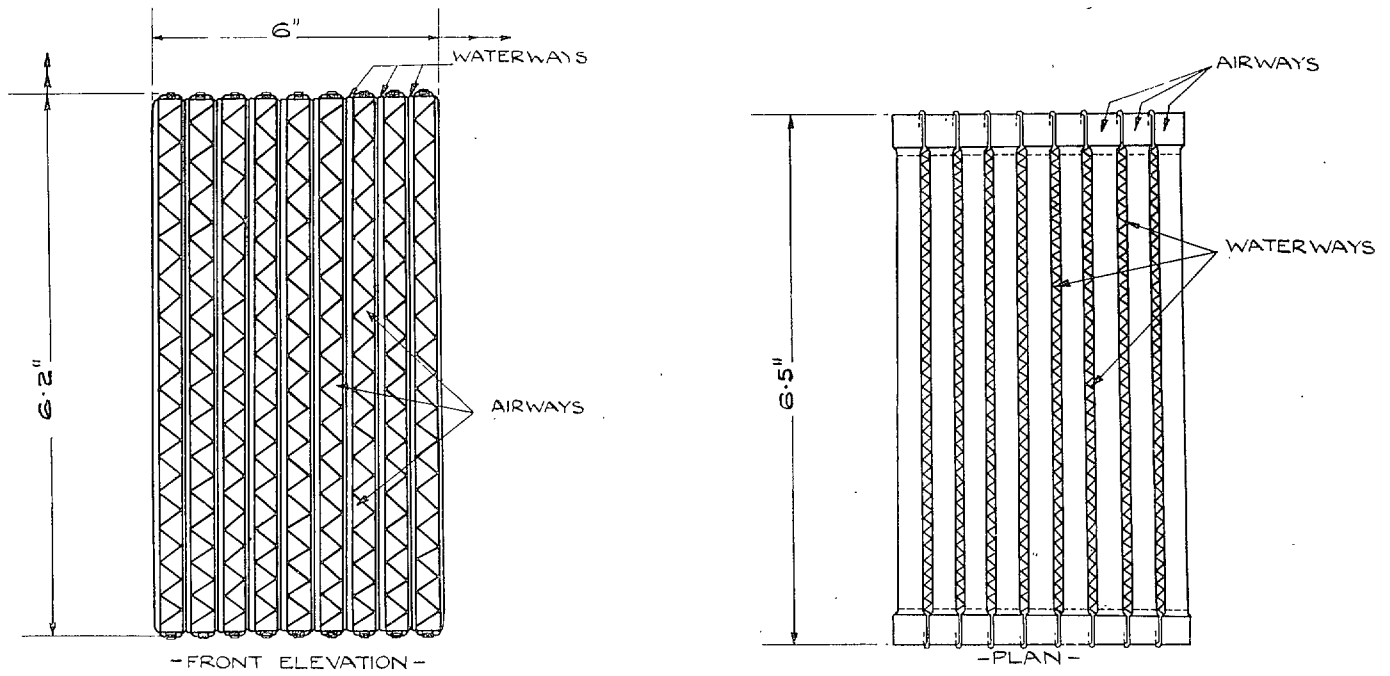


FIG. 13. Unit No. 6.

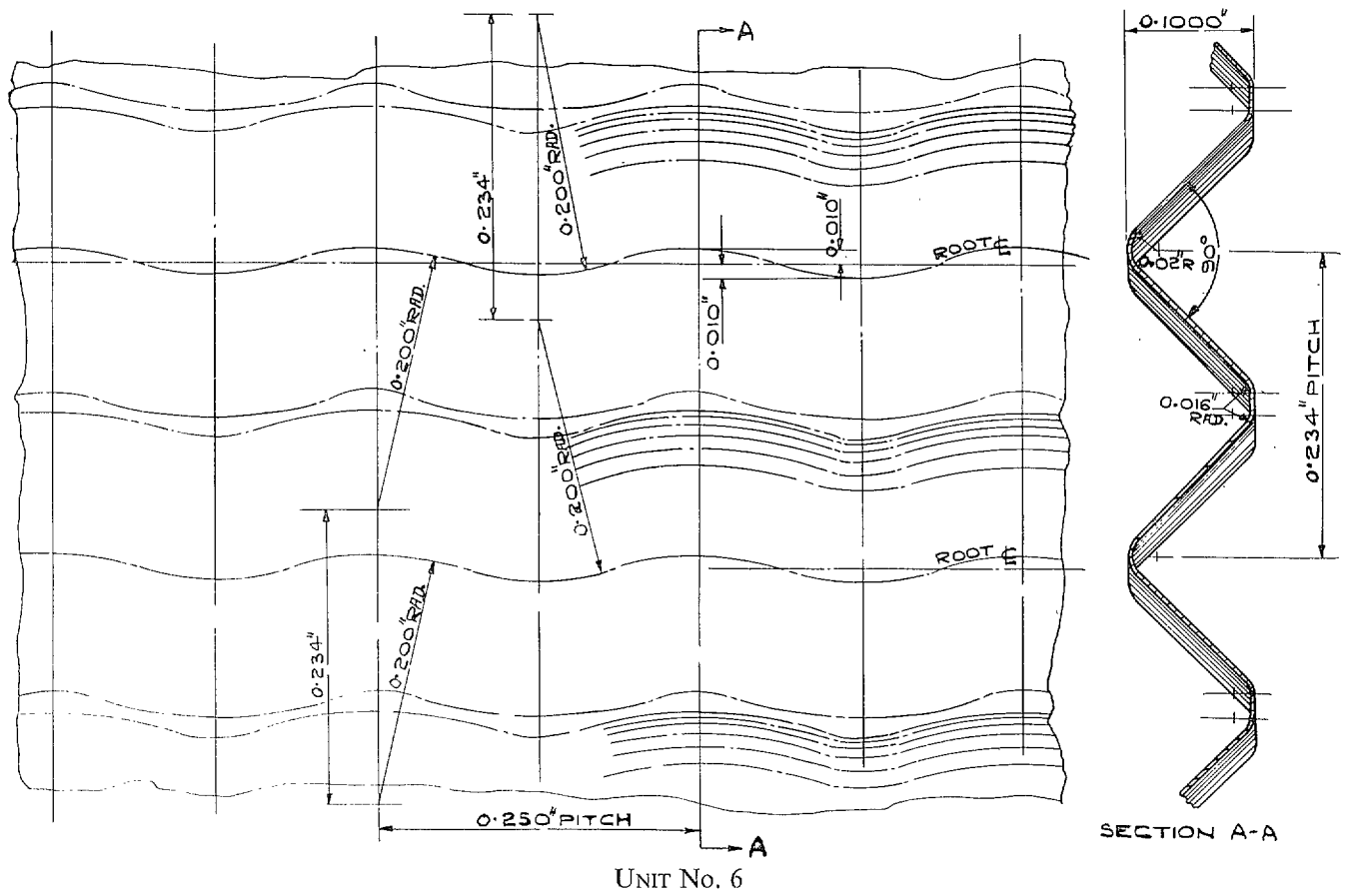


FIG. 14. Waved corrugated-foil for radiator.

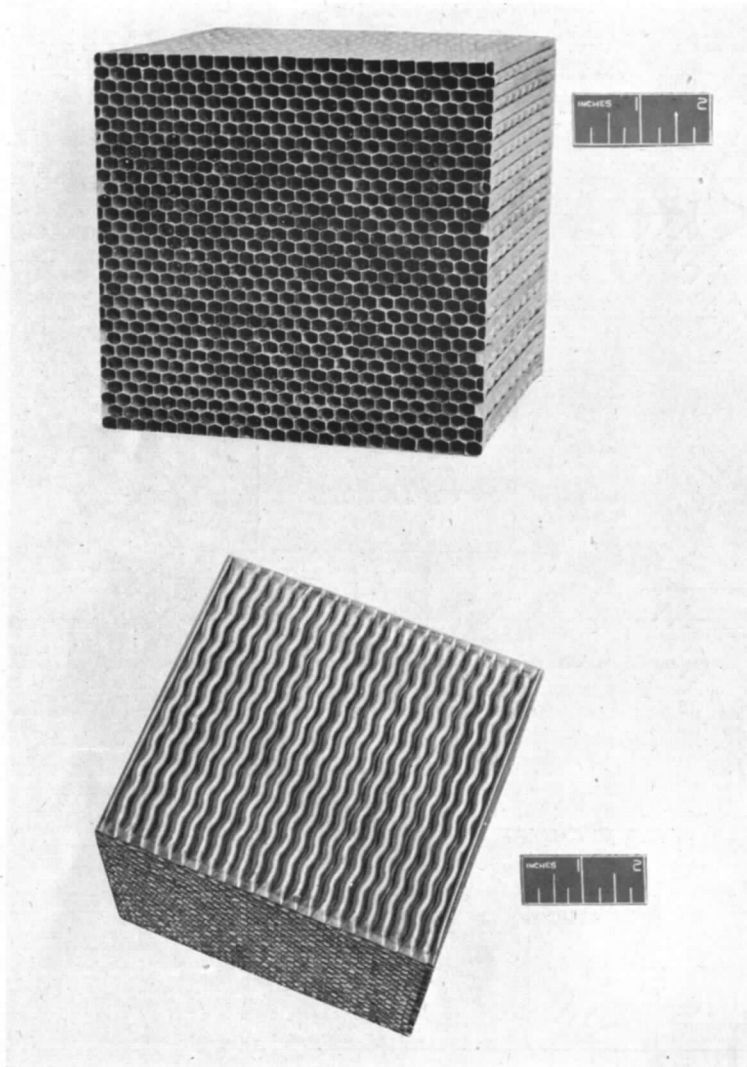


PLATE 5. Unit No. 9.

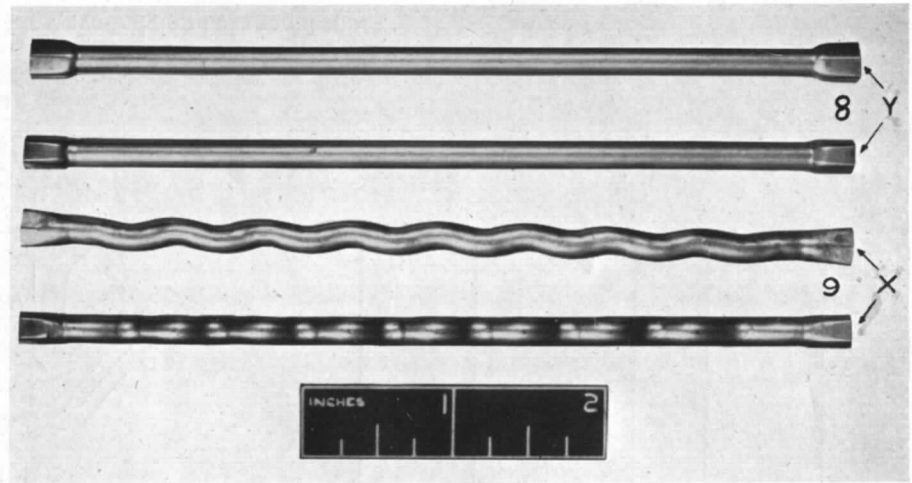


PLATE 4. Units Nos. 8 and 9.

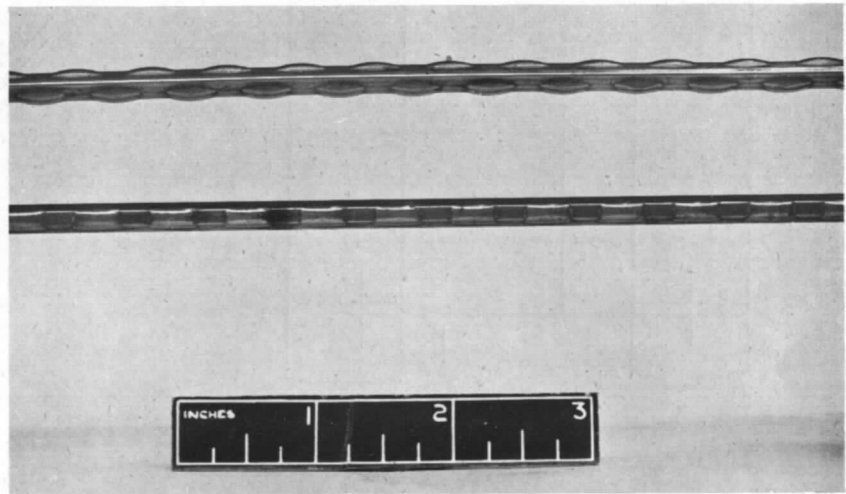
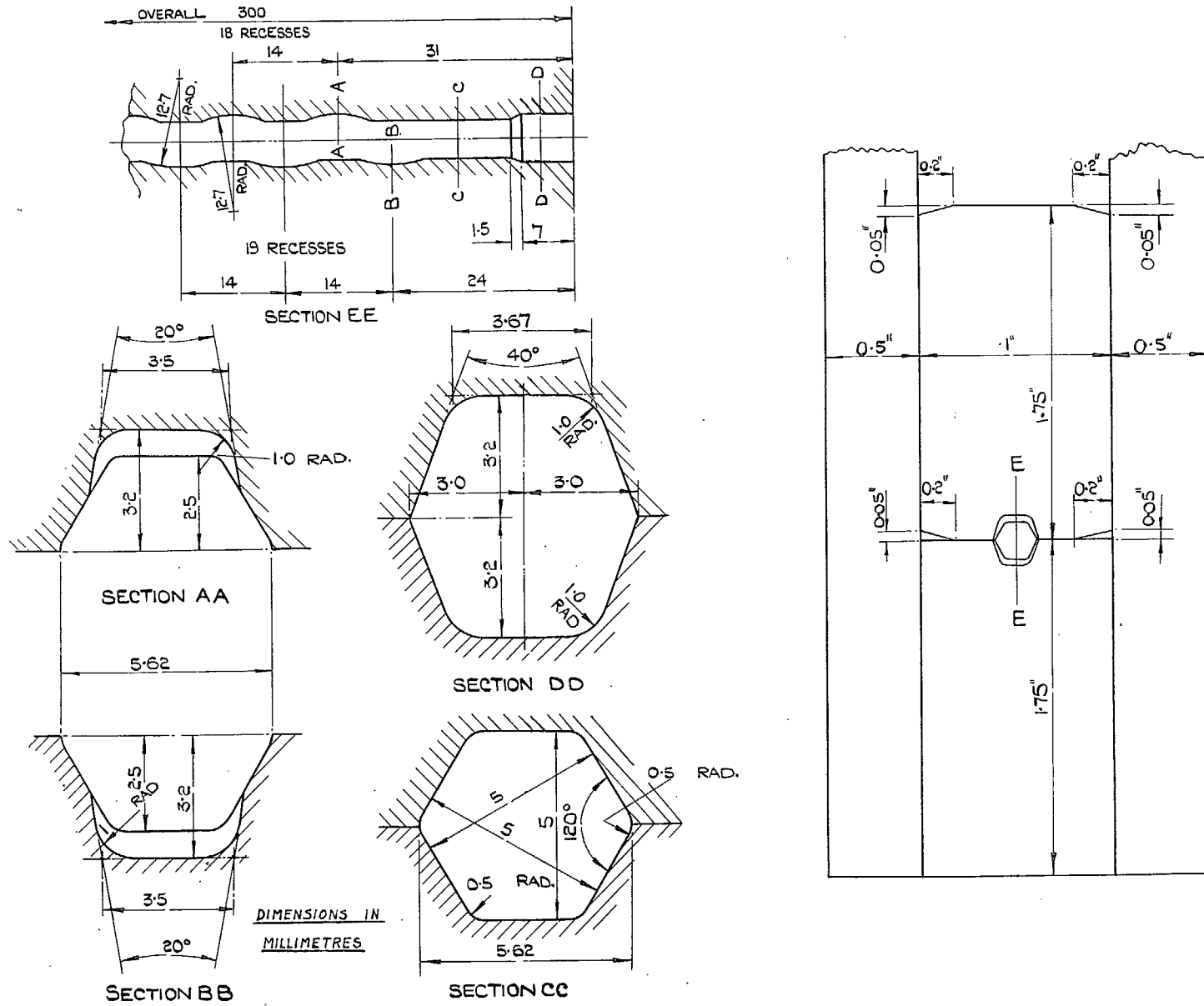
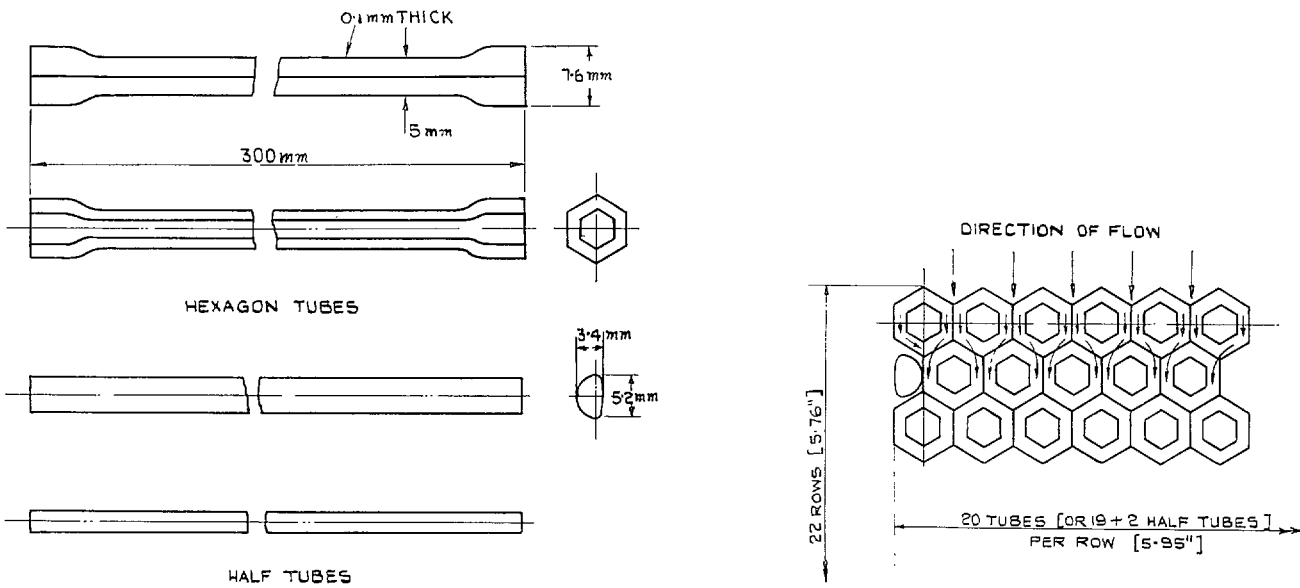


PLATE 6. Unit No. 17.



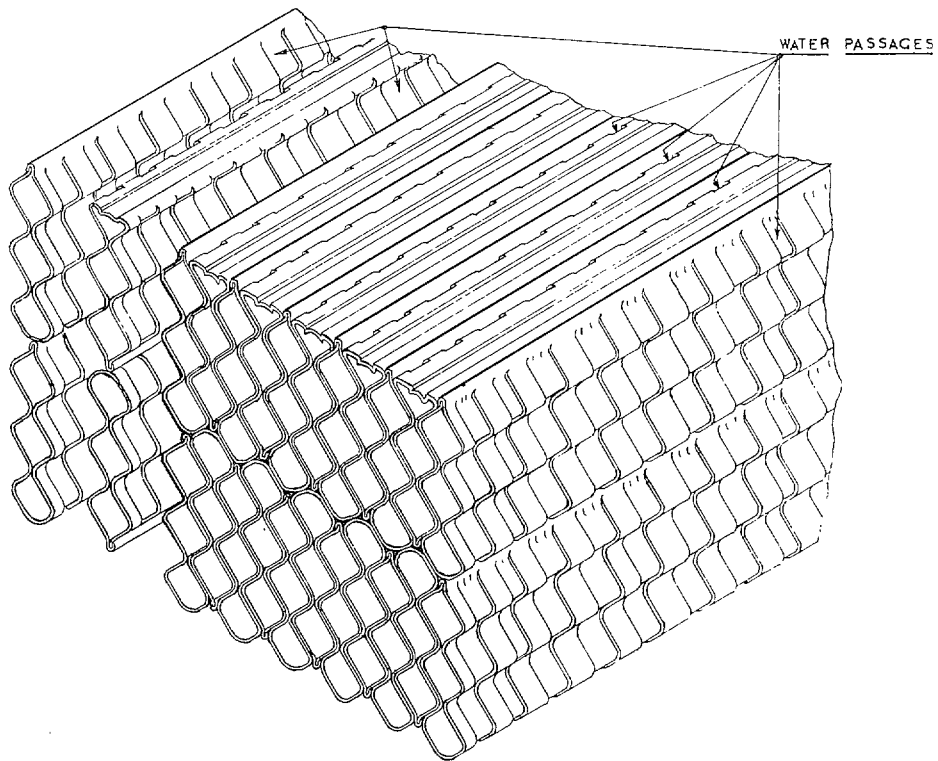
UNIT No. 17

FIG. 15. Dies for wave-bulging hexagonal tubes.



UNITS Nos. 18 and 19

FIG. 16. Tubular charge cooler with 5 mm × 300 mm hexagonal tubes with 7.6 mm end expansions.



UNIT No. 21

FIG. 17. Construction of 'Gallay' radiator.

TABLE 2
PARTICULARS OF EXPERIMENTAL CORRUGATED-FOIL COOLING BLOCKS

Unit No. Block		1 (a passages) A	2 (a passages) D	3 (b passages) D	4 (a passages) E	5 (b passages) E	6 B	7 C
Air passages	Length of passages .. L_a ft	0.301	0.500	0.500	0.500	0.500	0.500	0.500
	Matrix frontal area .. A sq ft	0.244	0.259	0.266	0.255	0.263	0.249	0.249
	Throughway area .. A_t sq ft	0.113	0.114	0.121	0.119	0.124	0.162	0.173
	Ratio A_t/A	0.464	0.440	0.454	0.467	0.474	0.650	0.698
	Swept surface .. A_a sq ft	20.09	29.11	30.73	30.44	32.50	40.01	43.75
	Mean hydraulic diameter .. D_a ft	0.00679	0.00785	0.00788	0.00782	0.00766	0.00808	0.00793
	Ratio L_a/D_a	44.3	63.7	63.5	63.9	65.3	61.90	63.05
Water passages	Length of passages .. L_b ft	0.525	0.500	0.500	0.500	0.500	0.500	0.500
	Matrix plan area .. B sq ft	0.136	0.266	0.259	0.263	0.255	0.230	0.236
	Throughway area .. B_t sq ft	0.060	0.121	0.114	0.124	0.119	0.040	0.042
	Ratio B_t/B	0.443	0.454	0.440	0.474	0.467	0.173	0.176
	Swept surface .. B_b sq ft	18.82	30.73	29.11	32.50	30.44	42.70	44.55
	Mean edge thickness at tube ends in.	0.0170	0.0160	—	0.202	0.0160	—	0.0214

TABLE 3
PARTICULARS OF EXPERIMENTAL TUBE BLOCKS

Unit No. Type of tube in block External diameter of tubes (mm)		8 Straight Round 5	9 'Sinuflo' Round 5	10 Straight Hexagonal 5†	11 R.T.7 Hexagonal 5†	12 R.T.7 Hexagonal 5†	13 R.T.7 Hexagonal 5†	14 R.T.5 Hexagonal 7†
Air passages	Length of passages .. L_a ft	0.4593	0.4593*	0.459	0.787	1.05	1.181	1.05
	Matrix frontal area .. A sq ft	0.2507	0.2435	0.246	0.250	0.246	0.248	0.251
	Throughway area .. A_t sq ft	0.1430	0.1369	0.161	0.159	0.154	0.157	0.176
	Ratio A_t/A	0.5704	0.5622	0.655	0.638	0.627	0.632	0.70
	Swept surface .. A_a sq ft	17.015	16.285*	18.90	31.9	41.25	46.98	33.82
	Mean hydraulic diameter .. D_a ft	0.01544	0.01544	0.01562	0.0157	0.0157	0.01575	0.0219
	Ratio L_a/D_a	29.75	29.75	29.4	50.0	66.87	75.00	48.07
Water passages	Length of passages .. L_b ft	0.5850	0.5787	0.636	0.640	0.626	0.638	0.649
	Matrix plan area .. B sq ft	0.2308	0.2297	0.228	0.394	0.528	0.591	0.525
	Throughway area .. B_t sq ft	0.0645	0.0654	0.047	0.0832	0.105	0.141	0.111
	Ratio B_t/B	0.280	0.285	0.208	0.212	0.199	0.239	0.212
	Swept surface .. B_b sq ft	16.1	15.4*	17.72	28.23	37.58	43.51	32.94
	Mean edge thickness at tube ends in.	0.0170	0.0160	—	0.202	0.0160	—	0.0214

* Nominal, neglecting waviness.

† Over flats.

TABLE 4
PARTICULARS OF EXPERIMENTAL TUBE BLOCKS

		Unit No. [Type of tube in block External diameter over flats (mm)]	15 R.T.5 Hexagonal 7	16 R.T.6 Hexagonal 7	17 Hexagonal 5	18 Straight Hexagonal 5	19 Rectangular 5	20 'Gallay' E.5 5	21 'Gallay' E 10
Air passages	Length of passages L_a	ft	1.05	1.05	0.984	0.984	0.585	0.983	1.037
	Matrix frontal area A	sq ft	0.246	0.246	0.181	0.238	0.462	0.249	0.232
	Throughway area A_t	sq ft	0.168	0.176	0.128	0.0908	0.222	0.166	0.1756*
	Ratio A_t/A		0.681	0.714	0.705	0.381	0.481	0.667	0.757*
	Swept surface A_a	sq ft	32.24	33.80	29.98	22.74	22.42	36.80	24.11*
	Mean hydraulic diameter .. D_a	ft	0.0218	0.0218	0.0168	0.0157	0.0232	0.0177	0.0302*
	Ratio L_a/D_a		48.10	48.10	58.69	62.65	25.24	55.5	34.3*
Water passages	Length of passages L_b	ft	0.631	0.643	0.435*	0.585	0.984	0.639	0.685
	Matrix plan area B	sq ft	0.528	0.522	0.410	0.462	0.238	0.484	0.4965
	Throughway area B_t	sq ft	0.0955	0.0845	0.0889	0.222	0.0908	0.0899	0.0564
	Ratio B_t/B		0.181	0.162	0.217	0.481	0.381	0.186	0.1133
	Swept surface B_b	sq ft	31.34	32.90	31.06	22.42	22.74	29.30	12.68*
	Mean edge thickness at tube ends	in.	0.0155	0.0261	—	—	—	0.0115†	0.039

* These quantities are derived by taking throughway and surface areas A_t , A_a and B_b as for plain square tubes 9.8 mm internal diameter and 0.1 mm thick.

† Nominal.

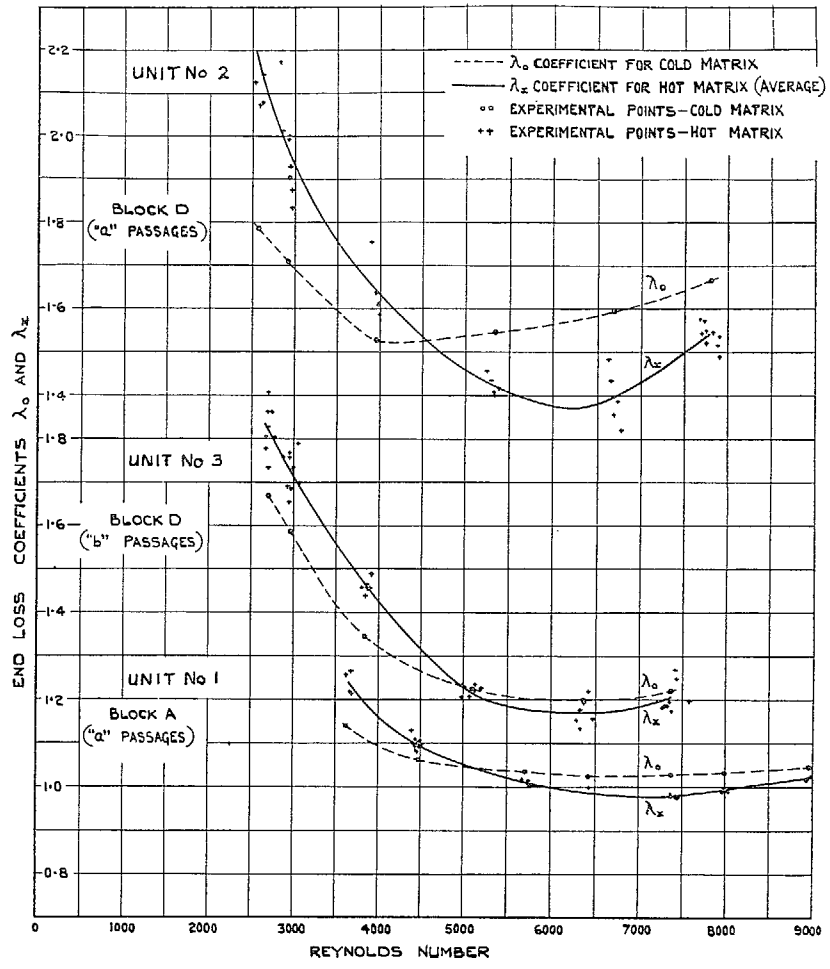


FIG. 18. Values of end-loss coefficient for blocks A and D.

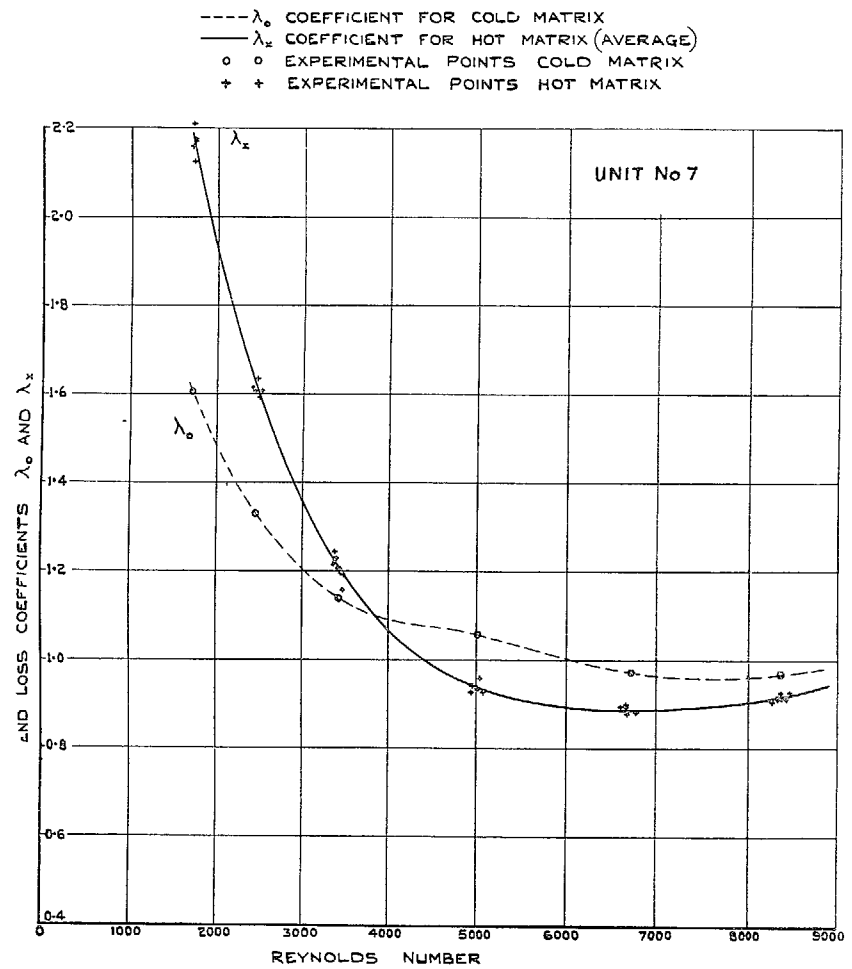


FIG. 19. Values of end-loss coefficient for block C.

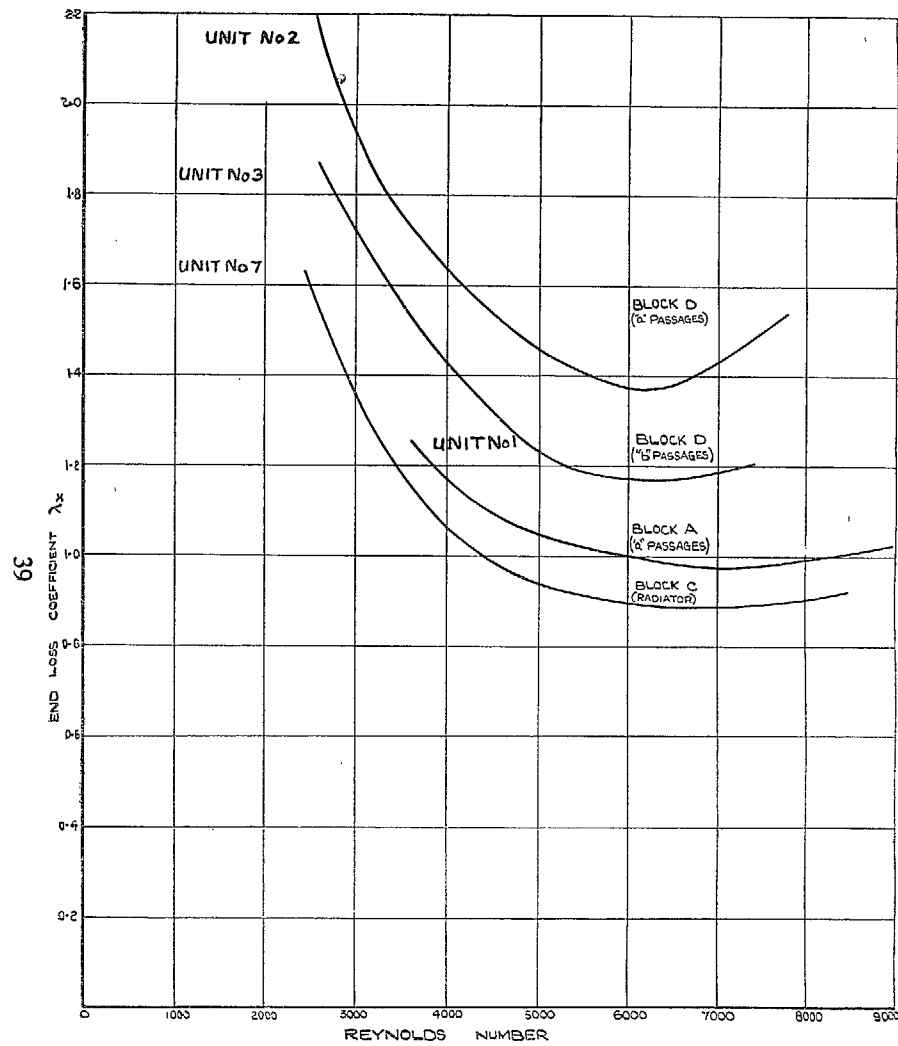


FIG. 20. End-loss coefficients for hot matrices.

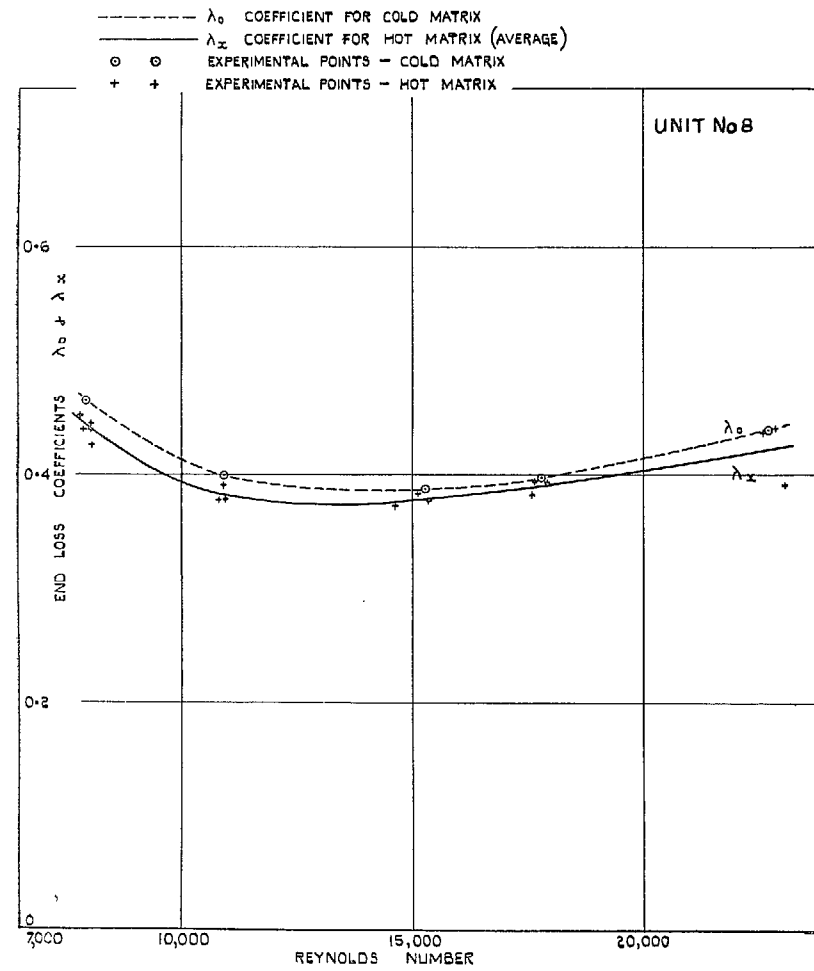


FIG. 21. Values of end-loss coefficients for straight round tube 5 mm \times 140 mm.

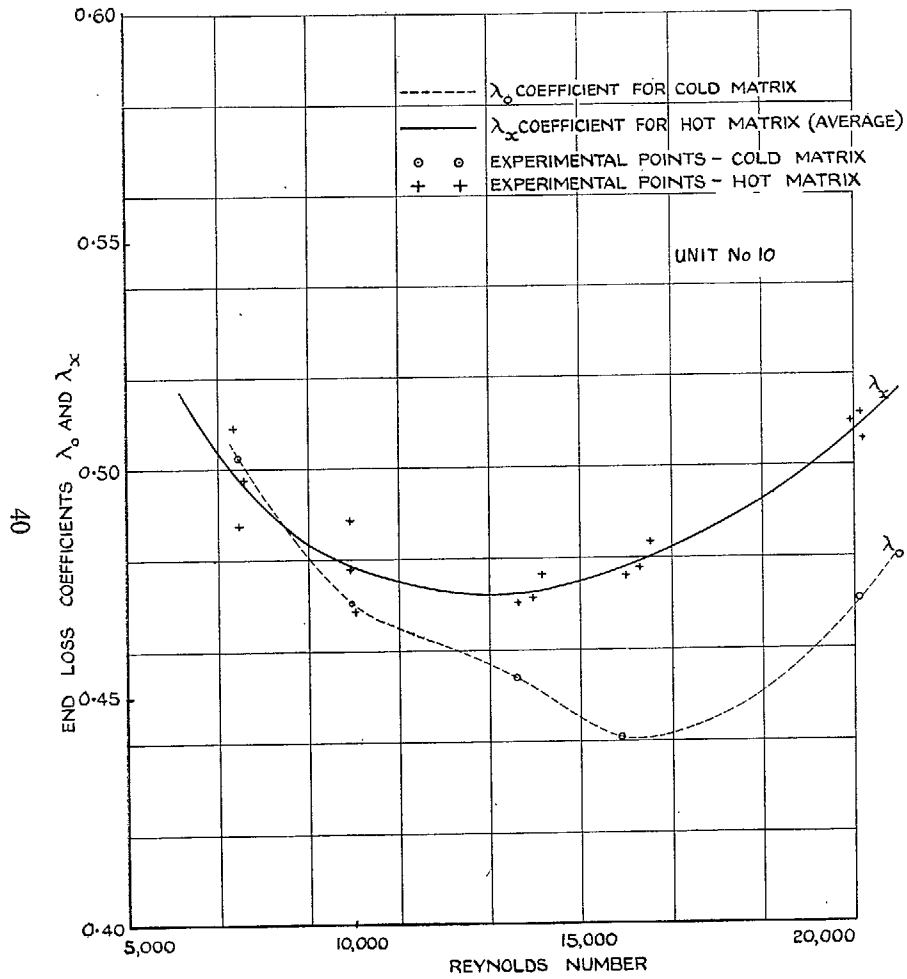


FIG. 22. Values of end-loss coefficient for 5 mm × 140 mm hexagonal tubes.

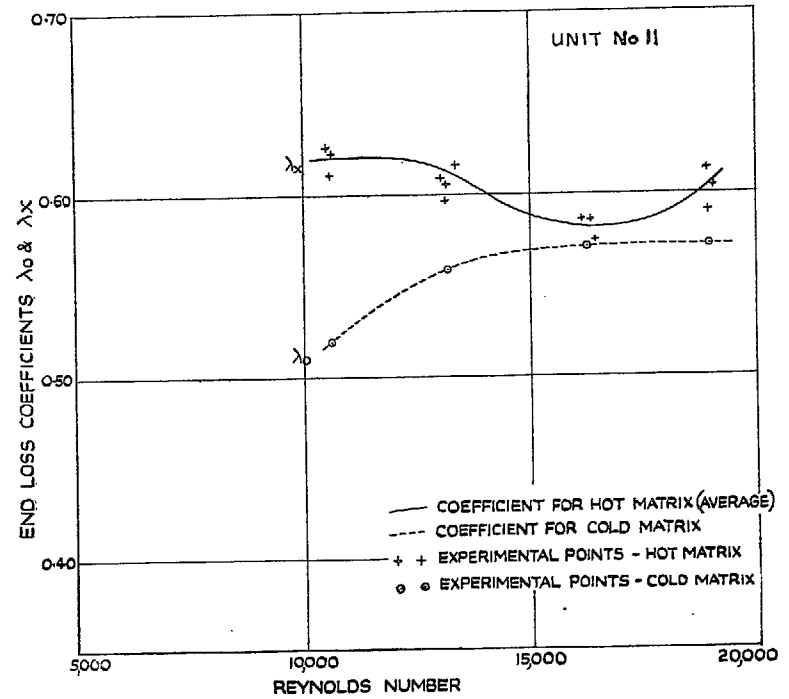


FIG. 23. Values of end-loss coefficients: hexagonal tubes 5 mm × 240 mm R.T.7.

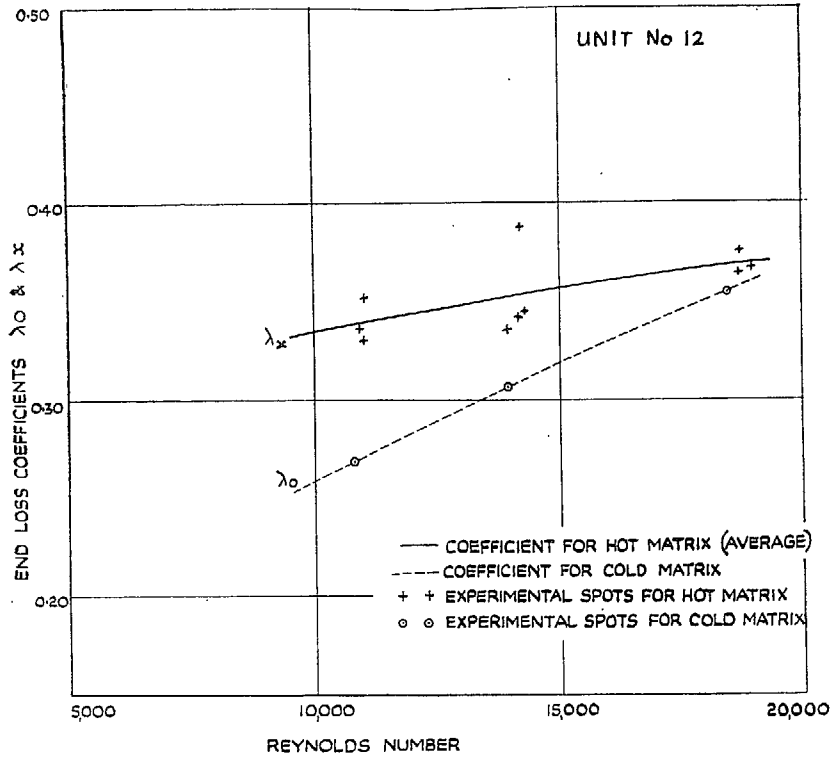


FIG. 24. Values of end-loss coefficients : hexagonal tubes 5 mm \times 320 mm.

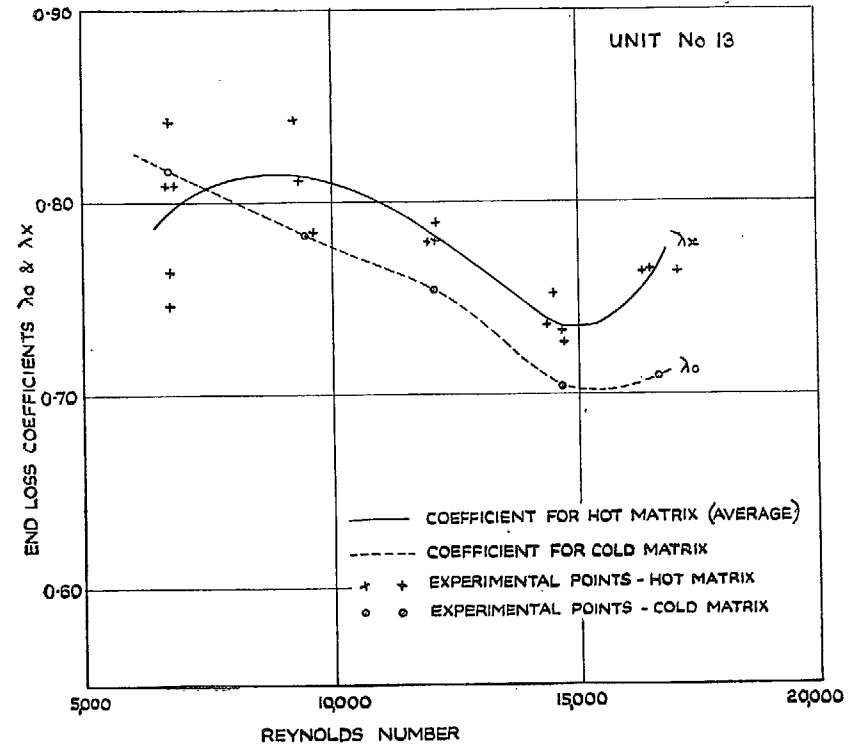


FIG. 25. Values of end-loss coefficients : hexagonal tubes 5 mm \times 360 mm R.T.7.

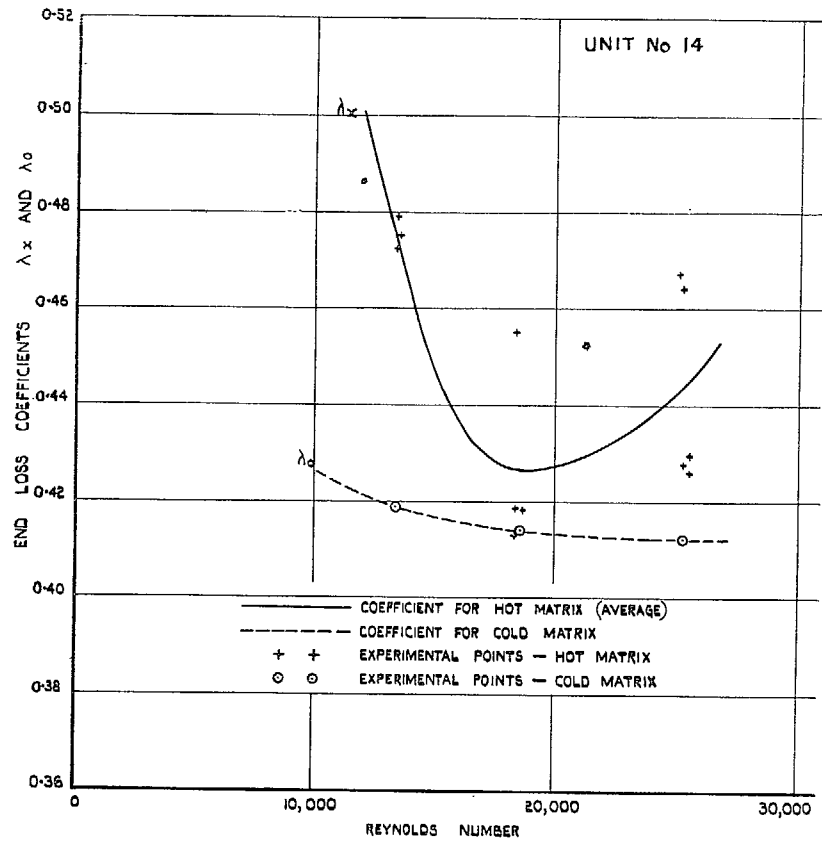


FIG. 26. Values of end-loss coefficients : hexagonal tubes
7 mm \times 320 mm R.T.5.

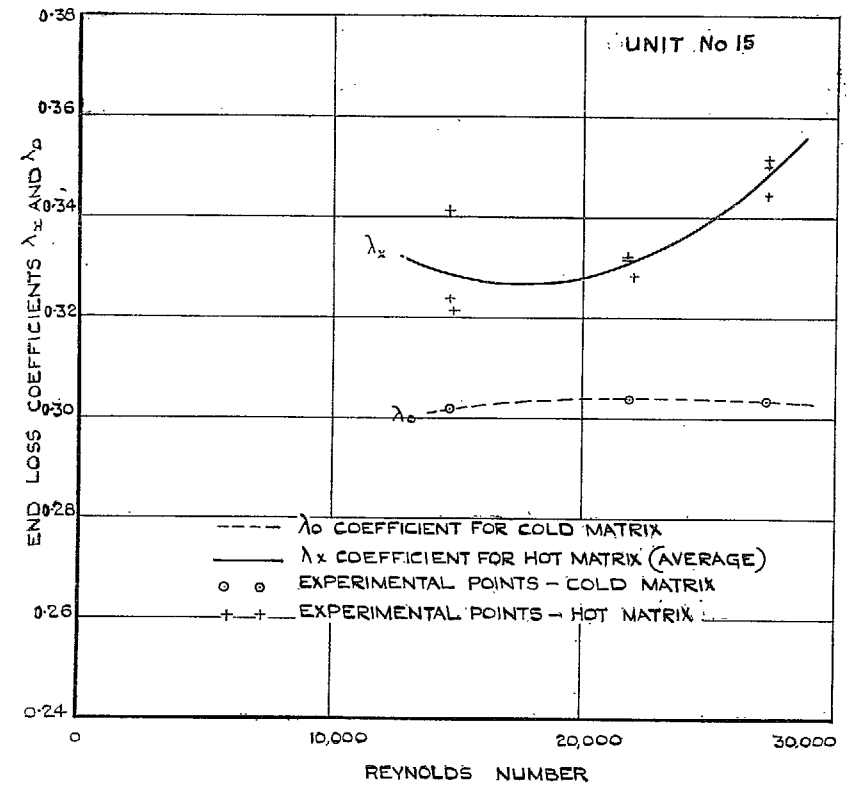


FIG. 27. Values of end-loss coefficients : hexagonal tubes
7 mm \times 320 mm R.T.5.

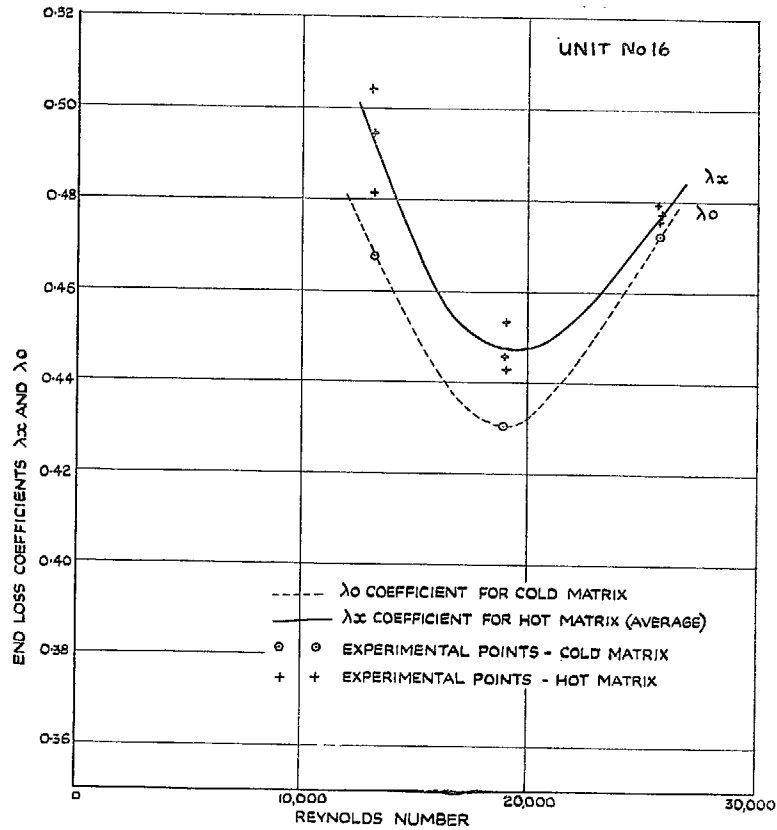


FIG. 28. Values of end-loss coefficients: hexagonal tubes 7 mm \times 320 mm R.T.6.

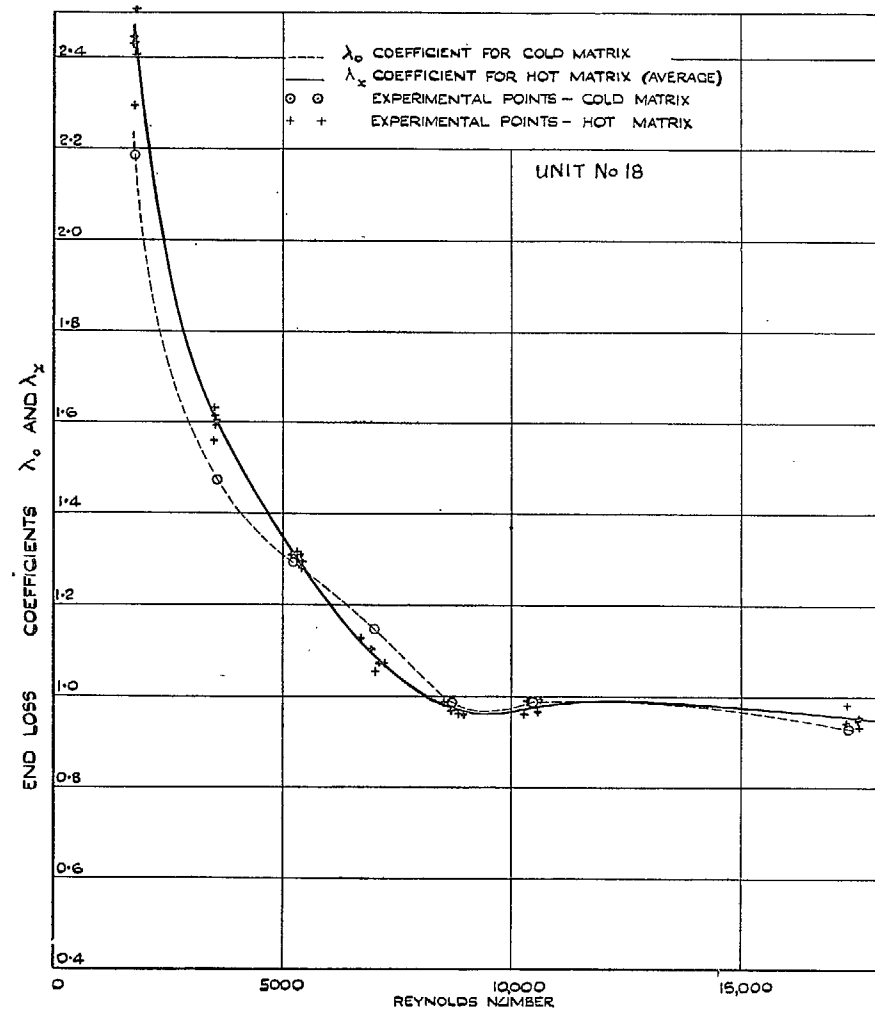


FIG. 29. Values of end-loss coefficient; inside tubes. Tubular charge cooler. Hexagonal tubes 5 mm \times 300 mm with 7.6 mm hexagonal end expansions.

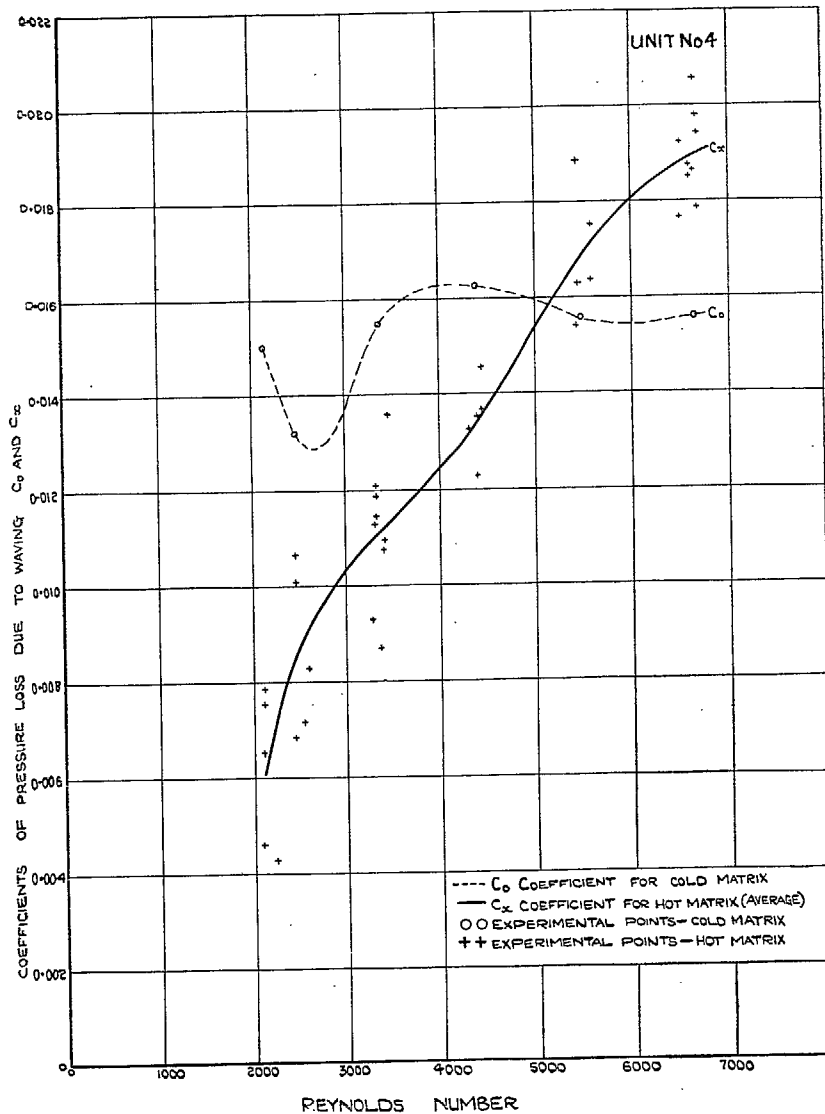


FIG. 30. Values of coefficients of pressure loss due to waving: block E ('a' passages).

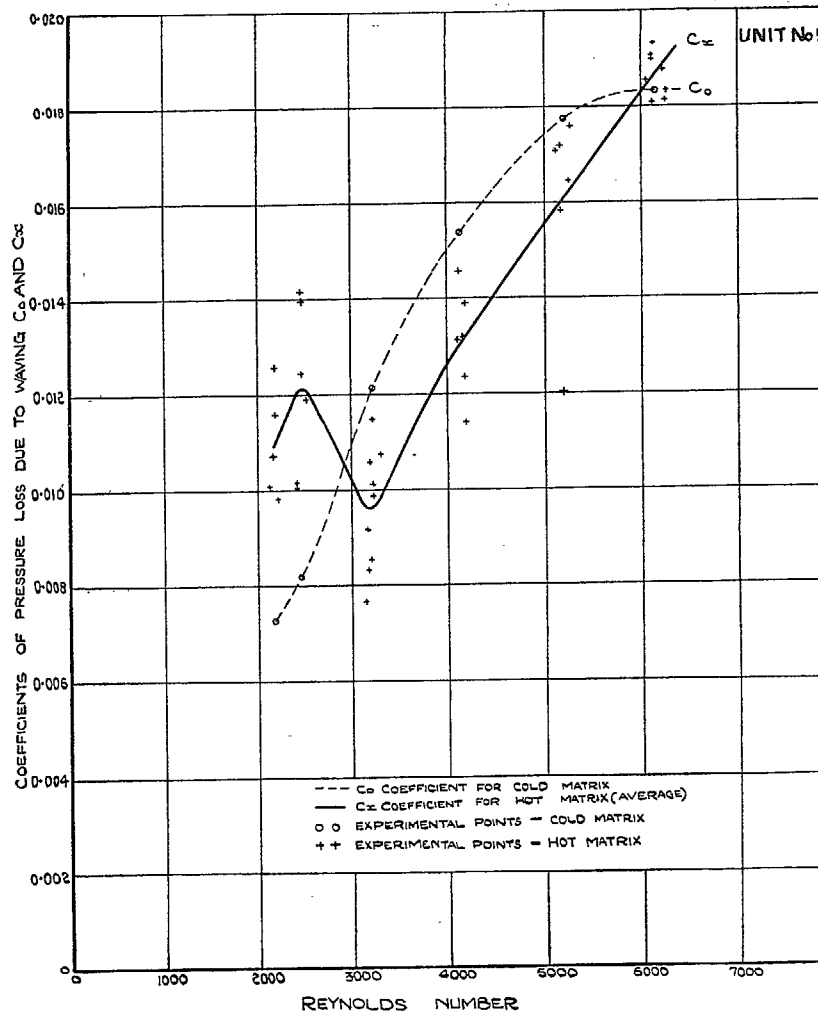


FIG. 31. Values of coefficients of pressure loss due to waving: block E ('b' passages).

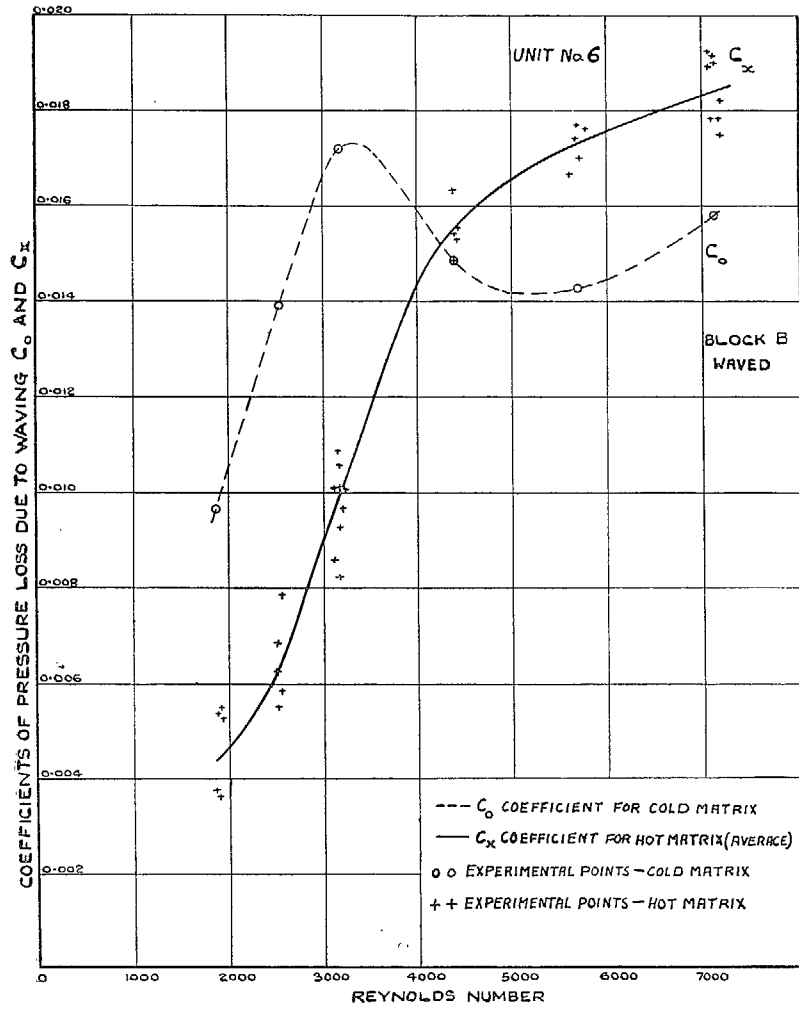


FIG. 32. Values of coefficient of pressure loss due to waving.

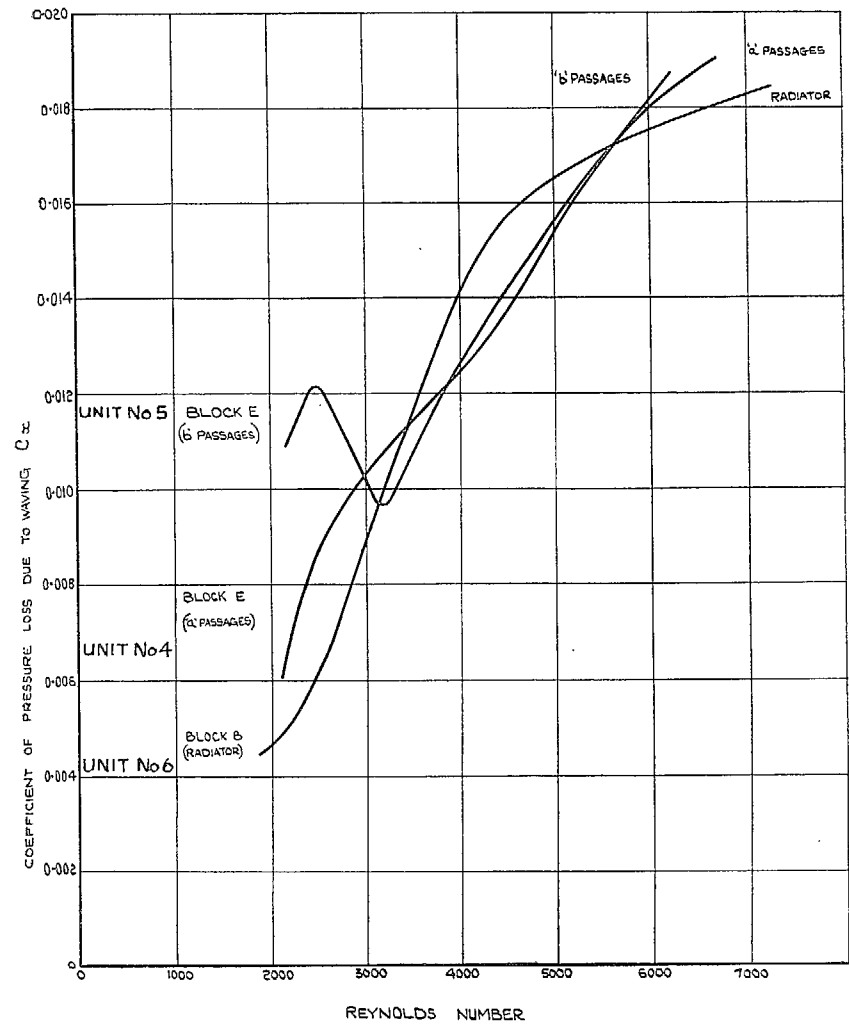


FIG. 33. Value of coefficient of pressure loss due to waving for hot matrices.

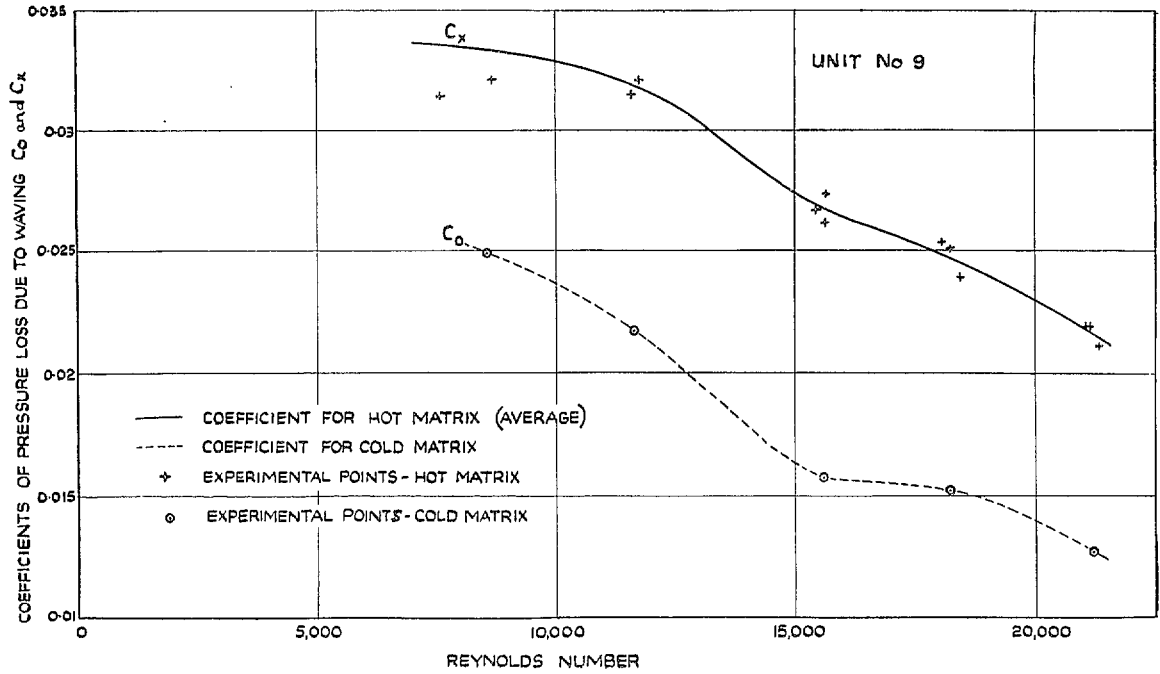


FIG. 34. Values of coefficients of pressure loss due to waving. 'Sinuflo' round tubes 5 mm x 140 mm.

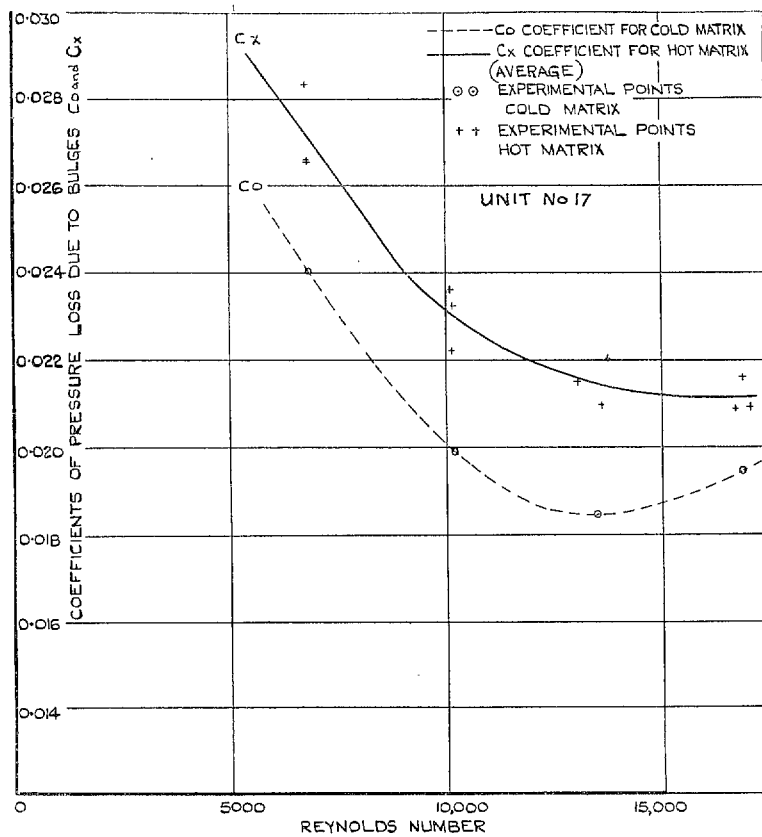


FIG. 35. Values of coefficient of pressure loss due to bulges. Wave-bulged hexagonal tubes 5 mm x 300 mm.

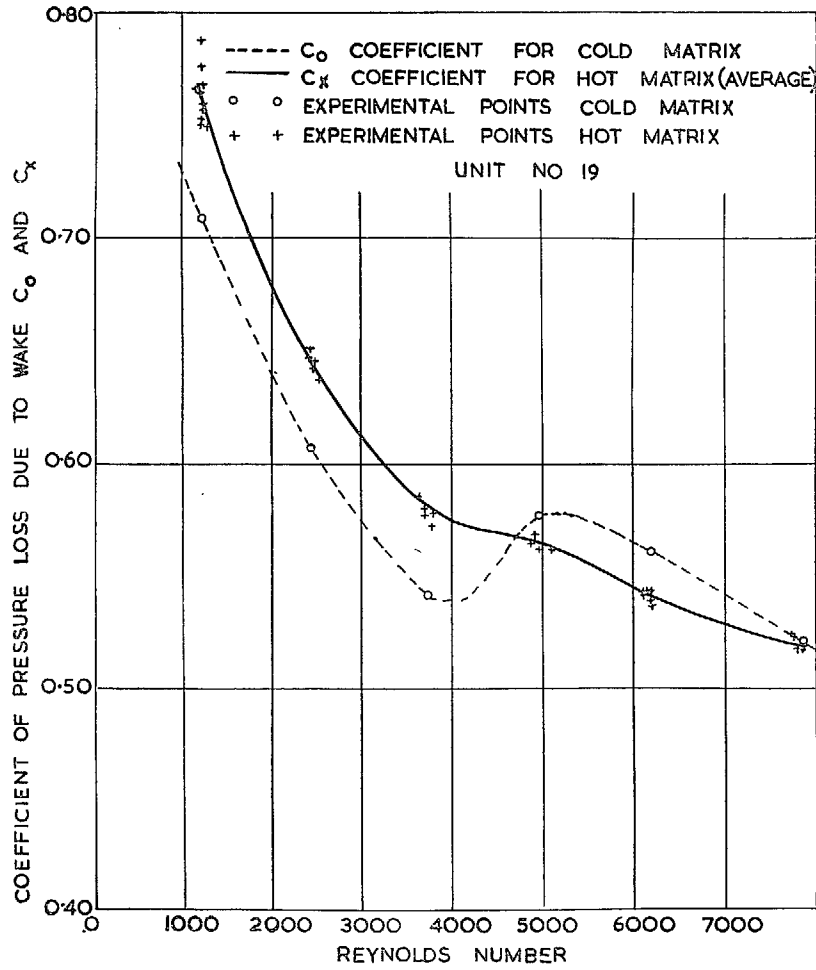


FIG. 36. Values of coefficient of pressure loss due to wake. Outside 5 mm x 300 mm hexagonal tubes with 7.6 mm hexagonal end expansions.

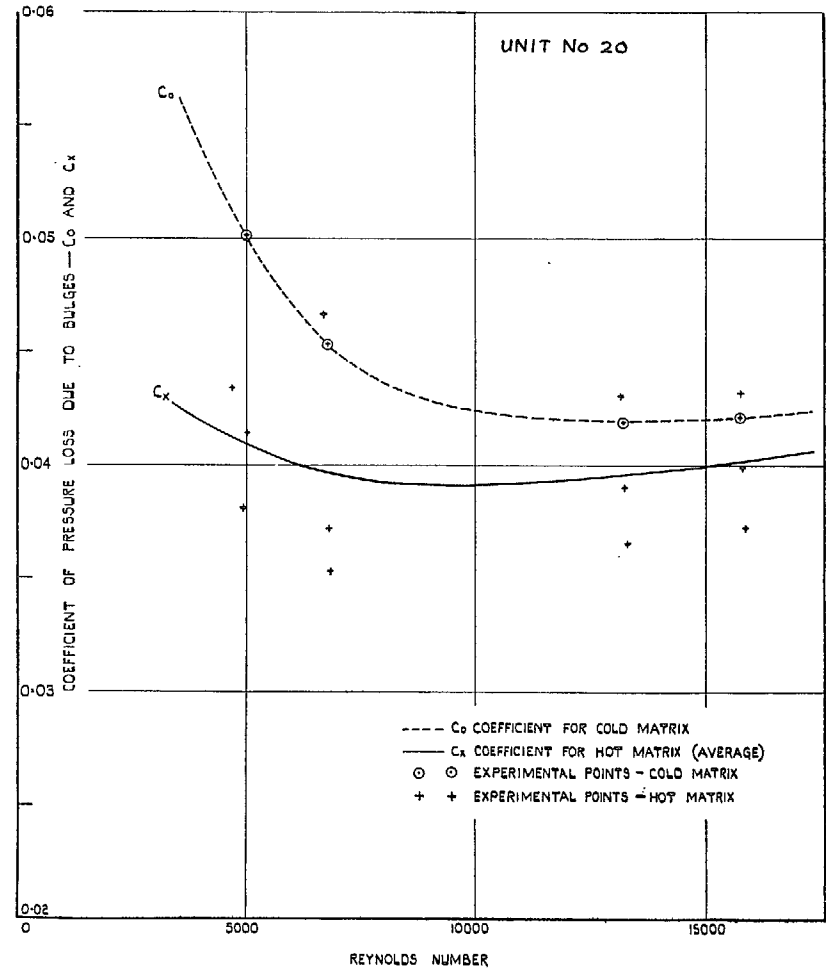


FIG. 37. Coefficient of pressure loss due to bulges. 'Gallay' radiator system E.5. 5 mm x 300 mm.

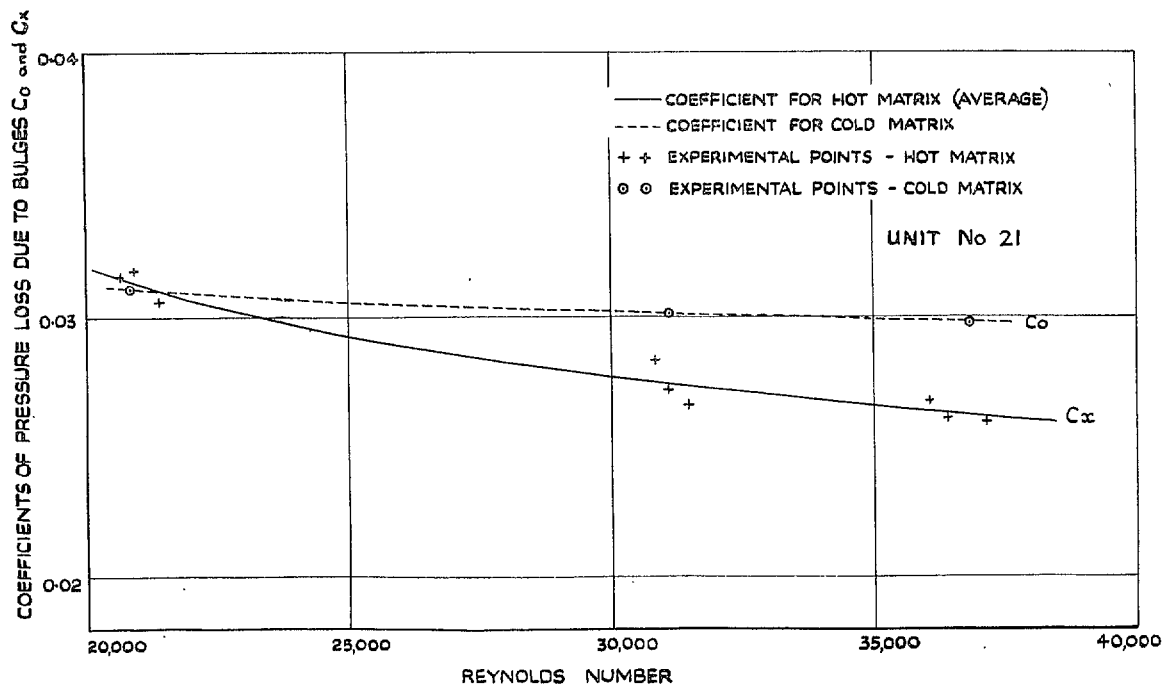


FIG. 38. Values of coefficients of pressure loss due to bulges. 'Gallay' radiator system E 10 mm x 316 mm.

APPENDIX V

Curves of Pressure-Drop Coefficients for Cold Units

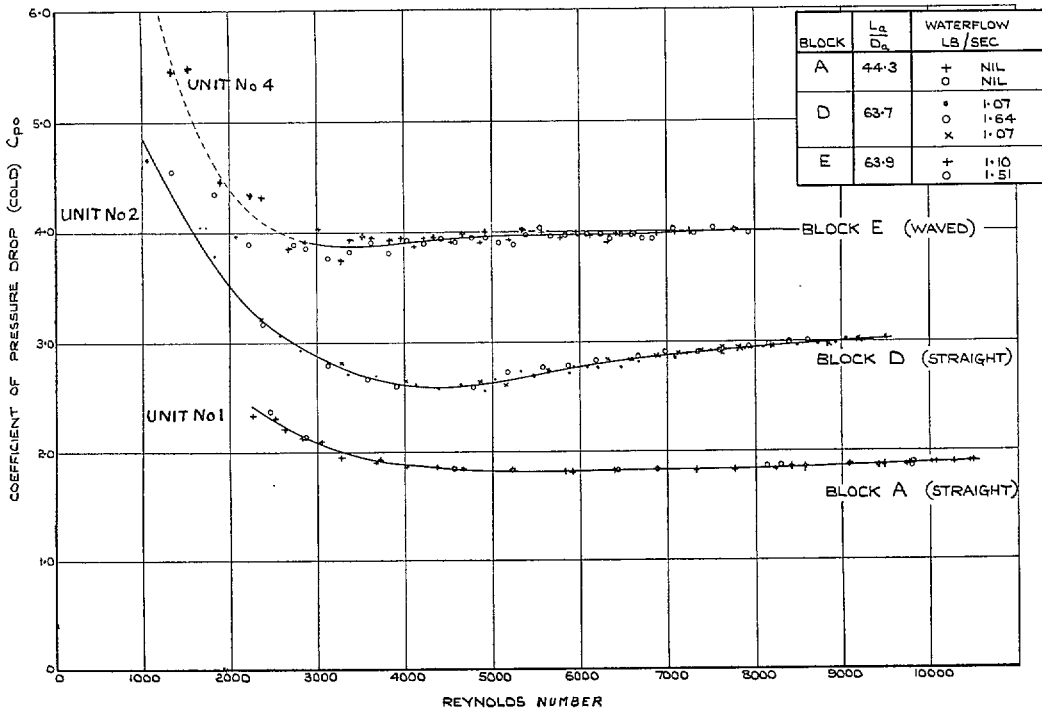


FIG. 39. Coefficient of air-pressure drop for cold matrices ('a' passages).

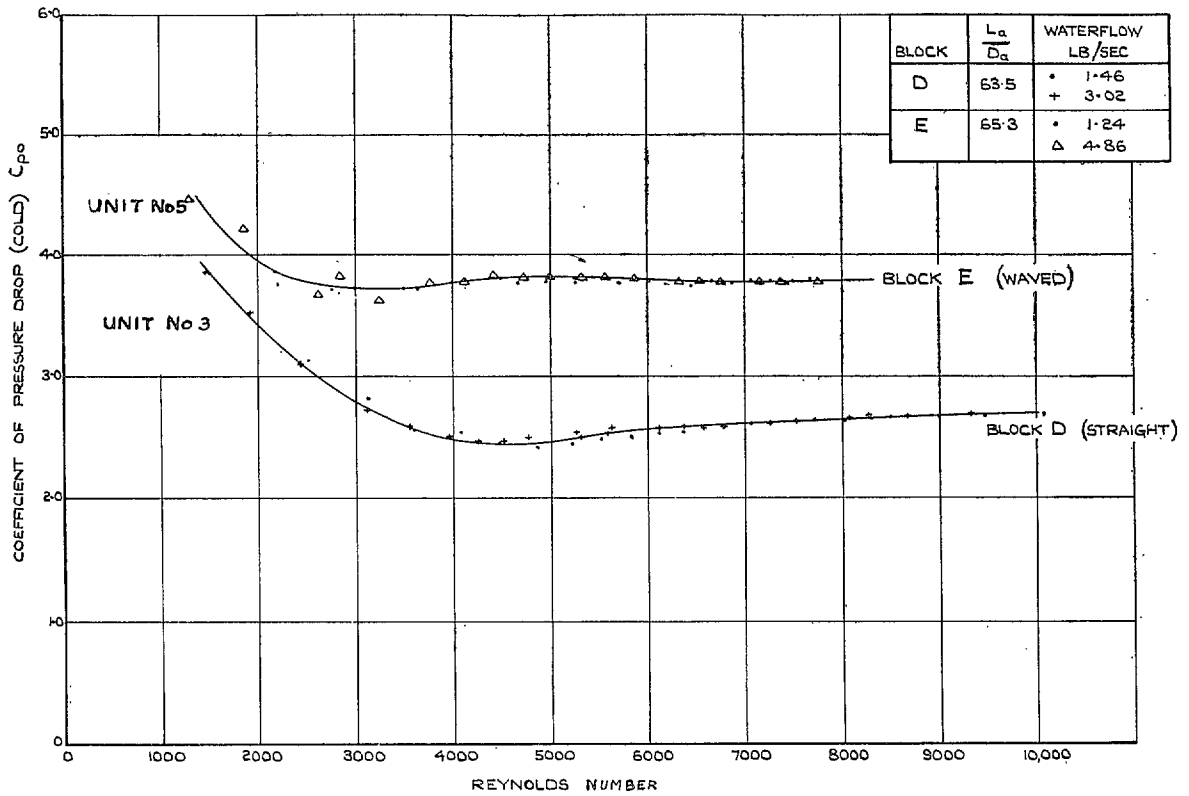


FIG. 40. Coefficient of air-pressure drop for cold matrices ('b' passages).

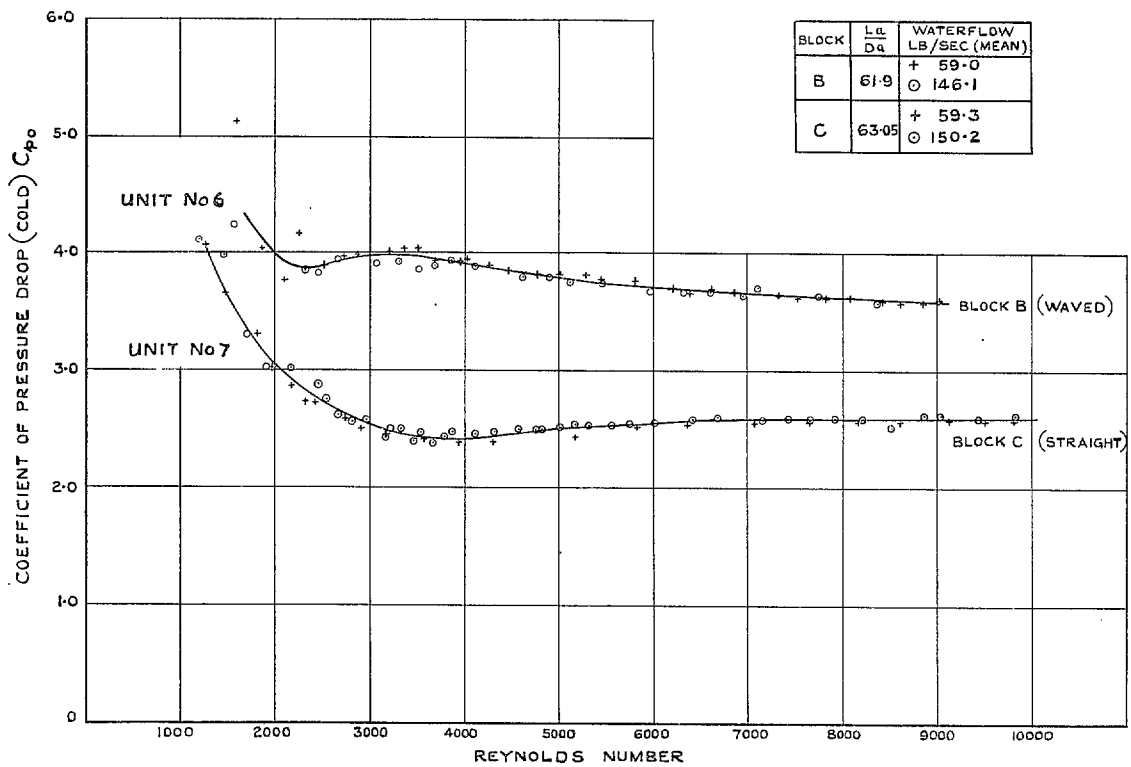


FIG. 41. Coefficient of air-pressure drop for cold matrices.

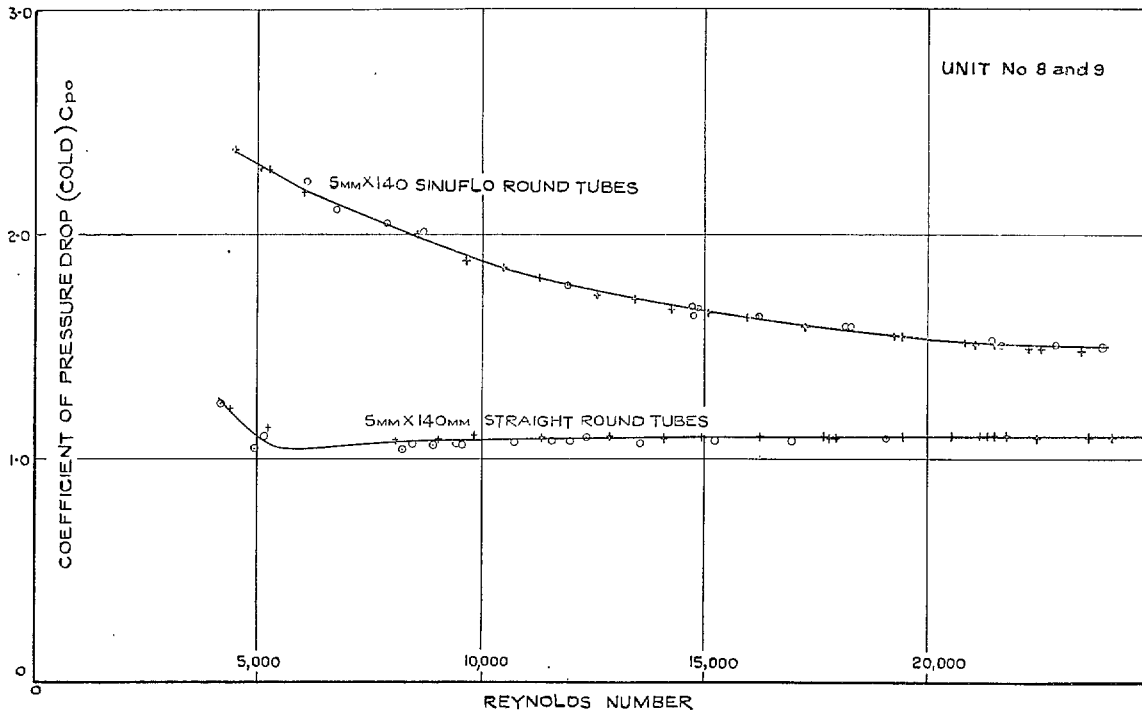


FIG. 42. Coefficient of air-pressure drop for cold matrices. 'Sinuflo' and straight round tubes 5 mm × 140 mm.

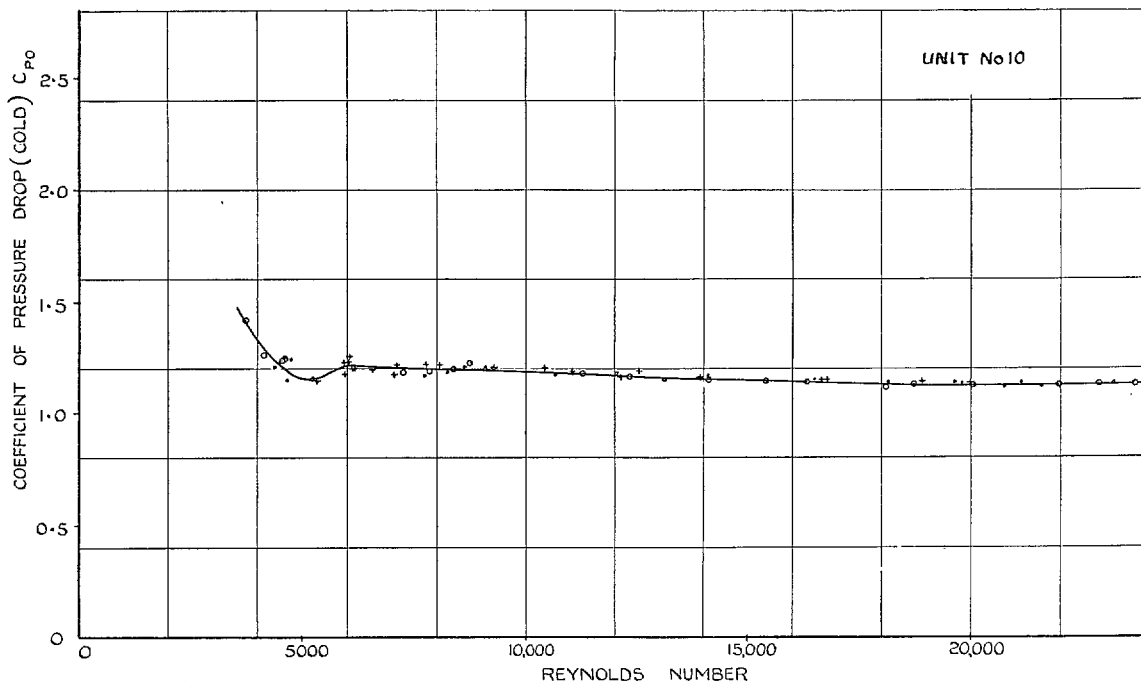


FIG. 43. Coefficient of air-pressure drop for cold matrix. 5 mm × 140 mm hexagonal tubes.

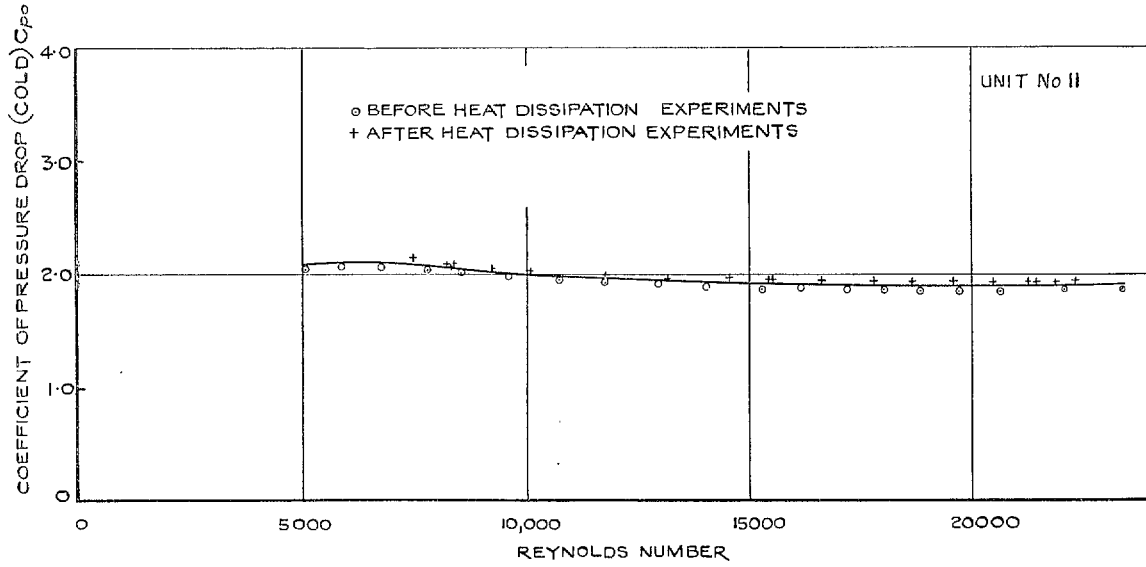


FIG. 44. Coefficient of air-pressure drop for cold matrix. Hexagonal tubes 5 mm \times 240 mm R.T.7.

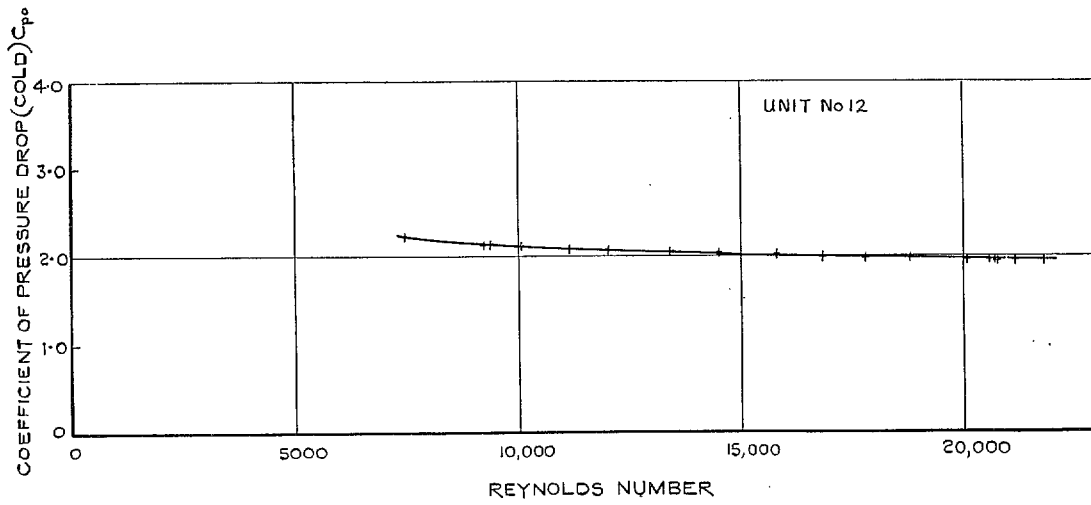


FIG. 45. Coefficient of air-pressure drop for cold matrix. Hexagonal tubes 5 mm \times 320 mm R.T.7.

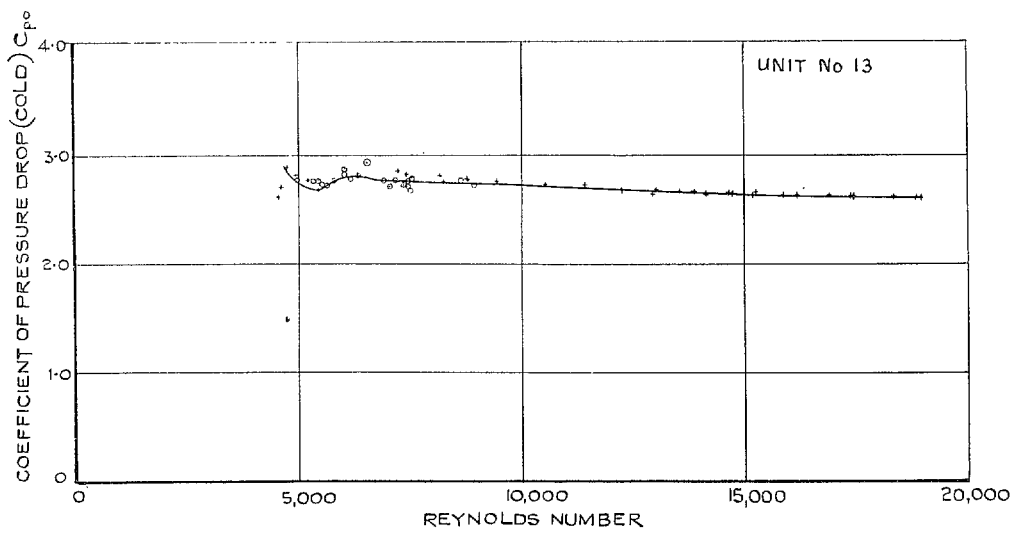


FIG. 46. Coefficient of air-pressure drop for cold matrix. Hexagonal tubes 5 mm \times 360 mm R.T.7.

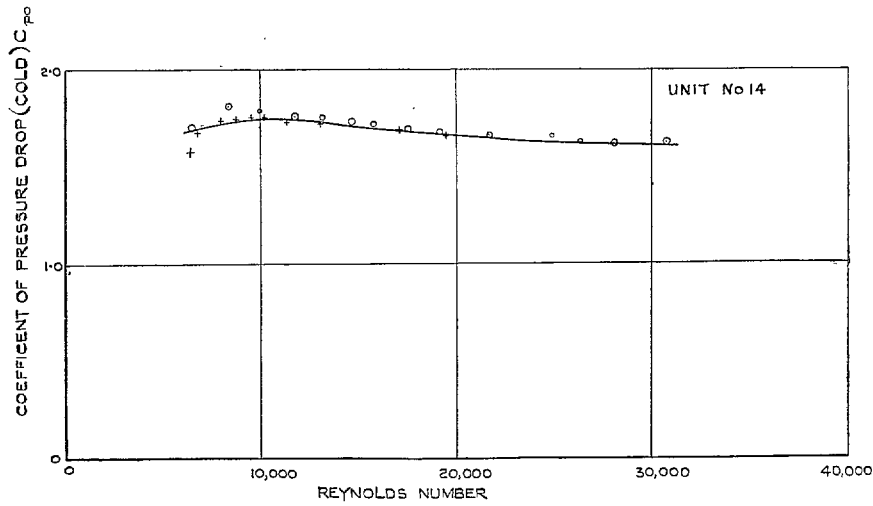


FIG. 47. Coefficient of air-pressure drop for cold matrix. Hexagonal tubes 7 mm \times 320 mm R.T.5.

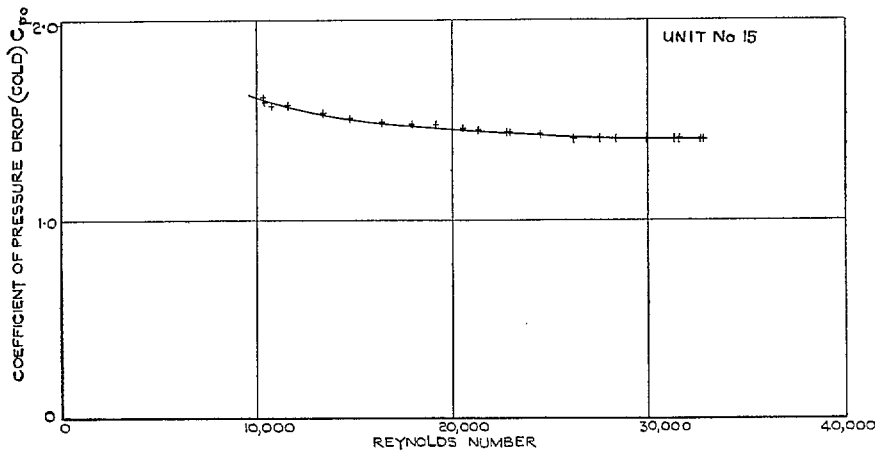


FIG. 48. Coefficient of air-pressure drop for cold matrix. Hexagonal tubes 7 mm \times 320 mm R.T.5.

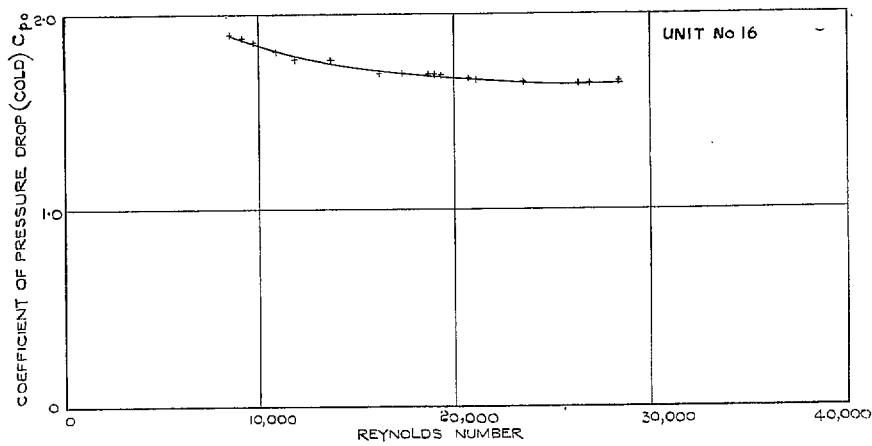


FIG. 49. Coefficient of air-pressure drop for cold matrix. Hexagonal tubes 7 mm \times 320 mm R.T.6.

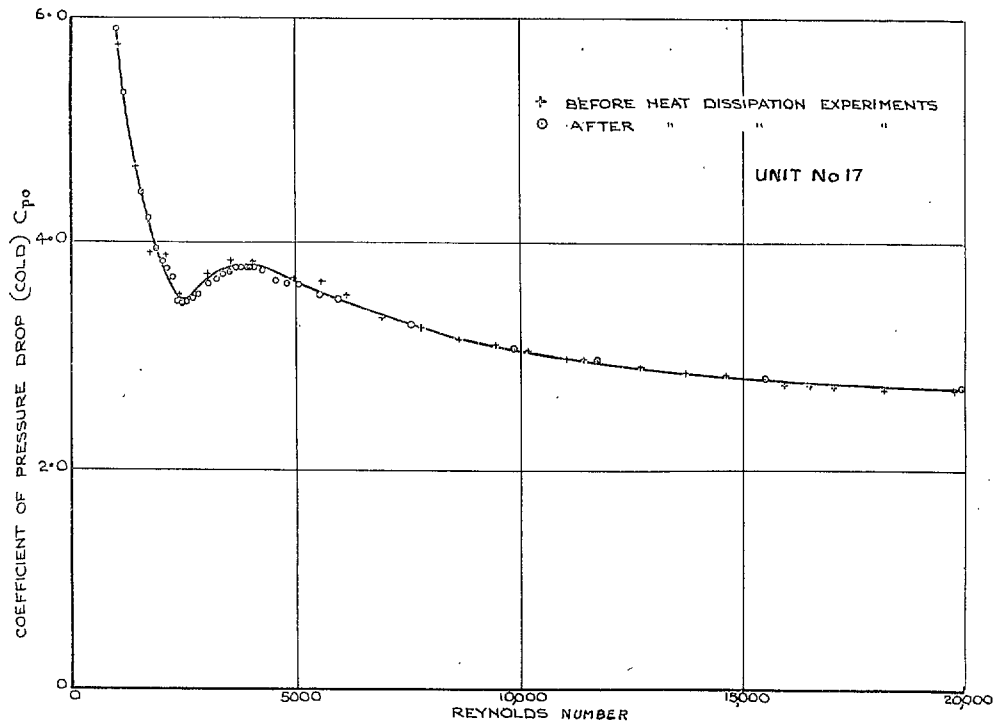


FIG. 50. Coefficient of air-pressure drop for cold matrix. Wave-bulged hexagonal tubes 5 mm × 300 mm.

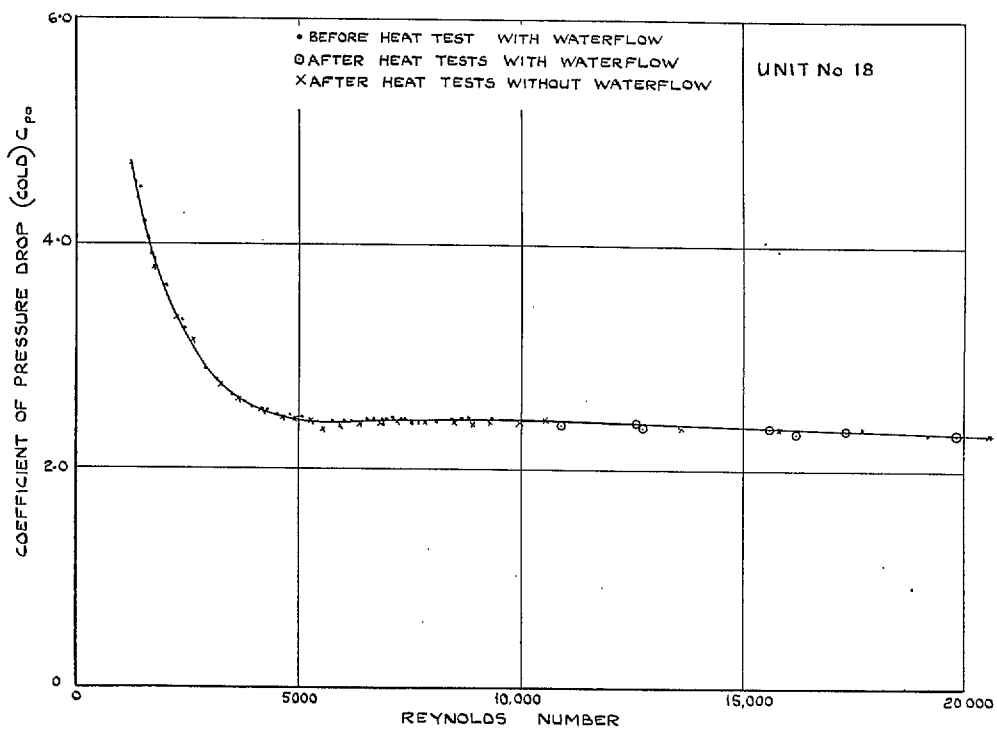


FIG. 51. Coefficient of air-pressure drop for cold matrix—inside tubes. Tubular charge cooler; hexagonal tubes 5 mm × 300 mm with 7.6 mm hexagonal end expansions.

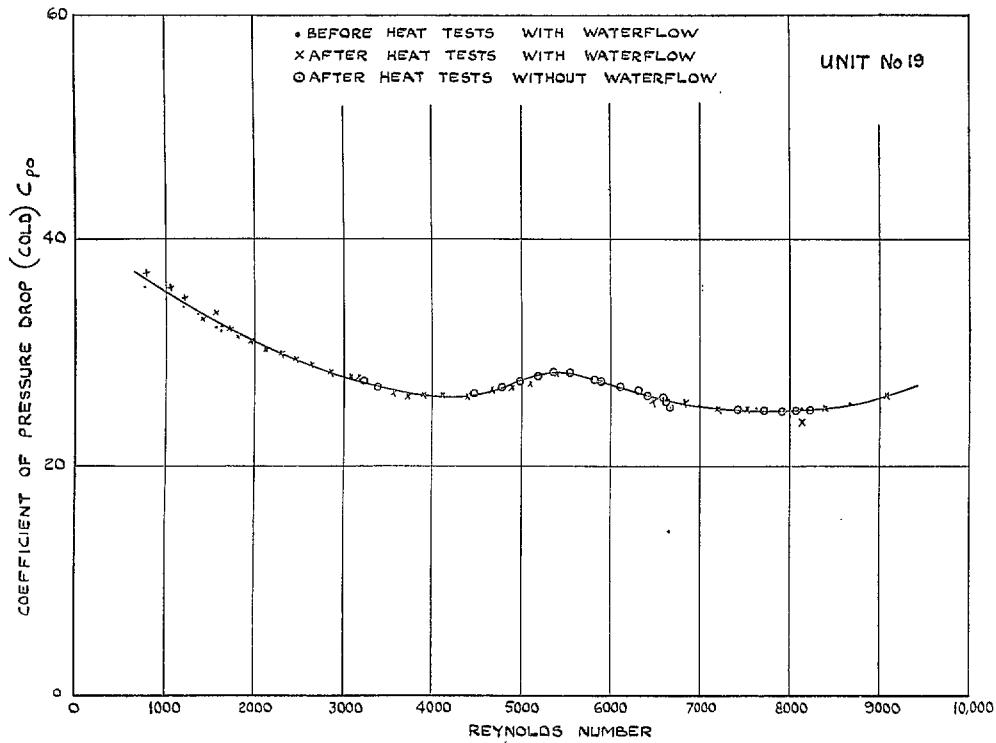


FIG. 52. Coefficient of air-pressure drop for cold matrix—outside tubes. Tubular charge cooler; hexagonal tubes 5 mm × 300 mm with 7.6 mm hexagonal end expansions.

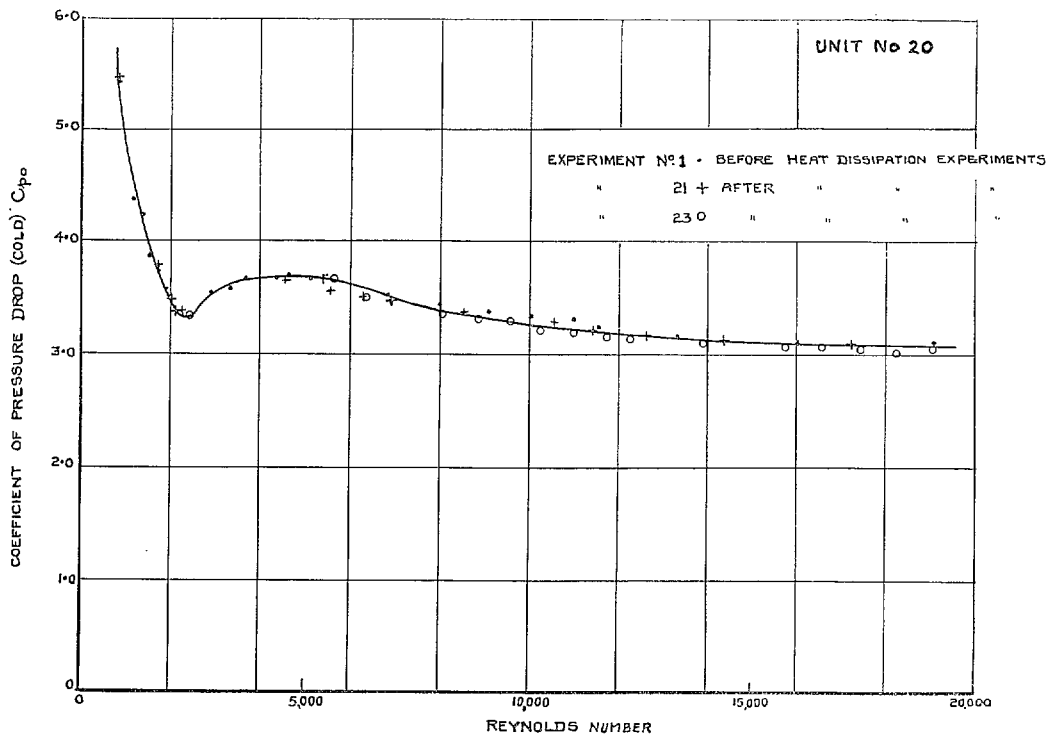


FIG. 53. Coefficient of air-pressure drop for cold matrix. 'Gally' radiator or system E.5. 5 mm × 300 mm.

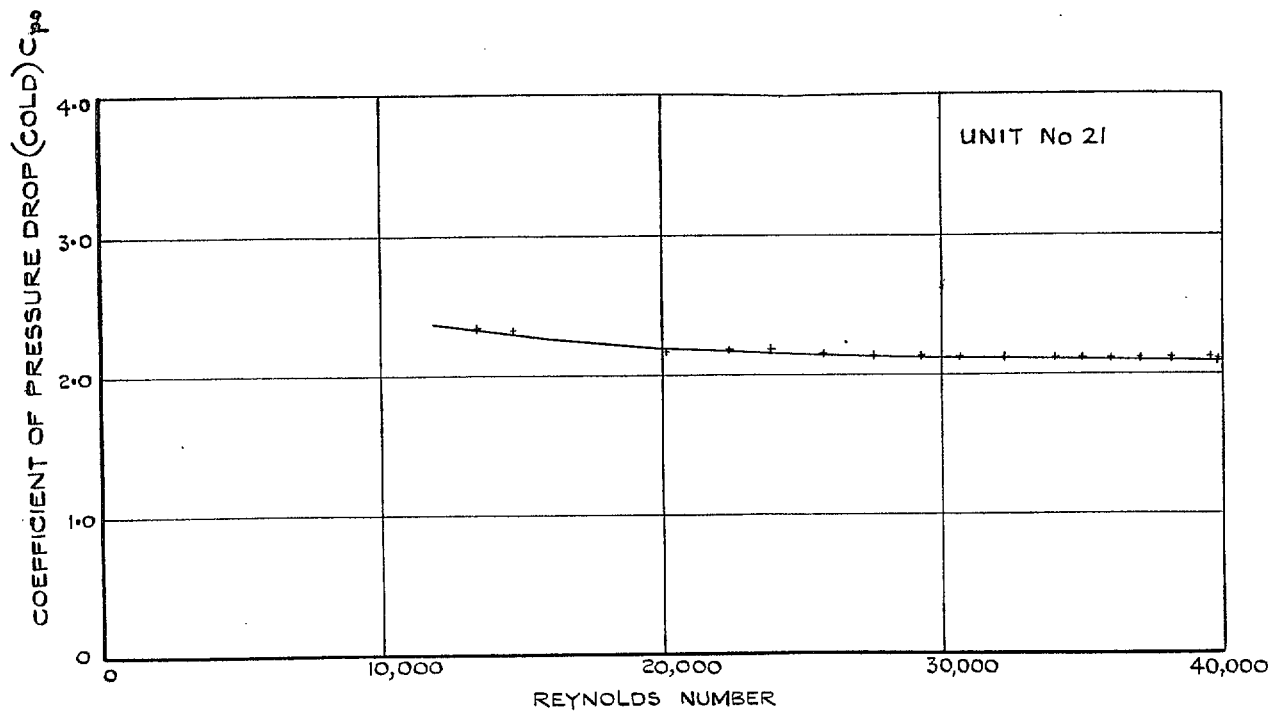


FIG. 54. Coefficient of air-pressure drop for cold matrix. 'Gallay' radiator system E' 10 mm × 316 mm.